UNIVERSITY OF NAPLES
FEDERICO II

DOCTORATE SCHOOL IN

BIOLOGY

XXX CYCLE

Novel functions of the p14ARF tumor suppressor: deciphering cell fate at the crossroad of adhesion and survival

FONTANA ROSA

Coordinator:
Prof. Salvatore Cozzolino

Tutor:
Prof. Girolama La Mantia

2017

Table of Content

SUMMARY

Background: the $p14^{ARF}$ tumor suppressor is an important sensor of oncogenic stimuli inducing cell cycle arrest and or apoptosis through both p53-dependent and independent pathways. It is widely demonstrated that ARF prevalent nucleo/nucleolar localization plays an important role in its tumor suppressor functions.

Nevertheless, recent studies show that, despite its role in growth suppression, ARF is overexpressed in a significant fraction of human tumors, suggesting that it may possess a pro-survival function. Accordingly, in our lab it has been demonstrated that, following PKC stimulation, ARF protein is phosphorylated and accumulates in the cytoplasm where it is unable to efficiently control cell proliferation both in tumor and immortalized cell lines. These observations led to the hypothesis that ARF expression in cancer cells could aid tumor progression by conferring pro-survival properties to the cells. On the other hands, ARF cytoplasmic localization could highlight physiologic and novel roles of this versatile protein.

In this scenario, the aim of my studies was to better understand ARF functions in HeLa, HaCaT and H1299 cell lines, where ARF is highly expressed and mainly localizes in the cytoplasm.

Results and Conclusions: We unexpectedly found that ARF plays a role in cytoskeleton organization. Interestingly, during cytoskeleton remodelling induced by cell spreading, we observed a strong PKC activation resulting in an ARF protein levels increase and stabilization in the cytoplasm. Moreover, we demonstrated that, by aiding cytoskeleton assembly during spreading, ARF protects cells from anoikis blocking DAPK (Death Associated Protein Kinase) dependent apoptosis and promoting cell survival through FAK stabilization. Interestingly, we found that the ARF T8D mutant, mimicking the phosphorylation status of the protein, is able to mediate both cell spreading, FAK activation and cell proliferation through inhibition of DAPK functions. On this basis, we propose that the role of ARF in cell adhesion and survival strictly depends on both cell context and post-translational modifications.

CHAPTER 1

INTRODUCTION

1.1 INK4b-ARF-INK4a locus: a puzzling genomic structure

The INK4b-ARF-INK4a locus, located on human chromosome 9p21 and on mouse chromosome 4, is conserved between human, mouse, rat and opossum (Quelle et al., 1995; Swafford et al., 1997; Sherburn et al., 1998). It encodes for three proteins that regulate the pathways of two potent cell cycle regulators: the retinoblastoma protein (pRB) and the p53 transcription factor.

INK4a and INK4b genes encode for $p16^{INK4a}$ and $p15^{INK4b}$, two important members of the INK4 family (inhibitors of the cyclin-dependent kinases (CDKs)). In response to specific signals, they block the assembly of the catalytically active cyclinD-CDK4/6 complex. In this way, the pRB protein, maintained in an active hypophosphorylated state, sequesters E2F transcription factors, causing G1 phase cell cycle arrest. (Sharpless and DePinho, 1999; Serrano, 2000) (Fig.1).

The simple tandem arrangement of this locus is complicated by the insertion of an exon (called exon 1β) that is located 22kb upstream to the exon 1α of INK4a. Exon 1β is transcribed from its own promoter and the resulting transcript also includes the exon 2 and 3 of INK4a (Duro et al.,1995; Mao et al., 1995; Stone et al., 1995) (Fig.1). Nevertheless, the protein product doesn't share any amino acid homology with p16 because the exon 2 is translated in a different open reading frame (Quelle et al.,1995). For this reason, the name of this protein is ARF (*Alternative Reading Frame*).

Interestingly, ARF (known as $p14^{ARF}$ in human and $p19^{ARF}$ in mouse), like $p16^{INK4a}$, is a potent tumor suppressor, but is involved in the regulation of p53 pathway (Fig.1). The sharing of exon 2 and the fact that both $p16^{INK4a}$ and ARF have the capacity to induce cell-cycle arrest raise intriguing questions about how this unique genomic arrangement might have come about (Gil and Peters, 2006). Evolutionary studies show that in the puffer fish *Fugu rubripes* genome, the region equivalent to the mammalian INK4b-ARF-INK4a locus specifies only a single gene (Fugu INK4a/b), that is a

homologue of INK4b, without any associated ARF-encoding potential region. This suggests that INK4b was the primordial gene at this locus and after the divergence of the lineage leading to mammals from fish, 450 million years ago, a gene duplication event generated the adjacent INK4a gene. No evidence for ARF has been found at the Fugu INK4 locus or in nearby surrounding regions (Gilley and Fried, 2001). Given that ARF protein is poorly conserved even between human and mouse, its evolutionary origins remain still unknown. Interestingly, Kim and colleagues (2003) reported that in chicken genome, which represents an intermediate between fish and man in the evolution, the INK4b-ARF-INK4a locus encodes the homologues of both $p15^{INK4b}$ and ARF. Interestingly, the exon 1β has replaced the exon 1α causing the loss of $p16^{INK4a}$ expression. Moreover, despite chicken ARF is encoded only by exon 1β because the splicing to exon 2 takes place in a different register to that used in mammals, the protein is yet functional. This finding is consistent with studies indicating that exon 1β-encoded N-terminal region (aa. 1-64 for $p14^{ARF}$) is necessary and sufficient for the known ARF tumor suppressor functions, while residues specified by exon 2 are dispensable (Quelle et al., 1997; Zhang et al., 1998; Lohrum et al., 2000; Weber et al., 2000; Llanos et al., 2001).

Nevertheless, recent evidences have shown that the exon 2-encoded sequences contribute significantly to ARF function in mammalian cells (see section 1.2 "ARF role in the cytoplasm").

Interestingly, it has been demonstrated that ARF constitutes a link between the pRb and p53 pathways and may act as a safety valve that triggers a p53-dependent checkpoint when the pRb pathway is compromised. Specifically, the inactivate pRb causes the release of E2F transcription factors, which induce ARF transcription (Stott et al., 1998; De Stanchina et al., 1998).

The unique genomic arrangement of INK4b-ARF-INK4a locus reflects a common purpose for the encoded products. Indeed, all three proteins are main regulators of cellular senescence, a growth-arrest mechanism that protects cell from hyperproliferative signals and various forms of stress and, together with apoptosis, represents an important barrier against tumor formation (Gil and Peters, 2006). Understanding $p16^{INK4a}$ and ARF role in this process is complicated by apparent differences in their behaviour between human and mouse cells. Indeed, while $p16^{INK4a}$

takes centre stage in senescence in human cells, ARF assumes a more prominent role in mouse cells. A possible explanation could be the fact that the stimuli that can lead to senescent states are different among the species. For example, while the replicative senescence of human fibroblasts appears to be mediated in large part by telomere attrition, senescence of mouse fibroblasts is completely independent of the telomere clock and is induced like a stress response (Collins and Sedivy, 2003).

ARF and p16 seem to have a different behaviour between human and mouse cells also for their tumor suppressor function. In human cancer, although in most cases all three genes of this locus are lost (Chin et al.,1998; Sherr, 2001; Saporita et al., 2007), INK4a is inactivated by loss of function "mutations" (point mutation and deletion) and promoter methylation events more frequently than ARF or INK4b. Specifically, INK4a mutation occurs in a significant fraction of familial melanoma (Kamb et al., 1994), sporadic esophageal and pancreatic adenocarcinomas (Schutte et al., 1997; Liggett and Sidransky, 1998). Conversely, it has been reported that some tumour types, like leukaemias and lymphomas, are associated with the specific inactivation of INK4b without any documented effects on INK4a (Ruas and Peters, 1998; Serrano, 2000; Sharpless and DePinho, 1999; Sherr, 1998).

The first studies carried out in mouse model showed that, respect to p16, ARF seems to assume a more prominent role as tumor suppressor in mouse rather than in man, where the mutation frequency of its gene is very low. $p19^{ARF}$ null mice develop tumors such as sarcomas (43%), lymphoid malignancies (29%), carcinomas (17%), and tumors of the nervous system (11%) early in life (after 9,5 months), and they die after one year. Furthermore, heterozygous mice also develop tumors, albeit after a longer latency compared to $p19^{ARF}$ -/- mice. In $p19^{ARF}$ +/- mice, it has been demonstrated that the tumor formation is accompanied by loss of the remaining allele (Kamijo et al.,1999).

Recently, specific $p14^{ARF}$ alterations have been identified in different human tumor contexts. Deletions and point mutations of exon 1β are frequent in familial melanoma (Rizos et al., 2001; Laud et al., 2006). Nine of fifty glioblastoma patients have a specific deletion of ARF (Nakamura et al, 2001). Furthermore, the promoter methylation of $p14^{ARF}$ is frequent in a wide spectrum of human cancers such as colorectal (Esteller et al., 2000), gastric (Tsujimoto et al., 2002) and prostate

carcinomas (Konishi et al., 2002). Moreover, in breast cancer, homozygous deletion, loss of heterozygosity and promoter hypermethylation have been described (Silva et al., 2001). Interestingly, in the majority of non-small cell lung cancer (NSCLC), $p14^{ARF}$ protein is expressed at low levels albeit there are no gene mutations and transcriptional alterations, indicating an inactivation mechanism not yet identified (Vonlanthen et al., 1998).

In conclusion, the INK4b-ARF-INK4a locus, whose evolutionary origins are not yet totally clear, plays an important role in human cancers showing a mutation frequency that is second only to the p53 locus (Hall et al.,1996; Hainaut et al., 1997), because encodes for master regulators of mechanisms (apoptosis, senescence, and cell cycle regulation) which represent an important barrier against tumor formation.

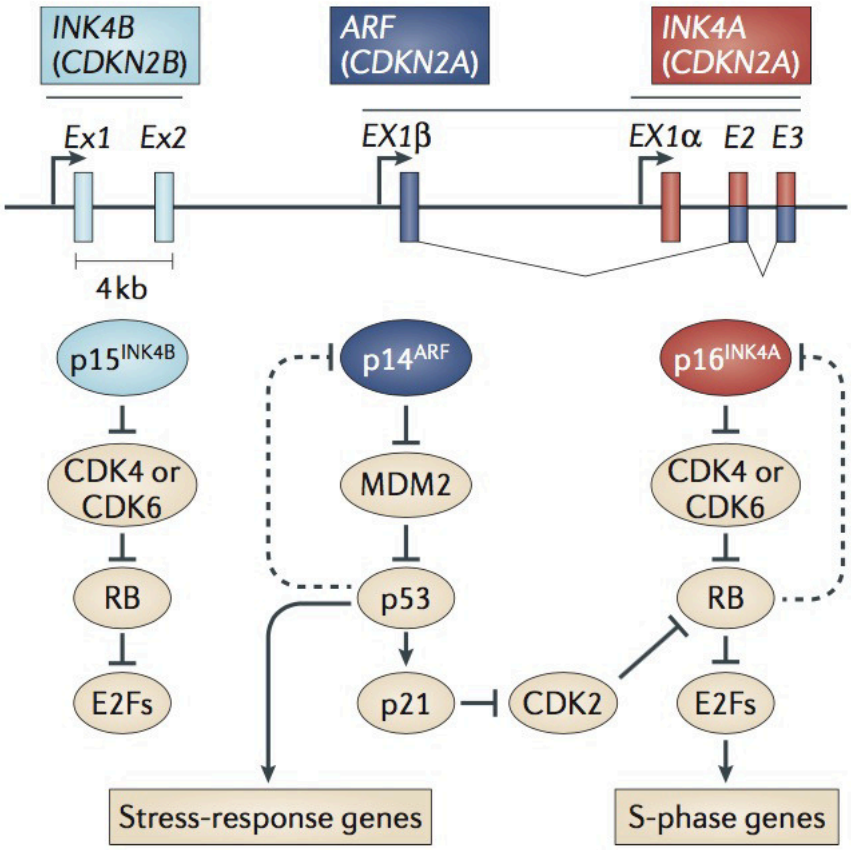

Figure 1: INK4b-ARF-INK4a locus and its protein products

INK4b-ARF-INK4a locus, located on human chromosome 9p21, is less than 50 kb in length. It encoded for three tumor suppressor proteins: $p15^{INK4b}$, $p14^{ARF}$ ($p19^{ARF}$ in mouse) and $p16^{INK4a}$. In light blue, it is represented the *CDKN2B* gene, which encodes $p15^{INK4b}$, and is composed by two exons. The *CDKN2A* gene encodes for $p14^{ARF}$ (exons in dark blue) and $p16^{INK4a}$ (exons in red). p16 transcript is composed by EX1α- Ex2- Ex3, while ARF transcript is composed by EX1β- Ex2-Ex3 and is translated in a different ORF respect to p16. The $p16^{INK4a}$ and $p15^{INK4b}$ proteins inhibit cyclin D-dependent CDK4 and CDK6 to prevent phosphorylation of the retinoblastoma protein (RB). The hypophosphorylated form of RB sequesters E2F transcription factors, blocking the transcription of different genes required for DNA replication, causing G1 phase cell cycle arrest. The ARF protein, biding the MDM2 E3 ubiquitin ligase, prevents p53 polyubiquitylation and induce p53 activation. In turn, the p53 transcription factor can induce the activation of p21CIP1, which inhibits CDK2-mediated RB phosphorylation causing G1 phase cell cycle arrest. If the cell damage is very strong, p53

activates other genes, that induce apoptosis. Inactivation of p53 leads to *ARF* induction, whereas inactivation of RB induces $p16^{INK4A}$ expression (Sharpless and Sherr, 2015).

1.2 Role of ARF in tumor suppression

One of well-studied ARF functions is its ability to suppress aberrant cell growth in response to altered mitogenic signals (such as Ras, c-Myc, E1A, E2F and v-Abl) through p53 dependent and independent pathways (Ozenne et al., 2010).

The ARF-MDM2-p53 pathway

p53 has been labeled the "guardian of the genome" and its gene is mutated in approximately half of all human cancers (Vousden et al., 2002; Maggi et al., 2014). In response to a wide variety of cellular stresses, such as DNA damage and inappropriate oncogenic signaling, p53 is able to induce the expression of a plethora of target genes involved in cell cycle arrest, apoptosis, senescence, autophagy and DNA repair (Junttilla and Evan, 2009).

Given the strong importance of p53 in the preservation of cell integrity, it is essential to keep its expression under tight modulation (Maggi et al., 2014).

One of the most important negative regulators of p53 is the E3 ubiquitin ligase MDM2. It was reported that MDM2 binds p53 transcriptional activation domain to interfere with the recruitment of basal transcription machinery, blocking in this way the expression of p53-responsive genes (Momand et al., 1992; Oliner et al., 1993). Moreover, MDM2 regulates p53 protein stability because, through its intrinsic E3 ubiquitin ligase activity, it promotes p53 polyubiquitylation and translocation from nucleoplasm to cytoplasm with resulting proteasomal degradation (Honda et al., 1997; Roth et al., 1998; Freedman and Levine, 1998; Tao and Levine,1999). In this way, MDM2 can keep the basal cellular levels and activity of p53 low enough to avoid interference with cell cycle progression and cell survival. Furthermore, a negative feedback loop exists because p53 can bind MDM2 promoter and stimulates its transcription (Maggi et al., 2014).

ARF is an upstream regulator of MDM2-p53 axis. The interaction between MDM2 and ARF has been documented both *in vivo* and *in vitro* (Kamijo et al.,1998; Pomerantz et al., 1998; Stott et al., 1998; Tao and Levine, 1999; Weber et al., 2000; Zhang et al., 1998). For the first time, Weber et colleagues (2000) identified the minimal interaction domains between ARF and MDM2 using specific deletion mutants. They demonstrated that the $p19^{ARF}$ N-terminal domain contains two non-

contiguous binding sites for MDM2 restricted to residues 1 to 14 and 26 to 37, respectively. Interestingly, the domain 26-37 has a dual function, because it is also necessary to induce $p19^{ARF}$ nucleolar localization. Although $p19^{ARF}$ Δ26-37 mutant retains the ability to bind MDM2 both *in vitro* and *in vivo*, it is strongly delocalized to the nucleoplasm, largely defective in inducing p53 accumulation and cell cycle arrest. These data indicate that the relocalization of Mdm2 to nucleoli by ARF is a necessary event to induce cell cycle arrest. Furthermore, the authors demonstrated that not only ARF but also MDM2 contributes to nucleolar localization of the ARF-MDM2 complex. Indeed, they reported that in the nucleoplasm ARF binding to MDM2 causes the exposure of a cryptic NoLS (nucleolar localization signal) within MDM2. In line with this, in the human $p14^{ARF}$ protein the region 2 to 14 is necessary both to bind MDM2 and allow ARF nucleolar localization (Weber et al., 2000; Zhang and Xiong, 1999; Tao and Levine, 1999). Moreover, it has been reported that the interaction of ARF with MDM2 inhibits the ubiquitin ligase activity of MDM2 to promote p53 stabilization (Honda and Yasuda, 1999). In the same way, ARF can also promote p53 stabilization blocking the ubiquitin ligase activity of ARF-BP1/Mule (ARF-binding protein1/Mcl1-ubiquitin ligase E3) (Chen et al., 2005). Furthermore, a negative feedback loop exists to limit p53 activation because ARF transcription is negatively regulated by p53 (Maggi et al., 2014).

p53-indepedent functions of ARF

There are different evidences indicating that ARF can also perform its tumor suppressor function in a p53 independent manner. Indeed, ARF-/- and ARF +/- mice develop a broader spectrum of tumors than p53-null animals (Kamijo et al., 1999). It has also been reported that mice lacking ARF, MDM2 and p53 (TKO) develop multiple tumors at a frequency greater than those observed in animals lacking both p53 and Mdm2 (DKO). Moreover, reintroduction of $p19^{ARF}$ into p53 null or TKO MEF can induce a G1 arrest (Carnero et al., 2000; Weber et al., 2000). It has also been described that $p14^{ARF}$ is able to stop the cells in S phase and/or trigger apoptosis in p53-deficient human tumor cell lines (Yarbrough et al., 2002; Hemmati et al., 2002). In particular, in human lung tumor, $p14^{ARF}$ induces G2 arrest followed by apoptosis both *in vitro* and *in vivo* (Eymin et al., 2003 and 2006).

All these data support the idea that ARF can play an independent role from MDM2-p53 axis in tumor surveillance.

In line with this, the discovery of multiple ARF interactors and the observation that, aside oncogenic stimuli, also viral, genotoxic, hypoxic and oxidative stresses activate an ARF-dependent response, suggest that this protein could exert a wider role to protect the cell (Eymin et al., 2006; Fatyol and Szalay, 2001; Garcia et al., 2006; Menendez et al., 2003).

It has been hypothesized that ARF could play a role in ribosome biogenesis because it is mainly localized in the nucleolus, the most prominent substructure within the nucleus, site of rRNA transcription, processing and of ribosome assembly. Sugimoto and colleagues (2003) demonstrated for the first time that $p19^{ARF}$ inhibits production of ribosomal RNA, retarding processing of 47/45S and 32S precursors. In line with this, Itahana and colleagues (2003) showed that in the nucleolus ARF is associated in high-molecular mass complexes with NPM (also known as B23), an abundant nucleolar phosphoprotein that is involved in different cellular processes such as ribosome biogenesis. The same authors demonstrated that ARF is able to regulate ribosome biogenesis inhibiting the endoribonuclease activity of NPM, promoting its poli-ubiquitylation and degradation through 26S proteasomal pathway. In spite of this, Brady and colleagues (2004) proposed that ARF sequesters NPM in the nucleolus and interferes with NPM shuttling. In this way, ARF impedes the ribosome export from nucleus to cytoplasm and induces growth arrest in a p53 independent manner.

Additionally, chromatin immunoprecipitation experiments identified $p14^{ARF}$ at the promoter of rDNA loci, suggesting a possible role in the regulation of rRNA transcription (Ayrault et al., 2004). In line with this hypothesis, it has been demonstrated that ARF negatively regulates the activity of UBF-1 and TTF-1, two important transcription factors involved in rRNA transcription (Ayrault et al., 2006; Lessard et al., 2010).

Taken together these data indicate that, through the interaction with different molecular partners, ARF regulates all three phases of ribosome biogenesis (transcription, processing and export) and, in this way, it can coordinate cell growth (increase of cell size) with proliferation (increase of cell number).

It has been reported that ARF can also contribute to the DNA damage response, one of the main process involved in cancer development. Indeed, after cell exposure to DNA genotoxic agents (such as UV irradiation), PARP-1 activates ARF transcription at the sites of unrepaired SBs (DNA single strand breaks) (Orlando et al., 2014). In response to these signals, ARF can induce cell cycle arrest and/or apoptosis through p53 dependent and independent pathways. In particular, it has been reported that ARF can trigger the activation of ATM/ATR signaling pathway inducing the stabilization of Tip60 protein, a histone acetyltransferase that activates ATM through acetylation (Sun et al., 2005). In this way, ARF can induce p53-independent G2 cell cycle arrest (Eymin et al., 2006) or TNFα-dependent apoptosis (Rocha et al., 2003 and 2005). Other studies demonstrated that ARF can also regulate the nucleotide excision repair (NER) mechanism, stimulating XPC expression (Dominguez-Brauer et al., 2009) and control chromosomal stability regardless of p53 (Di Tommaso et al., 2009).

Another p53-independent tumor suppressor function of ARF is its ability to regulate tumor angiogenesis, an important process that promotes cancer proliferation and metastatic spread providing an adequate supply of oxygen and nutrients and the removal of waste products to cancer cells. For the first time, Fatyol and Szalay (2001) reported that $p14^{ARF}$ can directly inhibit the transcriptional activity of hypoxia-inducible factor 1α (HIF-1α) by sequestering its α subunit into the nucleolus. HIF-1α is a critical transcription factor that regulates the expression of the vascular endothelial growth factor A (VEGFA), which is a key mediator of angiogenesis (Ferrara and Davis Smyth, 1997) and also acts as a potent tumor angiogenic factor (Carmeliet, 2005). Later, Kawagishi and colleagues (2010) demonstrated that $p19^{ARF}$ suppresses the translation of VEGFA mRNA in absence of p53 and inhibits VEGFA-dependent tumor angiogenesis in nude mice. Additionally, they reported that $p14^{ARF}$ expression and micro-vessel density are inversely correlated in human colon carcinomas (Kawagishi et al., 2010).

ARF- induced sumoylation

Equally remarkable is the fact that the enforced expression of ARF promotes the p53-independent sumoylation of several binding partners. The sumoylation is a

reversible post-translational modification that provides the covalent binding of small ubiquitin-like modifier (SUMO) to lysyl ε-amino groups located in the specific consensus sequence ΨKXE (Ψ = hydrophobic amino acid) of target proteins. It occurs through three enzyme cascade: an E1 activing enzyme, an E2 conjugating enzyme and an E3 ligase in analogous way used for ubiquitylation (Sheer, 2006). This process can have different functions, including alteration of protein trafficking, interference with ubiquitination and protein turnover, changes in DNA repair and sister chromatid cohesion, and regulation of gene expression (Tago et al, 2005; Sheer, 2006). It has been reported that ARF can facilitate the transfer of SUMO from the E2 complex to its binding proteins through a direct interaction with the SUMO-conjugating enzyme (E2) Ubc9 (Rizos et al., 2005), and it can also inhibit the function of a desumoylating protein, SENP3 (Haindl et al., 2008).

Both human $p14^{ARF}$ and mouse $p19^{ARF}$ promote the sumoylation of MDM2 and NPM (Xirodimas et al., 2002; Tago et al, 2005). Tago and colleagues (2005) reported that the ARF sequence, that is required for the binding to MDM2 and NPM, is also necessary to induce their sumoylation.

Although the functional significance of ARF-induced sumoylation is largely unknown, it has been reported that $p14^{ARF}$ induces the sumoylation of Werner syndrome helicase (WRN) causing its redistribution from the nucleolus to the nucleoplasm (Woods et al., 2004). Later, Liu and colleagues (2007) demonstrated that ARF-induced sumoylation of NPM regulates its subcellular localization, cell proliferation, and survival activities. It has also been described that *in vivo*, $p14^{ARF}$ promotes EGR1 transcription factor sumoylation through ARF/Ubc9/SUMO system leading to the activation of the PTEN tumor suppressor gene (Yu et al., 2009).

Moreover, ARF interacts with p63 (Calabrò et al., 2004), a member of p53 family of transcription factors involved in the development of skin and limb, to induce its sumoylation and proteasome mediated degradation (Vivo et al., 2009).

Recently, it has been reported that ARF can bind REG-γ, an ubiquitin-independent activator of the proteasome, to promote its sumoylation as well as its translocation in the cytoplasm, where in turn it induces proteasome degradation of $p16^{INK4a}$ as well as itself. Thus, these findings have uncovered a novel crosstalk of two key tumor

suppressors, ARF and $p16^{INK4a}$, through ARF-induced sumoylation of REG-γ (Kobayashi et al., 2013).

ARF role in the cytoplasm

Since its initial discovery, ARF was described with a prevalent nucleo/nucleolar localization, playing an important role in its stability and tumor suppressor functions. Nevertheless, different groups reported that ARF can also localize in the cytoplasm.

Careful sequence analysis showed that $p14^{ARF}$ and $p19^{ARF}$ transcripts contain a single internal methionine residue (Met 48 and Met 45, respectively), which is absent in other species (rat, opossum, pig and chicken). The translation from this methionine residue produces a short isoform of ARF protein called smARF (*short mitochondrial ARF*), which lacks N-terminus end required for MDM2 binding, p53-dependent cell cycle arrest and inhibition of rRNA processing. smARF is a short-lived protein (half-life <1hrs) that is rapidly degraded by proteasome, indeed represents less than 5% of total protein. In response to viral and cellular oncogenes, smARF is upregulated and localizes to mitochondria, where it is stabilized by the interaction with the mitochondrial p32 protein (Reef et al., 2007). It induces the dissipation of mitochondrial membrane potential in a p53 and Bcl-2 family independent manner, without the release of cytochrome c to the cytoplasm, suggesting that there is no apoptotic cell death. Furthermore, the overexpression of smARF in 293T cells causes caspase-independent cell death characterized by the accumulation of autophagic vacuoles. Interestingly, the knockdown of ATG5 or Beclin1, two important members of autophagy pathway, attenuates cell death in smARF-expressing cells, suggesting that the autophagic machinery contributes to the caspase-independent cell death process (Reef et al., 2006).

Autophagy is an evolutionarily-conserved homeostatic process where cytosolic components are targeted for removal or turnover in membrane-bound compartments (autophagosomes) that fuse with the lysosome. This process targets damage or excess organelles, misfolded proteins and proteins too large to be delivered to the proteasome for degradation. It occurs constitutively at low levels to regulate the turnover of

cytoplasmic components and is greatly induced during periods of metabolic stress. In these conditions, lysosome-mediated digestion of proteins serves to release free amino acids that can be used to fuel ATP generation, thereby promoting cell survival (Balaburski et al., 2010). Nevertheless, it seems that autophagy can also result in cell death as described in the case of smARF.

Interestingly, the role of smARF in autophagy is still subject of great debate. Indeed, Abida and Gu (2008) engineered a version of ARF in which the internal methionine is mutated in alanine, and showed that this nucleolar form, like the wt protein and the N-terminal region alone, could still induce autophagy and caspase independent cell death in transfected cells. So, they suggest an important role of autophagy in tumor suppression via full-length ARF. In line with this, a recent paper published by Murphy's group reported that $p14^{ARF}$ and $p19^{ARF}$ can induce autophagy, while mouse smARF localizes to mitochondria to induce mitophagy, a specific type of autophagy that selectively removes damaged or excessive mitochondria. Moreover, the authors identified a highly conserved domain located at the 5' end of ARF exon 2 that is necessary for autophagy induction by both human and murine protein. Interestingly, mutations in exon 2, that affect the coding potential of ARF, but not of $p16^{INK4a}$, impair its ability to induce autophagy (Budina-Kolomets et al., 2013).

The molecular mechanism through which ARF can promote autophagy in the cells is not yet clear. Abida and Gu (2008) demonstrated that ARF can induce autophagy in a p53 dependent and independent manner, depending on the cellular context. It has been reported that p53 itself can be a positive or negative regulator of autophagy based on its cellular localization and type of stress. In response to genotoxic stress, in the nucleus, p53 transcriptionally activates different genes with direct roles in autophagy, such as DRAM, or that encode inhibitors of mTOR activity. Instead, in unstressed cells cytosolic p53 inhibits autophagy (Balaburski et al., 2010).

It has also been reported that at the mitochondria ARF physically interacts with the Bcl2 family member BCL-xL, that plays an important role in autophagy. BCL-xL interacts with Beclin-1 and negatively regulates the kinase activity of the Vps34/Beclin-1 complex, which is a key mediator of autophagy (Maiuri et al.,2007; Pattingre et al.,2005). Notably, ARF blocks the BCL-xL/Beclin-1 complex, releasing Beclin-1 to induce autophagy.

The role of ARF in the cytoplasm is further complicated as ARF full length protein can localize to the mitochondria not only to induce autophagy but also to induce apoptotic cell death. Indeed, Itahana and Zhang (2008) demonstrated that in the mitochondria, ARF interacts with p32 through the exon 2-encoded C-terminus causing a decrease in $\Delta\psi_m$ leading to release of cytochrome c and apoptotic cell death.

A recent paper published by Per Guldberg group demonstrated that endogenous ARF is constitutively expressed as a cytoplasmic protein in melanocytes. Interestingly, ARF is recruited to dysfunctional mitochondria to induce the dissipation of membrane potential and maintain low steady-state levels of intracellular superoxide, suggesting a new ARF role in oxidative stress regulation. This mechanism could be activated by pharmacological inhibition of oxidative phosphorylation in normal melanocytes, as well as in senescent melanocytes and in melanoma cells undergoing a metabolic shift in response to inhibition of glycolysis. This mitochondrial activity of ARF is independent of its known autophagic and p53-dependent functions and involves the evolutionarily conserved acidic motif GHDDGQ (residues 65-70 in $p14^{ARF}$), which mediates interaction with BCL-xL, that is also an important regulator of mitochondrial redox homeostasis. Interestingly, among 23 germline INK4a-ARF mutations found in human melanoma, six of these affect this acidic motif. In conclusion, the authors identified a new cell-protective mechanism of ARF in melanocytes that is targeted in familial melanoma (Christensen et al., 2014).

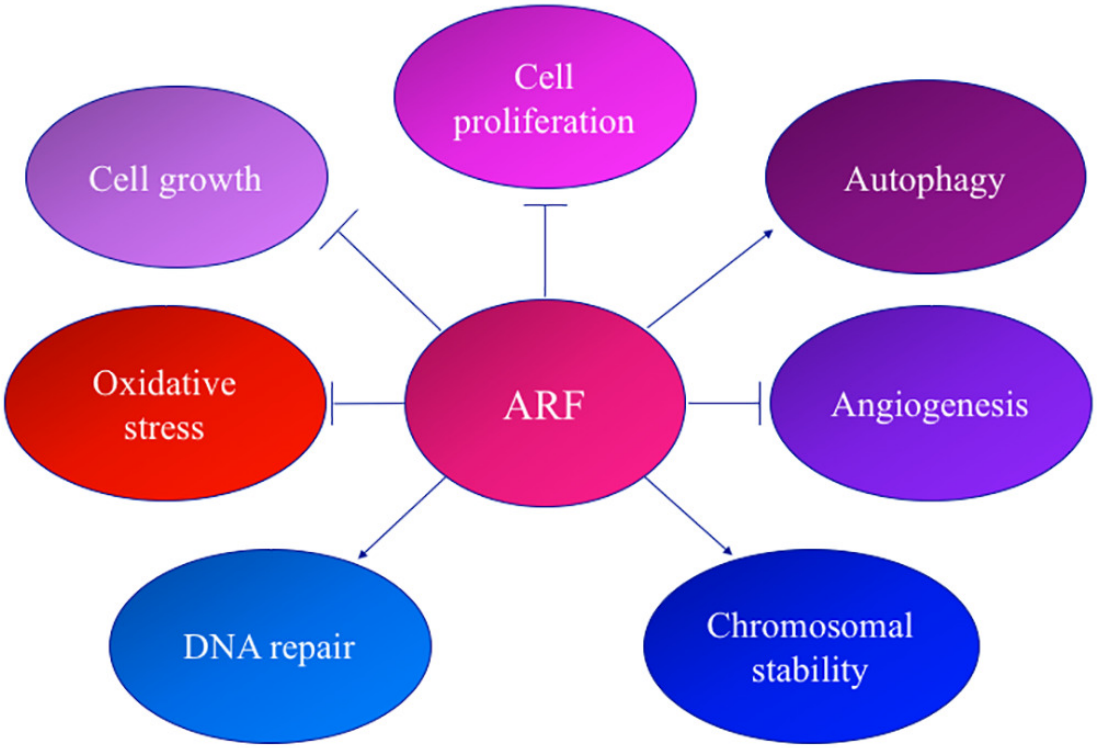

Figure 2: Schematic representation of p53 dependent and independent tumor suppressor functions of ARF

1.3 ARF physiological functions

ARF is not detectably expressed in most normal tissues during mouse fetal development or in young adult mice.

Interestingly, it has been reported that ARF is expressed transiently in at least 3 normal cell types: mural components of the hyaloid vasculature system (HVS) within the vitreous of the developing eye (McKeller et al., 2002), male spermatogonia (Zindy et al., 2003; Gromley et al., 2009), and fetal yolk sac (Li et al., 2013).

The first evidence of ARF involvement in eye development has been obtained from the observation that ARF-/- mice have slightly smaller eyes compared to wild type mice (Kamijo et al., 1999; Saporita et al., 2007; McKeller et al., 2002). Histological studies revealed the presence of a funnel-shaped retrolental mass of cells present in the vitreous of ARF-/- eyes on postnatal day 1 (P1) through P10. Normally, the retrolental vitreous in the newborn mouse eye contains elements of the hyaloid vascular system (HVS), that is composed of endothelial cells, several types of perivascular cells and regresses during the first 2 weeks of postnatal development (P6-P10). Interestingly, the presence of HVS elements in ARF-/- mice eyes suggests that ARF is involved in the physiological regression of HVS, a process that is required to ensure normal vision. Indeed, in wild type mice, ARF is expressed transiently in cells within the vitreous at P5 before the HVS regression. Importantly, these characteristics are not observed in p53−/− mice, indicating that this new ARF function is independent of p53 (McKeller et al., 2002).

ARF is also expressed transiently during mouse male germ cell development. Spermatogenesis is a spatio-temporally coordinated process by which undifferentiated spermatogonia evolve into spermatocytes in the lumen through a series of mitotic and meiotic cellular divisions (Kotsinas et al., 2014). In mice, it occurs during the first month after birth and $p19^{ARF}$ is selectively expressed in mitotic spermatogonia, but not in intratubular spermatocytes, suggesting that it may regulate the switch from mitotic to meiotic division. Interestingly, detachment of ARF-null progenitors from the tubular lining triggers DNA damage and p53-dependent apoptosis (anoikis) of primary spermatocytes, resulting in a reduced number of mature sperm and testicular atrophy.

These data surprisingly indicate that, in primary spermatocytes, ARF prevents p53 from inducing apoptosis (Gromley et al., 2009).

Li and colleagues (2013) reported that ARF is physiologically expressed in the fetal yolk sac, a tissue derived from the extraembryonic endoderm (ExEn), and marks late stages of ExEn differentiation in cultured embryoid bodies (EBs). ARF inactivation delays differentiation of the ExEn lineage within EBs. Interestingly, during ExEn formation, $p19^{ARF}$ induces the expression of microRNA-205 (miR-205), that regulates a suite of genes that govern cell migration and adhesion. The re-expression of this miRNA is able to rescue ExEn formation in ARF-null embryonic or induced pluripotent stem cells.
Interestingly, a paper published this year from Sherr group demonstrated that the re-expression of smARF in ARF null mice is able to correct the developmental phenotypes of these mice, such as the block of HVS regression in the eyes and the reduction of sperm production, suggesting that these two p53-independent phenotypic defects depend on smARF alone (Van Oosterwijk et al., 2017).

Vivo and colleagues (2009) demonstrated that the induction of the differentiation program in human primary keratinocyte and in HaCaT cells (immortalized keratinocytes) causes an increase of ARF levels leading to ΔNp63α sumoylation and proteasomal degradation. ΔNp63α, a specific isoform of the transcription factor p63, is strongly downregulated during keratinocyte differentiation.
On the other hand, mice lacking p63 cannot form skin, exhibit craniofacial and skeletal defects, and die soon after birth. Interestingly, Su and colleagues (2009) reported that inactivation of p63 in mice is accompanied by aberrantly increased expression of the INK4a and ARF tumour suppressor genes. In turn, the anomalies of p63-null mice affecting the skin and skeleton are partially rescued in mice lacking either INK4a or ARF. In conclusion, the authors demonstrated that p63 negatively regulates the expression of both INK4a and ARF and that abnormal upregulation of these genes in the absence of p63 inhibits skin development.

All together, these data suggest that ARF protein plays an important role in physiological processes like angiogenesis, cell migration and differentiation.

1.4 ARF turnover

$p14^{ARF}$ (132 aa, 14 kDa) and $p19^{ARF}$ (169 aa, 19 kDa) are highly basic (>20% arginine) and hydrophobic proteins. The basic nature of ARF renders it a highly insoluble protein and is likely the reason for its lack of structure. Indeed, neither NMR nor crystal structure have been determined despite its small size. ARF probably needs to form complexes with other molecules to assume specific spatial conformation and to neutralize its charge at physiological pH. This would explain the incredible number of ARF binding partners, which make it difficult to formulate a single model that expresses the role of this protein in cellular physiology (Sherr, 2006).

ARF study is further complicated by the fact that human and mouse protein share only 50% of homology. Interestingly, the exon 1β-encoded N-terminal region, that is necessary and sufficient for the known ARF tumor suppressor functions, is only modestly conserved between species, whereas the exon 2-encoded C-terminal region shows a strong degree of identity between human and mouse (57% of identity) (Stott et al., 1998).

The mechanisms that regulate ARF protein turnover represent another dark side in the study of this protein.

In eukaryotic cells, the pathways that degrade most cellular proteins are: the ubiquitin–proteasome system (UPS), which usually degrades the majority of proteins, and autophagy, primarily responsible for the degradation of most long-lived or aggregated proteins and cellular organelles (Lilienbaum, 2013).

The initial event in UPS degradation is the conjugation of ubiquitin to internal lysines of protein target through three enzyme cascade (E1-E2-E3) in analogous way used for sumoylation. Then, ubiquitinated proteins bind to the 19S particles, whose function is to open the 20S catalytic barrel-shaped proteasome core and allow protein entry and degradation (Hershko and Ciechanover, 1998; Pollice et al., 2008).

Early studies excluded the possibility that ARF turnover is regulated by UPS because human protein is lysine-less and the murine one has a single lysine residue not required

for proteasome degradation. Nevertheless, the first evidence of a link between ARF and the proteasome is the observation that in primary cells, where the half-life of this protein is extremely short, both human and mouse ARF accumulate following treatment with proteasome inhibitor MG132, without effect on the transcriptional level (Pollice et al., 2004; Kuo et al., 2004; Rodway et al., 2004). Unlike to primary cells, ARF protein is very stable in cancer cells, where the proteasome degradation is strongly compromised (Chen et al., 2010).

It has been reported that, although it lacks lysine, ARF can undergo to N-terminal polyubiquitination (Kuo et al., 2004). Indeed, through biochemical purification, it has been identified a specific ubiquitin ligase for ARF named ULF. ULF interacts with ARF both *in vitro* and *in vivo* and promotes the lysine-independent ubiquitylation and degradation of ARF. In human primary cells, ULF knockdown causes a strong stabilization of ARF, triggering ARF-dependent p53-mediated growth arrest. Moreover, NPM and c-Myc abrogate ULF mediated ARF ubiquitylation through distinct mechanisms, promoting ARF stabilization in cancer cells (Chen et al., 2010). NPM is not only a binding partner through which ARF regulates the ribosome biogenesis, but also plays an important role in the control of ARF turnover. Indeed, in response to increased levels of NPM, the turnover of $p19^{ARF}$ is retarded, whereas NPM short hairpin RNAs accelerates its degradation (Kuo et al., 2004). In agreement, when NPM is inactivated, $p19^{ARF}$ is excluded from nucleoli and destabilized, suggesting that the binding to NPM and nucleolar localization seems to be two important events to promote ARF stabilization (Columbo et al., 2005). In contrast to ARF, ULF is predominantly located in the nucleoplasm, suggesting that NPM overexpression in cancer cells induces ARF stabilization by keeping it away from its nucleoplasmic ubiquitin ligase. Indeed, ULF-dependent polyubiquitylation of ARF is severely inhibited by NPM overexpression.

c-Myc, instead, binds ULF both *in vivo* and *in vitro* and stabilizes ARF, inhibiting the ULF-ARF interaction, through a transcription-independent mechanism (Chen et al., 2010).

Interestingly, it has been demonstrated that ARF can be degraded by 20S/REG-γ proteasome in a ubiquitin-independent manner (Pollice et al., 2007; Chen et al., 2007). REG-γ belongs to the REG or 11S family of proteasome activator, that has been shown

to bind and activate 20S proteasomes (Ma et al., 1992; Dubiel et al., 1992). It resides in the nucleus of the cells in interphase and is used for the degradation of small, unstructured proteins like p19 and $p14^{ARF}$, p21, $p16^{INK4a}$, that have no structural motifs when not associated with specific binding partners (such as cyclins and CDKs, for p21 and p16, and NPM in the case of ARF) (Chen et al., 2007; Li et al., 2006).

Pollice and colleagues (2004) demonstrated that one of the ATPases, component of the 19S proteasome, TBP-1/PSMC3, interacts with $p14^{ARF}$ but, unexpectedly, instead of bringing it to degradation, it induces ARF stabilization. Indeed, overexpression of TBP-1 in various cell lines results in a strong increase of both transfected and endogenous ARF protein levels followed by the activation of p53 pathway.

Later, the same group demonstrated that TBP-1 blocks, *in vitro*, the degradation of ARF by the 20S proteasome, in absence of an assembled 19S regulative cap. The first N-terminal 39 amino acids in $p14^{ARF}$ are necessary for both interaction with and stabilization by TBP-1. They hypothesized that, upon binding, TBP-1 could cause a folding of ARF, rendering it a poor substrate for proteasome destruction (Pollice et al., 2007).

Altogether these data indicate that among the plethora of ARF interacting partners, only TBP-1 and NPM/B23 are involved in ARF stabilization using two different ways. Indeed, while NPM prevents ARF degradation retaining it into the nucleolus in an inactive form (Chen et al., 2010), TBP-1 is clearly excluded from the nucleolus and binds to ARF mainly in the nuclear compartment. This interaction causes an accumulation of ARF that results in the activation of the p53/MDM2 pathway (Pollice et al., 2008).

Recently, it has been reported that also MDM2, another classical ARF biding partner, is able to regulate ARF protein stability. Specifically, Vivo and colleagues (2015) showed that MDM2 overexpression causes both endogenous and transfected $p14^{ARF}$ degradation through the proteasome in different cancer cell lines. This event does not require the ubiquitin ligase activity of MDM2 and preferentially occurs in the cytoplasm. Indeed, immunofluorescence experiments clearly show that MG132 treatment causes an increase of ARF levels in the cytoplasm, strongly suggesting that

the reason why ARF is not usually detectable in this subcellular compartment resides in a more rapid turnover.

Furthermore, it has also been reported that the Protein Kinase C (PKC) is involved in the regulation of ARF stability. PKC represents a family of serine/threonine kinase, located typically under the plasma membrane and involved in the regulation of a wide variety of cellular processes such as proliferation, differentiation, apoptosis and cell survival (Nishizuka, 1995). For this reason, a strong activation of PKC has been observed in different types of tumors, but also in dermatological, autoimmune and neurodegenerative diseases and in many other important human diseases (Mochly-Rosen et al., 2012).

For the first time, Inoue and Shiraishi (2005) reported that the phorbol ester TPA, a known activator of PKC, increases the stability of transfected $p14^{ARF}$ protein in a p53-independent manner. In addition, the knockdown of PKCα, but not PKCδ, attenuates TPA-mediated $p14^{ARF}$ stabilization.

Vivo and colleagues (2013) demonstrated that in H1299 (human lung tumor cells, ARF+/+) and in HaCaT (immortalized keratinocytes) cell lines, endogenous $p14^{ARF}$ is a PKC target. Indeed, upon the treatment of HaCaT cells with two major activators of PKC, TPA and Ca^{2+}, $p14^{ARF}$ levels are strongly increased; conversely, the treatment with Bisindolylmaleimide-I, a known inhibitor of the catalytic activity of this kinase, causes drastically decrease of $p14^{ARF}$ protein levels. *In vitro* phosphorylation assay confirmed that ARF can be phosphorylated by PKC, while co-immunoprecipitation assay identified the physical interaction between active PKC and ARF in H1299 cells. Moreover, nucleo-cytoplasmic fractionation assay in H1299 cells showed that ARF is located in both cell compartments, but after TPA treatment, $p14^{ARF}$ protein levels increase only in the cytoplasmic portion. Subsequently, treating the H1299 and HaCaT cytoplasmic protein extracts with λ phosphatase, it has been confirmed that the cytoplasmic portion of $p14^{ARF}$ is actually phosphorylated.

A careful protein sequence analysis of ARF revealed the presence of three potential PKC phosphorylation sites: the Threonine 8 and Serine 52 in the functional active domain of the protein, and the Serine 127 in the C-terminal region of the protein.

Interestingly, the Threonine 8 is located in a conserved domain (aa. 2-14) among all ARF orthologs (Fig. 3).

To functionally characterize the role of Threonine 8, the authors constructed two single mutants: the T8A mutant, where Thr 8 is replaced by an Alanine residue, that cannot be phosphorylated; and the T8D mutant, where Thr 8 is replaced with an Aspartic Acid residue, that mimics the phosphorylation status of the protein.

Although the T8A mutant has a very short half-life (about 2h), it retains both the nuclear/nucleolar localization and the ability to block cell proliferation with the same efficiency of wt protein. Surprisingly, the T8D mutant has a stability comparable to wt form (half-life about 6h), but it is located not only in the nucleus but also in the cytoplasm. Although T8D is able to bind MDM2 and stabilize p53, the ability to block cell proliferation is severely compromised. These data seem to suggest that the partial loss of the tumor suppressor function in mutant T8D could be ascribed to an alteration of a p53-independent ARF function.

In conclusion, these data indicate that following the PKC activation in tumor cells (H1299) and immortalized keratinocytes (HaCaT), $p14^{ARF}$ is phosphorylated and predominantly accumulates in the cytoplasm, where it is not able to efficiently control cell proliferation.

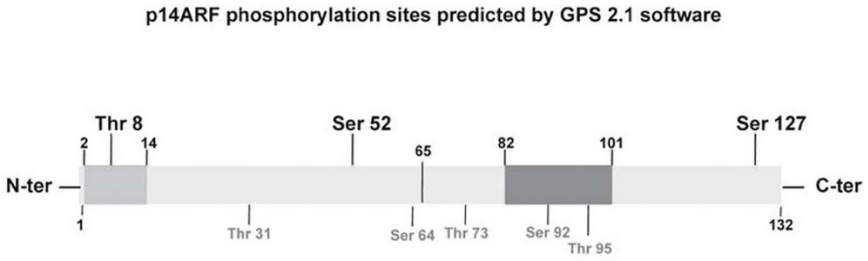

Figure 3: Schematic representation of p14^{ARF} phosphorylation sites identified in silico analysis.

In light grey is indicated the conserved region aa. 2-14, that represents the first NoLS signal (nucleolar localization signal), located in the N-terminal domain encoded by exon 1β (aa. 1-64), while in dark grey is represented the second NoLS signal (aa. 82-101) located in the exon 2. PKC phosphorylation sites are shown in bold above the scheme, while target sites of other kinases are represented in grey below the scheme (Vivo et al., 2013).

1.5 A new pro-proliferative function of the tumor suppressor ARF

Despite its multiple growth suppression functions, ARF is inexplicably overexpressed in a significant fraction of human tumors, such as Burkitt's lymphoma (Basso et al., 2005; Eischen et al., 1999), as well as the majority of tumors with mutant p53 (Kamijo et al., 1998). It has also been reported that $p14^{ARF}$ is over-expressed in 74 samples of aggressive B-cell lymphomas, where it mainly localizes in the nucleoplasm, and is associated with progression and unfavourable prognosis observed in this group of lymphomas (Sànchez-Aguilera et al., 2002).

Lee and colleagues (2003) reported that $p14^{ARF}$ mRNA is increased in patients with hematological malignancies, especially in the early stage of CML (chronic myelogenous leukemia), suggesting that this overexpression could be associated with CML development and loss of this gene could play a role in disease progression. Furthermore, inactivation of INK4a-ARF locus is rare in follicular adenomas and carcinomas, where $p14^{ARF}$ protein levels are strongly increased and, remarkably, a delocalization to the cytoplasm has been observed in some aggressive papillary carcinomas (Ferru et al., 2006).

Although sequencing analysis in these cancers didn't show any mutation in the ARF gene, an ARF increase has been explained as accumulation of non-functional protein.

Surprisingly, Humbey and colleagues (2008) reported that in myc-driven lymphomas cells, containing high levels of ARF and mutant p53, ARF silencing impairs autophagy induced by nutrient deprivation and hypoxia, leads to decrease cells viability and impedes the ability of these cells to establish tumors *in vivo*. In this paper, the authors proposed for the first time that ARF can promote the progression of specific type of tumors maybe through its ability to induce autophagy, that can help established tumors to survive during periods of metabolic or hypoxic stress.

Further evidences that support this new pro-oncogenic activity of ARF result from different studies performed in prostate cancer models.

Pandolfi group reported that in mouse prostate, the concomitant inactivation of the genes encoding both Pten and p53 leads to a rapidly lethal prostate cancer phenotype. Surprisingly, they noted that in Pten-deficient mice, the loss of $p19^{ARF}$ expression in

prostate epithelium does not accelerate the prostate cancer phenotype as expected, but rather these mice ($p19^{ARF}$-/- Pten-/-) exhibit a decrease in pre-neoplastic lesions. They also found that in TMAs (tissue microarrays) from human prostate specimens, complete loss of $p14^{ARF}$ is extremely rare and increased levels of this protein are correlated with disease aggressiveness. In conclusion, they proposed that ARF could affect *in vivo* tumor growth in a tissue specific and p53-independent manners, possibly due to interactions with different targets in different cell types (Chen et al., 2009).

Later, Xie and colleagues (2014) demonstrated that $p19^{ARF}$ inactivation represses the EMT (epithelial-mesenchymal transition) phenotype of Pten/Trp53 double null mice through regulation of SLUG, a protein that promotes cell migration and cancer metastasis through the repression of E-cadherin and the regulation of EMT. Specifically, in the nucleus of PC3 cells, $p14^{ARF}$ induces SLUG sumoylation to increase the stability of this protein resulting in down-regulation of E-cadherin and of cell-cell junctions. In this way, ARF can promote cell proliferation and migration in prostate cancer.
In a recent paper, the same group demonstrated that ARF is able to induce EMT in prostate cancer also through the upregulation of MMP7, a member of the matrix metalloproteinases protein family, that induces ECM degradation to promote cell migration in a physiological context and invasion and metastasis in cancer (Xie et al., 2016).

Taken together, these data suggest that in addition to its well known tumor suppressor role, ARF can also perform a pro-proliferative function depending on cellular and genetic context and on the state of tumor aggressiveness.

CHAPTER 2

AIM OF THE STUDY

The majority of studies carried out on $p14^{ARF}$ protein are focused on its important role as suppressor of cell proliferation in response to oncogenic stimuli in mammalian cells. Through the interaction with different biding partners, this protein plays a pivotal role in cellular processes that are essential to safeguard cell integrity, such as apoptosis, cell cycle regulation, senescence, DNA repair and chromosomal stability.

Surprisingly, recent data from several laboratories demonstrated that ARF is overexpressed in a significant fraction of human tumors (Eischen et al., 1999; Sànchez-Aguilera et al., 2002, Basso et al., 2005; Ferru et al., 2006), and it can also perform a pro-proliferative function depending on cellular and genetic context and on the state of tumor aggressiveness (Humbey et al., 2008; Chen et al., 2010; Xie et al., 2014 and 2016).

When I joined the Prof. La Mantia lab, dott. M. Vivo had already demonstrated that, following activation of PKC, ARF protein is phosphorylated and accumulates in the cytoplasm, where it appears unable to efficiently control cell proliferation both in tumor and immortalized cell lines (Vivo et al., 2013). These findings can be explained proposing that ARF phosphorylation in these cell lines could be a way to escape ARF surveillance following oncogenic stress. Alternatively, these data raise the possibility that ARF expression in cancer cells could aid tumor progression by conferring unknown pro-survival properties to the cells. On the other hands, the cytoplasmic localization could highlight more physiologic roles for this versatile protein.

On the basis of these hypotheses, the aim of my studies was to better understand ARF functions in HeLa, HaCaT and H1299 cell lines, where ARF is highly expressed and mainly localizes in the cytoplasm.

Interestingly, we found that ARF plays an unexpected role in the organization of the cytoskeleton. Moreover, we demonstrated that, by aiding cytoskeleton assembly during spreading, ARF protects cells from anoikis blocking DAPK (Death Associated

Protein Kinase) dependent apoptosis and promoting cell survival through FAK stabilization (Vivo et al., 2017).

In addition, we sought to investigate if ARF role in cell spreading and its functional relation with FAK could be regulated by PKC dependent phosphorylation (Fontana et al., submitted paper).

CHAPTER 3

p14ARF INTERACTS WITH THE FOCAL ADHESION KINASE AND PROTECTS CELLS FROM ANOIKIS

Maria Vivo*, Rosa Fontana, Michela Ranieri, Giuseppina Capasso, Tiziana Angrisano Alessandra Pollice, Viola Calabrò, Girolama La Mantia*

Dipartimento di Biologia, Università degli Studi di Napoli "Federico II"

Published in August 2017 on Oncogene 36(34):4913-4928

doi: 10.1038/onc.2017.104.

* corresponding authors

lamantia@unina.it

maria.vivo@unina.it

Running Title: p14ARF tumor suppressor promotes cell spreading

OPEN

Oncogene (2017), 1–16

www.nature.com/onc

ORIGINAL ARTICLE

p14ARF interacts with the focal adhesion kinase and protects cells from anoikis

M Vivo, R Fontana, M Ranieri, G Capasso, T Angrisano, A Pollice, V Calabrò and G La Mantia

The ARF protein functions as an important sensor of hyper-proliferative stimuli restricting cell proliferation through both p53-dependent and -independent pathways. Although to date the majority of studies on ARF have focused on its anti-proliferative role, few studies have addressed whether ARF may also have pro-survival functions. Here we show for the first time that during the process of adhesion and spreading ARF re-localizes to sites of active actin polymerization and to focal adhesion points where it interacts with the phosphorylated focal adhesion kinase. In line with its recruitment to focal adhesions, we observe that hampering ARF function in cancer cells leads to gross defects in cytoskeleton organization resulting in apoptosis through a mechanism dependent on the Death-Associated Protein Kinase. Our data uncover a novel function for p14ARF in protecting cells from anoikis that may reflect its role in anchorage independence, a hallmark of malignant tumor cells.

Oncogene advance online publication, 24 April 2017; doi:10.1038/onc.2017.104

INTRODUCTION

The ARF protein functions as sensor of hyper-proliferative stimuli restricting cell proliferation through both p53-dependent and -independent pathways.[1] In line with its tumor-suppressive role, ARF-deficient mice develop lymphomas, sarcomas and adenocarcinomas.[2] In humans, the importance of ARF inactivation in cancer development is less clear and p16INK4a appears to have a more relevant role in tumor protection.[3] More than 30 distinct ARF-interacting proteins have been identified, suggesting that ARF is involved in a number of different cellular processes.[4]

Although ARF expression levels in normal proliferating cells are very low, studies based on its loss have revealed its importance in different physiological and developmental mechanisms.[5–8]

Since its initial discovery, ARF has been described to have a prevalent nucleo-nucleolar localization. More recently, ARF has been reported to localize also in the cytoplasm mainly associated to mitochondria, and also because of its role in autophagy.[9]

Despite its role in growth suppression, ARF is overexpressed in a significant fraction of human tumors.[10] Increased expression of p14ARF has been associated with progression and unfavorable prognosis in hematological malignancies and in aggressive B-cell lymphomas, and predicts a shortened lifespan.[11] Furthermore, recent findings suggest that ARF loss hampers, instead of promoting, progression of prostate tumor,[12] and in mouse lymphomas displaying mutant p53, ARF has been described as having a tumor-promoting activity correlated with its role in autophagy.[13] Interestingly, it has been reported that the p14ARF protein level increases in thyroid cancer-derived tissues and, remarkably, a delocalization to the cytoplasm has been observed in some aggressive papillary carcinomas.[14] Although in these cancers ARF has been found to be wild-type, an ARF increase has been explained as accumulation of non-functional protein.

Our previous data suggest that, following activation of protein kinase C, ARF protein is phosphorylated and accumulates in the cytoplasm where it appears unable to efficiently control cell proliferation.[15] These findings, together with the observations in the cited literature, raise the possibility that ARF expression in cancer cells could aid tumor progression by conferring unknown pro-survival properties to the cells.

Here, we present data showing that during cell adhesion and spreading, p14ARF is delocalized from nucleoli to sites of actin polymerization concentrating at focal contacts where it colocalizes with the focal adhesion kinase (FAK). Moreover, we show that ARF depletion leads to defects in cell spreading and actin cytoskeleton spatial organization in both tumor and immortalized cell lines. Finally, we demonstrate that p14ARF can confer resistance to death-associated protein kinase (DAPK)-dependent apoptosis.

RESULTS

ARF localizes to focal contacts during spreading

Cancer-derived HeLa cells express high levels of p14ARF, whereas immortalized HaCaT keratinocytes express low levels of this protein. Remarkably, in HaCaT cells ARF is mainly localized to the cytoplasm.[8] By immunofluorescence analysis in HeLa and HaCaT cells, we noticed that ARF accumulated at the edge of cells, in particular to lamellipodia and filopodia where rapid actin filament dynamics take place. We therefore examined ARF localization during the process of cellular adhesion and spreading. To synchronize and follow the adhesion process, HeLa cells were detached from the plate by trypsinization, plated onto coverslips and collected at different time points. We analyzed ARF localization by IF (immunofluorescence) while actin cytoskeleton was visualized by tetramethylrhodamine-conjugated phalloidin staining. Thirty minutes after plating, p14ARF was detected along the plasma membrane, (Figure 1; 30 min). During spreading, ARF protein localizes first to cytoplasmic blebs and later on to filopodia (Figures 1, 3 and 5 h after plating). This localization was observed with two different ARF antibodies, and on transfected p14ARF,

Dipartimento di Biologia, Università Degli Studi di Napoli 'Federico II', Napoli, Italy. Correspondence: Dr M Vivo or Professor G La Mantia, Dipartimento di Biologia, Università Degli Studi di Napoli Federico II Via Cinthia, Napoli 80126, Italy.
E-mail: maria.vivo@unina.it or lamantia@unina.it
Received 1 July 2016; revised 1 March 2017; accepted 6 March 2017

either tagged with GFP or not (Supplementary Figures S1a–c). Similar results were obtained on cells plated within a three-dimensional substrate such as Matrigel thus suggesting that this localization does not depend on the specific substrate used for adhesion (Supplementary Figure S2a). Immunofluorescence staining of the nucleolar protein B23 showed that nucleoli were not disassembled at any time after seeding (Supplementary Figure S2b).

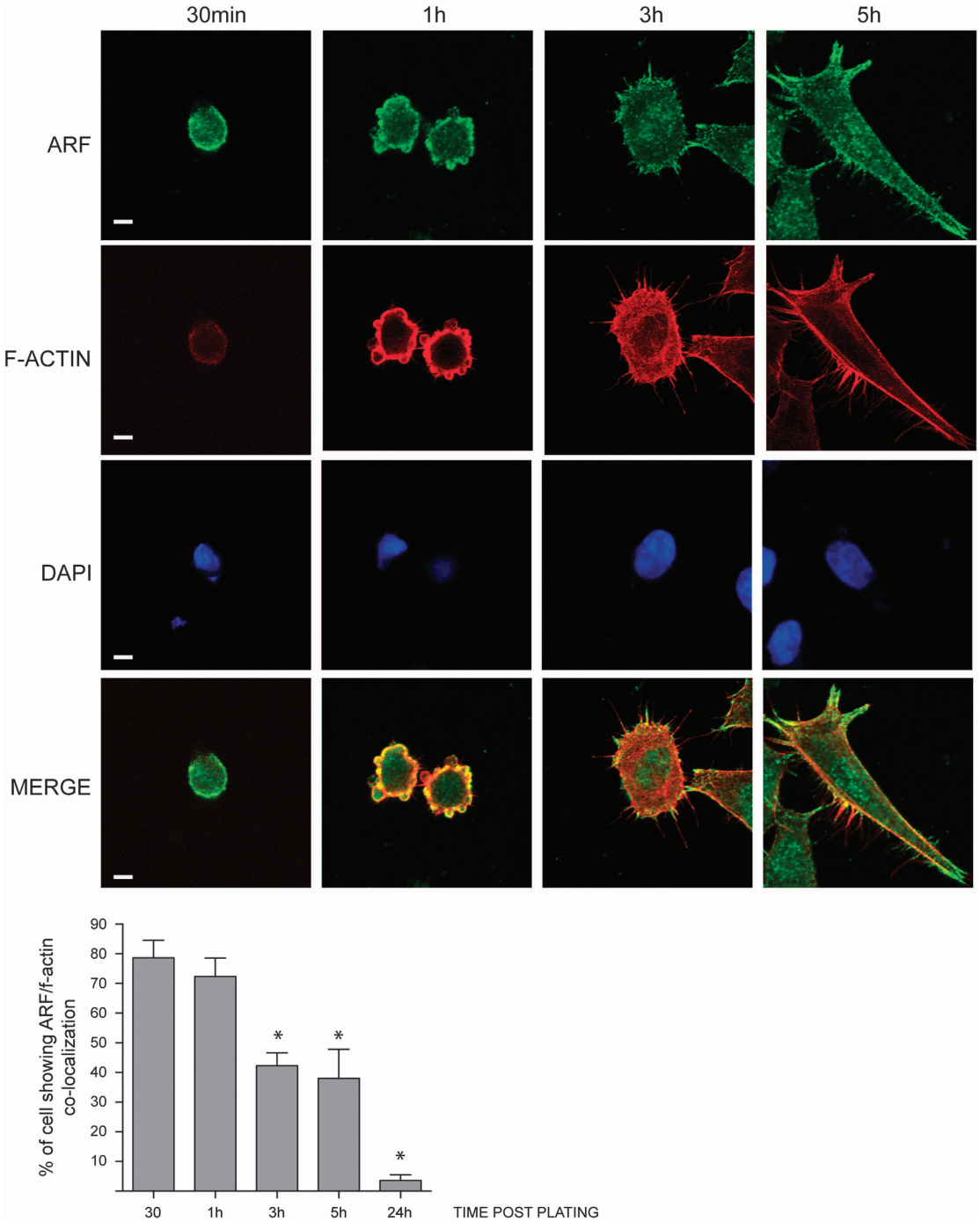

Figure 1. ARF localizes to the plasma membrane during adhesion/spreading process. HeLa cells were detached by gentle trypsin treatment, re-suspended in growth medium and allowed to adhere onto fibronectin-coated coverslip, and at various times following plating, rinsed in PBS (4 °C) and fixed with 3.75% PFA. Cells were fixed at different time points after plating (30′, 1 h, 3 h and 5 h), permeabilized and subjected to IF with anti-ARF antibody and both tetramethylrhodamine phalloidin and DAPI staining to visualize actin cytoskeleton and nuclei. Representative images of ARF subcellular localization are shown for each time point. Images were taken with a Zeiss confocal laser-scanning microscope LSM 510 (Oberkochen, Germany) (scale bar, 7μm). A 40× objective was used and image analysis was performed using ImageJ. Samples that were to be directly compared were imaged at the same sitting, and the same gain and exposure time were used. Histograms, representing the mean of three independent experiments, reports the percentage of cells in which ARF localize with f-actin. For each time point, 50 cells have been analyzed. S.d. are also shown. Asterisks (*) indicate statistically significant differences by unpaired two-tailed *t*-test with Welch correction: $*P < 0.001$ between each point and 1-h time point.

Cell interaction with the extracellular matrix results in integrin-mediated tyrosine phosphorylation and recruitment of FAK to focal adhesions.[16,17] We thus monitored ARF localization during spreading by following the localization of phosphorylated FAK and of its target, such as Paxillin phosphorylated on Tyrosine 118. Confocal analysis showed ARF/FAK and ARF/Paxillin colocalization at focal adhesions 5 h post-seeding (Figures 2a and b, IF and graph), while 24 h after seeding ARF was mainly localized to the

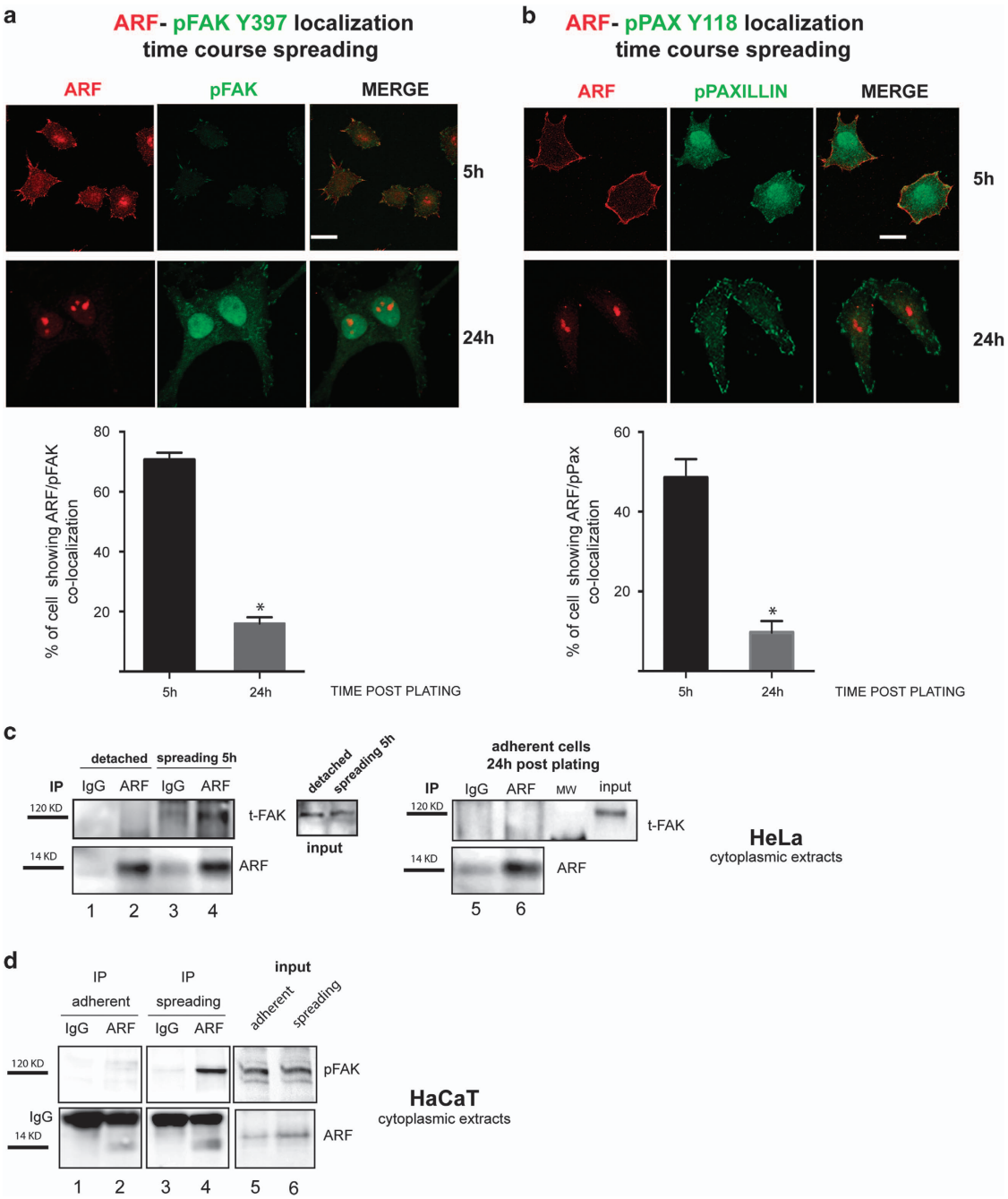

Figure 2. ARF interacts with active FAK during adhesion. ARF colocalizes with active FAK (phosphorylated FAK on Tyr397) and phosphorylated Paxillin during adhesion. HeLa cells were allowed to adhere onto fibronectin-coated coverslips for 5 and 24 h as described before, fixed and subjected to IF with anti-ARF and either pFAK Y397 antibody or pPaxillin Tyr118 antibody. Representative images showing ARF and pFAK (**a**) or ARF and pPaxillin (**b**). Subcellular localization are shown for each time point. Images were taken as described before (scale bar, 10 μm). Histograms below each panel, representing the mean of three independent experiments, reports the percentage of cells in which ARF colocalize with pFAK or pPAXillin Tyr118. S.d. are also shown. Asterisks indicate statistically significant differences ($P < 0.001$) as described in Figure 1. ARF and FAK co-immunoprecipitation. (**c**) Cytoplasmic HeLa extracts collected upon cell detachment (lanes 1–2), during spreading (lanes 3–4), and 24 h after adhesion (lanes 5–6) were subjected to immunoprecipitation with anti-ARF antibody or IgG as negative control and western blot with FAK and ARF antibodies. Inputs probed with anti-FAK antibody are shown. (**d**) Same experiment described in **c** performed on HaCaT cells except that IB was performed with anti-pFAK Y397. Molecular weights of both ARF and FAK are shown on the left of each western blot.

nucleoli. We next performed co-immunoprecipitation experiments of HeLa and HaCaT cytoplasmic extracts during cell spreading (Figures 2c and d) with anti-ARF antibody followed by immunoblot with FAK antibodies. We detected an interaction between p14ARF and FAK 5 h after plating (compare lane 4 with lane 2) that was lost or reduced 24 h after plating (Figure 2c). Incubation with anti-paxillin antibody did not show any interaction with ARF. Reverse co-immunoprecipitation with anti-FAK antibody shows interaction with both ARF and paxillin (Supplementary Figure S3). The experiments thus suggest the existence of a time window during spreading where a transient and specific ARF/FAK interaction takes place at points of focal contacts.

ARF depletion induces actin cytoskeleton defects and decrease of FAK levels

To analyze ARF role in cell spreading, we transiently transfected cells with three different small interfering RNAs (siRNAs; siARF-1, siARF-2 and siARF-3) targeting different regions of the unique exon 1β of the INK4a/ARF locus (Supplementary Figure S4a). As control, we found that p16INK4a levels were not significantly affected upon ARF silencing (Supplementary Figures S4a and b). Control and ARF-depleted cells were then detached and re-plated to follow the spreading process over time by phase-contrast microscopy. Five hours after seeding, control cells were almost completely spread, whereas ARF KD (Knock-Down) cells exhibited a clear round morphology (Figure 3a and Supplementary Figure S4c). The same effect was seen at 24 h after plating (Figure 3a). Quantification of spreading efficiency showed that less than 50% of ARF-depleted cells were able to properly spread (Figure 3b) As control, silencing of p16INK4a by RNA interference does not affect cell morphology (Supplementary Figure S4d). Staining with fluorescein isothiocyanate-conjugated phalloidin showed that ARF KD cells present blebs around the cell periphery and rare or shorter filopodia (Figure 3c). Similar results were obtained in both HeLa and HaCaT cells grown on Matrigel (Supplementary Figures S5a and b)

As it was previously shown that defects in FAK phosphorylation induces cells to acquire a round morphology,[18,19] we analyzed the levels of phospho-FAK in ARF-depleted cells by FAK immunoprecipitation and phospho-Tyr immunodetection in HeLa cells not subjected to re-plating (Figure 4a, left panels), and upon detachment and re-plating (Figure 4a, right panels). No significant change in FAK tyrosine phosphorylation occurred upon ARF KD before re-plating. Instead, we found a decrease of FAK tyrosine phosphorylation mirrored by total FAK levels reduction when ARF KD cells were induced to spread. Quantitative reverse transcriptase–PCR analysis showed no significant change in FAK mRNA levels upon ARF depletion, neither in the expression levels of genes involved in cell adhesion such as fibronectin, type IV collagen and integrin β1 (Figure 4b). In agreement with this, transfection of increasing amounts of ARF-expressing plasmid induces an increase in the protein levels of FAK in HeLa cells (Figure 4c). In addition to the 120 kDa FAK immunoreactive band, slow migrating species, previously demonstrated to correspond with SUMO-conjugated FAK forms,[20] appear to be stabilized upon ARF expression (Figure 4c, last lane). This is particularly evident in HaCaT cells, where ARF overexpression induces a strong increase of slow migrating FAK species (Figure 4d), and upon ARF and SUMO co-transfection (Figure 4e) thus suggesting that ARF could mediate FAK stabilization through sumoylation.[21]

ARF ectopic expression rescues both morphology and FAK phosphorylation defects of ARF-depleted cells

To test if the effects of ARF silencing observed in HeLa cells were strictly dependent on ARF, we performed a rescue experiment transfecting both human and mouse ARF protein. Upon transfection with either an empty or an ARF-expressing vector, cells were treated with scrambled or ARF-specific siRNA-1 for 48 h and then induced to spread. Both p14ARF and p19ARF expression rescued spread morphology defect caused by ARF silencing (Figure 5) thus suggesting the existence of an evolutionary conserved mechanism. In line with this, mouse protein also shows f-actin co-localization during spreading (Supplementary Figure S6a).

To map ARF region responsible of this function, we performed a rescue experiment by transfecting Hela cells with different ARF deletion mutants corresponding to either aa 1–64, encoded by the exon 1β, widely demonstrated to be necessary to elicit ARF cell cycle arrest,[22–24] or aa 65–132, encoded by the exon 2 (Figures 6a and b). Transfected cells were treated with luciferase or ARF-specific siRNA targeting the 5'-UTR region of endogenous transcript (siARF-3). As both ARF mutants migrate with approximately the same molecular weight of the endogenous protein, the silencing of endogenous gene was checked in cells transfected with the empty vector (data not shown). The evaluation of the spreading efficiency (Figure 6c) clearly indicated that the ARF region encoded by exon 2 was able to rescue the spreading defect induced by depletion of the endogenous protein. Regarding the exon 1β encoded domain, we noticed that its expression *per se* (1–64 siSCR) impairs spreading similarly to ARF depletion, and treatment with ARF siRNA (1–64 siARF) does not further affect cell spreading.

We next tested 65–132 mutant and p19ARF ability to rescue FAK phosphorylation by FAK immunoprecipitation followed by phospho-FAK immunodetection and observed that both proteins restore normal levels of active FAK (Figure 6d and Supplementary Figure S6b).

In order to map ARF domain required for ARF/FAK interaction during spreading, either wt or ARF 65–132 deletion mutant were transfected in HeLa cells and subjected to immunoprecipitation (Figures 7a and b) with anti-ARF antibody. The 65–132 mutant shows reduced pFAK binding (Figure 7b) thus suggesting that a FAK-binding domain is present in the 1–64 amino-acid region. We next analyzed binding efficiency of ARF 1–64 and of ARF 100–132 by immunoprecipitation with anti-GFP. Although ARF 100–132 is still able to bind pFAK, the reduced binding shown by ARF 1–64 could reflect its impairment to induce FAK stabilization. We thus probed the filter with antibody recognizing total FAK, thus demonstrating that ARF 1–64 is still able to bind the FAK although in a not phosphorylated form (Figure 7c).

We next analyzed the ability of these mutants to stabilize FAK, by transfecting them in HeLa cells and evaluating pFAK levels during spreading. We included in this analysis an ARF deletion mutant devoid of 100–132 domain. The experiment shows that only ARF 65–132 and ARF 100–132 are able to induce FAK stabilization with an efficiency similar to the wt (Figure 7d).

Finally, we tested different ARF point mutants derived from melanoma predisposing mutations[25] affecting single residues within an acidic motif (65–70 aa). We found that all of them are still able to induce pFAK stabilization, at efficiency similar or higher than the wt protein (Supplementary Figure S7). These experiments collectively show that ARF binding to FAK is mediated by at least two domains present in both the N-terminal and C-terminal protein region. Moreover, binding is not sufficient to induce FAK stabilization and this function is restricted to the 100–132 amino-acid region of p14ARF.

ARF depletion induces anoikis in HeLa and HaCaT cells

We next analyzed the relationship between cellular morphology and viability of ARF-depleted HeLa cells. Apoptosis analysis, by both western blot of PARP-1 cleavage and FACS-based Annexin V/7-aminoactinomycin D (7-AAD) assay, shows that ARF silencing induces 50% increase of the number of cells in apoptosis, as soon as cells were induced to spread (Figure 8a). As round cells could be easily separated from attached cells, we analyzed them separately. The experiment shows that round cells are

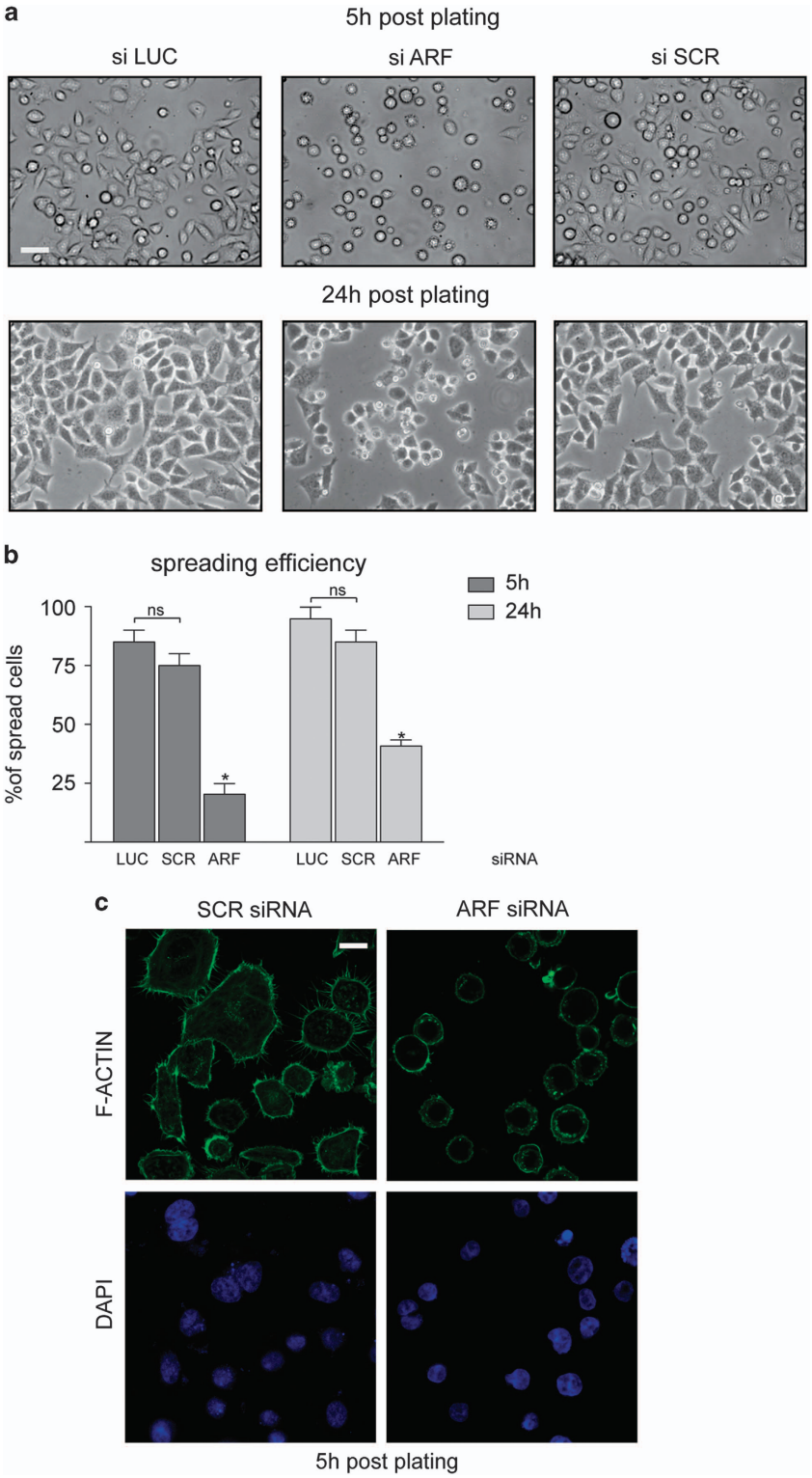

Figure 3. p14ARF depletion affects cell morphology. (**a**) Contrast images of HeLa cells transiently transfected with the indicated stealth siRNAs for 48 h, detached by trypsinization and re-plated at a density of 1×10^5/ml in six-well plates. Images were collected and analyzed by phase-contrast microscope 5 and 24 h after plating with a 20× objective (scale bar, 30 μm). (**b**) To quantify the percentage of each phenotype, for each transfection point, we counted adherent and round cells in five different fields and pooled data from three to five experiments. Spreading efficiency was measured by assaying the number of adherent cells relative on total cell number (graph). Cumulative data are expressed as a mean value ± s.e.m. of three independent experiments. Number of cells analyzed for each experiment: siSCR (200), siARF (200), siLUC (200). Asterisks (*) indicate statistically significant differences by unpaired two-tailed *t*-test between siARF and both siLUC and siSCR: $*P < 0.0002$, whereas NS indicates non statistical significant values. (**c**) Confocal images of HeLa cells treated with control or specific ARF siRNA for 48 h were left to adhere and doubly stained with fluorescein isothiocyanate (FITC)-conjugated phalloidin and DAPI (scale bar, 10 μm).

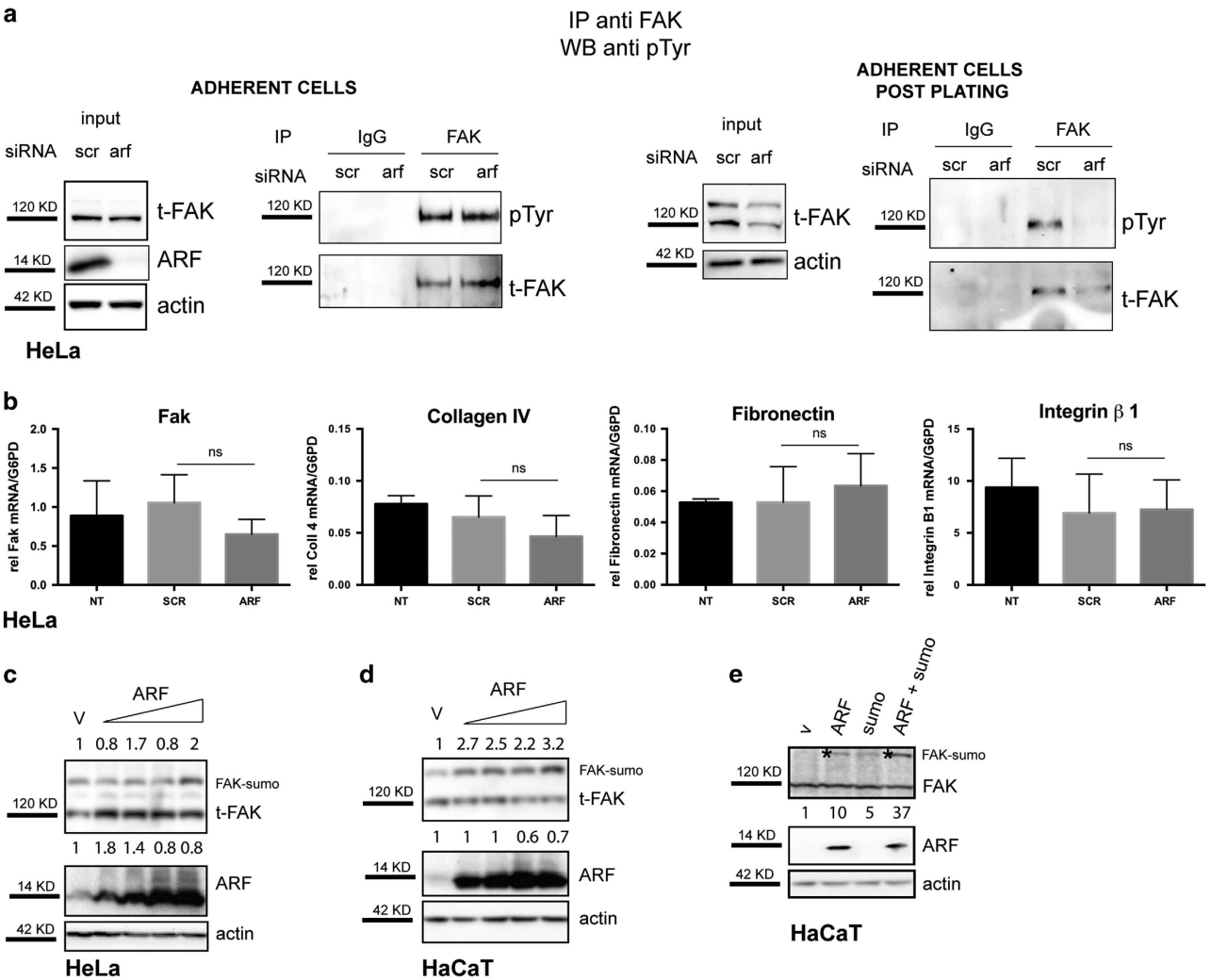

Figure 4. ARF depletion affects FAK activation. (**a**) HeLa total extracts of ARF and control-depleted cells (adherent cells) were immunoprecipitated with anti-total FAK antibody or with IgG as negative control and analyzed by western blot with anti-pTyr antibody and subsequently with anti-t-FAK antibody cells before (left panels) or after adhesion following detachment and re-plating (right panels). Panels of inputs probed with anti-FAK, ARF and actin antibodies are also shown on the left of each immunoprecipitation experiment. (**b**) Quantitative reverse transcriptase (qRT)–PCR analyses of FAK, collagen IV, fibronectin and integrin β1 mRNA levels normalized on G6PD expression in cells treated with the indicated siRNA are shown. Cumulative data are expressed as a mean value ± s.d. of three independent experiments. Statistical analysis performed by unpaired, two-tailed Mann–Whitney test show no statistical (NS) difference between siSCR and siARF samples. (**c**) HeLa and HaCaT cells were transfected with an empty vector (v) and increasing amount of p14ARF expression plasmid. Twenty-four hours after transfection, cells were lysed and cellular extracts were immunoblotted and analyzed with anti-FAK, anti-ARF antibody to detect exogenous ARF levels and anti-actin as loading control. (**d** and **e**) HaCaT cells were transfected with plasmids encoding ARF proteins alone or in combination with plasmid encoding SUMO protein. Cellular extracts were analyzed as described before in **b**. Asterisks indicate slow migrating FAK species. Western blots shown are representative of at least three independent experiments. Normalized FAK band intensities are shown below each corresponding band, whereas sumo FAK are indicated on top above, and are expressed as fold enrichment with respect to empty vector-transfected sample arbitrarily set to 1 (see Materials and Methods section for details).

7-aminoactinomycin D/Annexin V-positive and showed increased PARP-1 cleavage (Supplementary Figures S8c and d).

MTT (3-(4,5-dimethylthiazol-2-yl)-2,5-diphenyltetrazolium bromide) assay and crystal violet staining show that ARF silencing significantly reduced HeLa and HaCaT cell viability (Figures 8b and c).

To determine if apoptosis could be the cause of the so far described spreading defect, ARF knockdown cells were treated with the pan-caspase inhibitor Z-VAD-fmk. Quantification of spreading efficiency showed that apoptosis inhibition does not rescue the morphology defect of ARF silenced cells (Figure 8d). This could suggest that apoptosis could be induced in cells that cannot properly spread. To explore this hypothesis, we analyzed apoptosis in ARF-depleted HeLa cells grown in suspension as spheroids by changing the coating vessel surface. After 48 h of suspension culture, no PARP-1 cleavage was observed in control and ARF-depleted cells (Figure 9a) even if spheroids were disaggregated and cells re-placed under suspension culture conditions for additional 24 h (Figure 9b, left panel). Conversely, re-plating onto an adhesive substrate resulted in PARP-1 cleavage (right panel) thus indicating that cell-substrate contacts are required for apoptosis induction in cells devoid of ARF expression.

The DAPK, a pro-apoptotic serine/threonine kinase, is activated and induces apoptosis following cytoskeleton–matrix disengagement.[26,27] We thus investigated a possible involvement of DAPK in apoptosis induced by ARF silencing. Simultaneous abrogation of ARF and DAPK in HeLa and HaCaT cells by RNA interference rescues apoptosis induced by ARF depletion (Figure 9c; Supplementary Figure S9a) suggesting that ARF depletion induces anoikis through a DAPK-

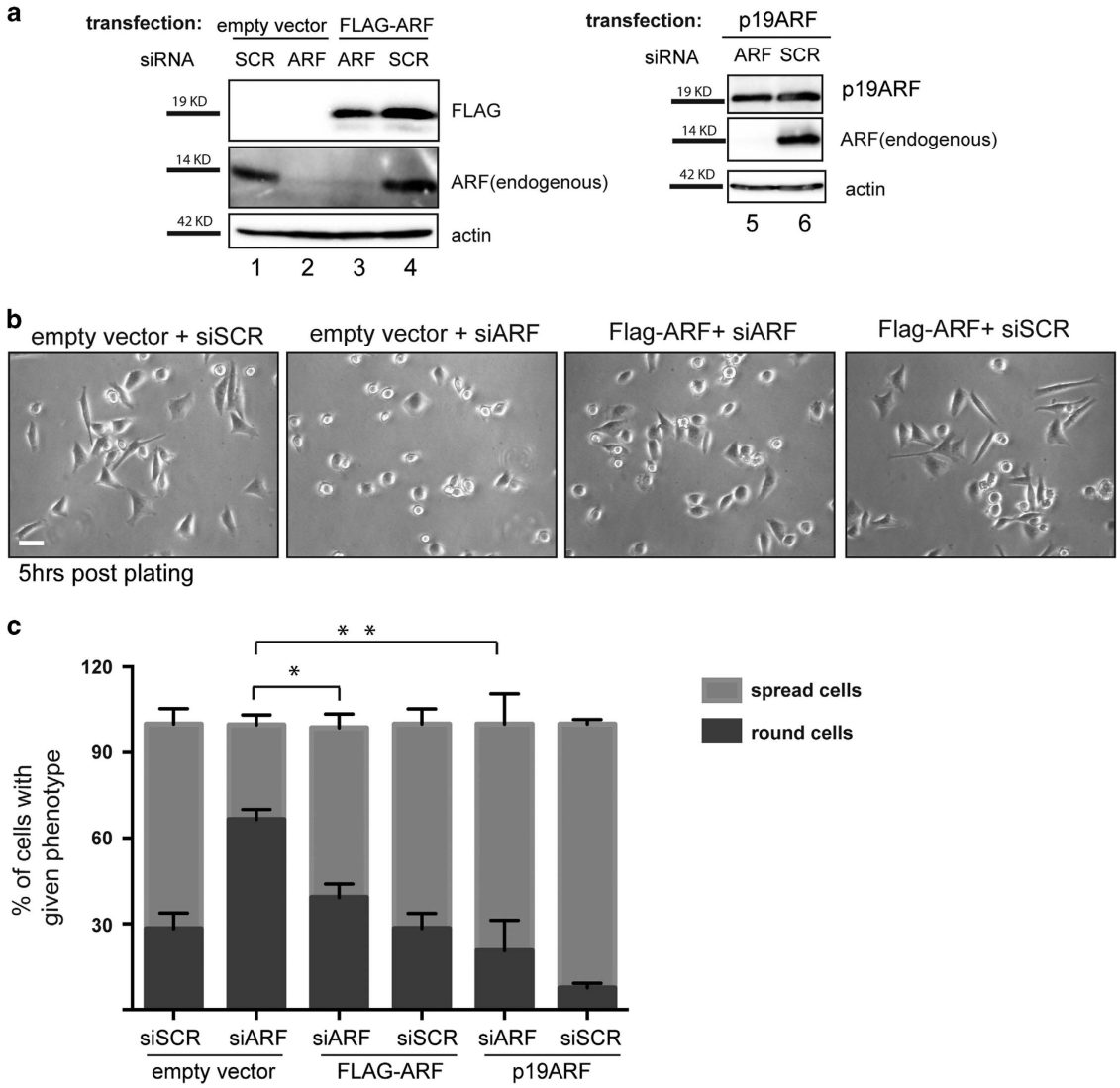

Figure 5. Both human and mouse ARF transfections rescue cell spreading defect of p14ARF-depleted cells. HeLa cells transiently transfected with empty, flag-ARF or p19ARF vector for 24 h were treated with the indicated siRNAs for 48 h, detached and re-plated as described above. (**a**) Western blot analysis with anti-Flag, ARF (human and mouse) and actin from collected cells. (**b**) Images of re-plated cells acquired by phase-contrast microscope (scale bar, 30μm). (**c**) Cumulative data are expressed as a mean value ± s.e.m. of at least three independent experiments. Single experiment data have been tested as described in Materials and methods section to analyze normal distribution. Asterisks (*) indicate statistically significant differences by paired two-tailed Wilcoxon test. $*P < 0.001$ and $**P < 0.01$ by paired Student's *t*-test. Number of cells analyzed for each experiment: SCR siRNA+ empty vector (350), ARF siRNA+empty vector (330), ARF siRNA+Flag-ARF (300), SCR siRNA+ Flag-ARF (350), SCR siRNA+p19ARF (336) and ARF siRNA+p19ARF (300).

dependent mechanism. Moreover, both cell round phenotype and the decrease of pFAK levels of ARF silenced cells were not affected by DAPK abrogation, suggesting that were not caused by apoptosis (Figure 9c, graph image and Supplementary Figure S9b). Interestingly, upon ARF silencing a slight but reproducible increase of p53 levels occurred both in HeLa, where the p53 pathway is not irreversibly disabled,[28] and HaCaT cells (Figure 9c and Supplementary Figure S9) and is reversed by concomitant DAPK depletion.

Finally, rescue experiments with wt and mutant ARF expression showed that both wt and ARF 100–132 are able to rescue cell viability (Figure 9d) thus establishing a positive correlation between increased pFAK levels and proliferation.

ARF depletion induces actin cytoskeleton defects but not anoikis in H1299 cells

To get further inside on the role of ARF in cell spreading and FAK phosphorylation, we extended our analysis to the H1299 cells, expressing robust endogenous levels of p14ARF. Upon ARF silencing, almost 50% cells failed to properly spread upon re-plating until 24h after seeding (Figure 10a). Analysis of ARF localization during adhesion and spreading by IF confirmed ARF recruitment at points of active actin polymerization in a time-dependent manner (Figure 10b, 8 h after plating).

Interestingly, we found that, in contrast with what described previously, FAK levels do not change upon ARF silencing (Figure 11a). In line with this, no difference in FAK RNA levels nor in other adhesion-related genes were found between ARF and control-depleted cells (Figure 11b). These results suggest that the spreading defect does not depend on FAK levels in these experimental conditions. Consistently, transient FAK silencing in HeLa cells does not completely phenocopy ARF depletion as cells retain the ability to spread (Supplementary Figure S10a). These experiments collectively show that in H1299 cells, the molecular circuitry linking cytoskeleton dynamics and FAK levels are

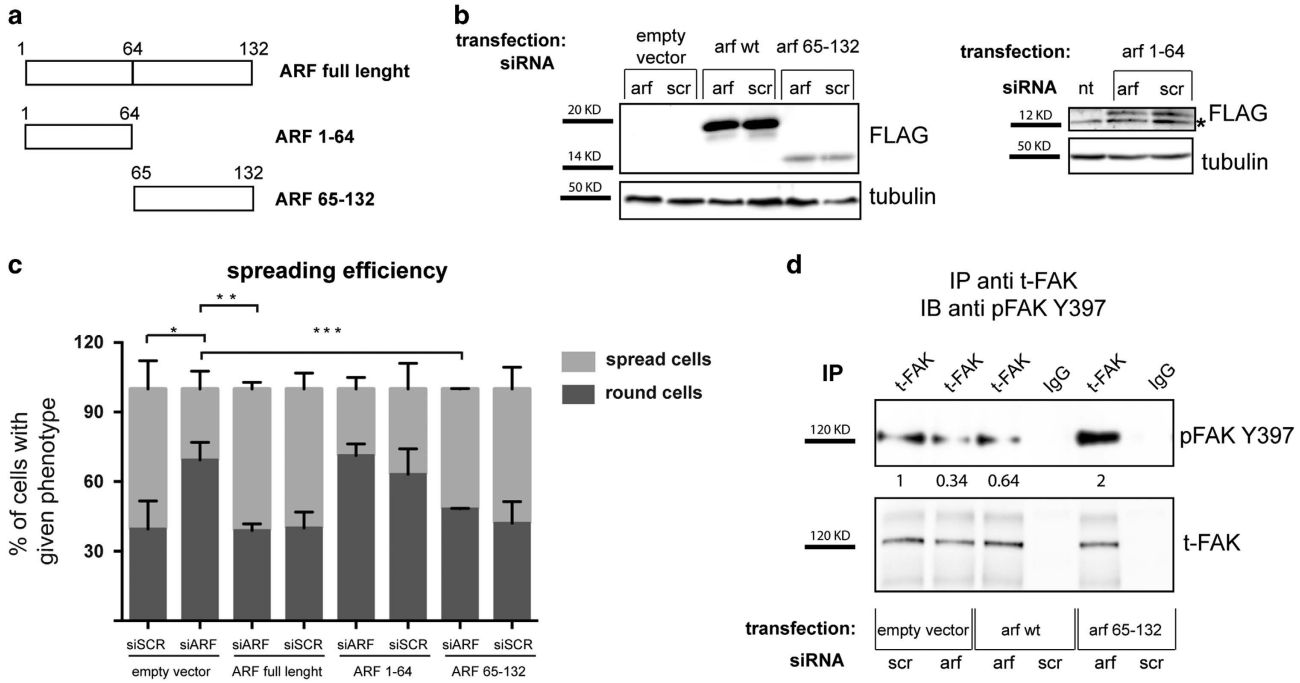

Figure 6. Re-introduction of ARF exon 2 encoded domain in ARF-depleted cells restore both spreading and pFAK expression. Rescue experiment was performed as described before, except that siRNA for the 5′-UTR of ARF gene was used (siRNA-3), and different ARF tagged forms were tested. (**a**) Scheme of N-ter flagged forms of ARF used in this study. (**b**) Immunoblot analysis of flagged 14 ARF mutants and tubulin (loading control) expression levels in whole-cell lysates of cells transfected and silenced with the indicated plasmids and siRNAs. Asterisks indicate an aspecific flag band. (**c**) Quantification of spreading efficiency of cells. Data were quantified from three or more experiments and 400 cells were analyzed for each transfection point in every experiment. Error bars represent the s.d. from the mean and statistical analysis performed as described in Figure 5. $*P < 0.02$ siARF-empty vector vs siSCR-empty vector; $**P < 0.0092$ siARF-Flag-ARF vs siARF-empty vector; $***P < 0.0112$ siARF-Flag 65–132 vs siARF-empty vector. (**d**) Analysis of pFAK and total FAK intracellular protein levels upon rescue experiment by IP with anti-t-FAK antibody and IB with anti-pFAK Y397 antibody performed as previously described. Representative western blots are shown. pFAK band intensities normalized versus t-FAK are shown below each corresponding band, and are expressed as fold value with respect to empty vector siSCR-transfected sample, arbitrarily set to 1 (see Materials and Methods section for details).

disconnected, thus implying that the round phenotype relies on specific ARF-dependent functions.

Interestingly, when we analyzed the role of ARF on cell viability in H1299, we found no effect on cell growth (Figure 11c). Moreover, cellular growth curves showed that, although ARF is required for proliferation of HeLa and HaCaT cells but it is dispensable for H1299, all tested cell lines require FAK expression to proliferate (Figure 11d and Supplementary Figure S10b). In agreement, western blot analysis shows that FAK-depleted HeLa and H1299 cells present PARP-1 cleavage and thus undergo apoptosis (Supplementary Figure S10a and data not shown), suggesting that, rather than having a role in spreading, FAK downregulation is the signal that halts cell growth in these cell lines.

We thus tested ARF ability to interact with FAK in this cell line. Moreover, as neither p53 nor DAPK are expressed in these cells, we tested if their exogenous expression could have a role in this interaction. The experiment shows that ARF and FAK interact in this cell line and the binding increases when DAPK is transfected (Figure 12a). Interestingly, transient transfection of both wt and DAPK K42A, a mutant defective in apoptosis induction, induce a decrease in FAK levels (Figure 12b). We thus wondered if it could be possible to induce apoptosis and FAK decrease upon ARF silencing in H1299 cells following DAPK and p53 re-introduction by transient transfection. As a key feature of apoptotic cell death is genomic DNA fragmentation, we extracted genomic DNA and analyzed its integrity by agarose gel electrophoresis. As expected, ARF silencing does not affect genomic DNA integrity in this cell line (Figure 13a). Transfection of p53 and wt DAPK slightly affect genomic DNA integrity, whereas DAPK K42A is not functional. Interestingly, ARF silencing further induces degradation of genomic DNA in cells expressing either p53 or WT DAPK, even more when both proteins are expressed, whereas it does not in cells expressing the inactive DAPK K42A mutant. Cells transfected with the DAPK constitutive active mutant (DAPK DCAM) strongly show DNA degradation irrespective of ARF status. Analysis of pFAK levels shows that ARF silencing has no effect of pFAK levels in untransfected cells (Figures 13a and b). DAPK expression instead induces a decrease of FAK expression when ARF is silenced (Figure 13b, compare lane 4 with lane 3). Expression of constitutive active DAPK DCAM strongly induces apoptosis and decrease of FAK levels. This effect is further exacerbated when cells are induced to spread (Figure 13c).

DISCUSSION

Here we show, for the first time, that although in adherent cells ARF localizes mainly in the nucleus, during the early phase of the spreading process the protein is recruited or stabilized to cell periphery at points of focal adhesions, in a precise time window. This localization is substrate independent, and is involved in the organization of actin structures during cell spreading. Reducing ARF expression levels leads to defects in the spatial organization of actin cytoskeleton during the process of cellular spreading. In line with a role in this phenomenon, we noted that during cell spreading ARF protein levels increase, through a protein kinase

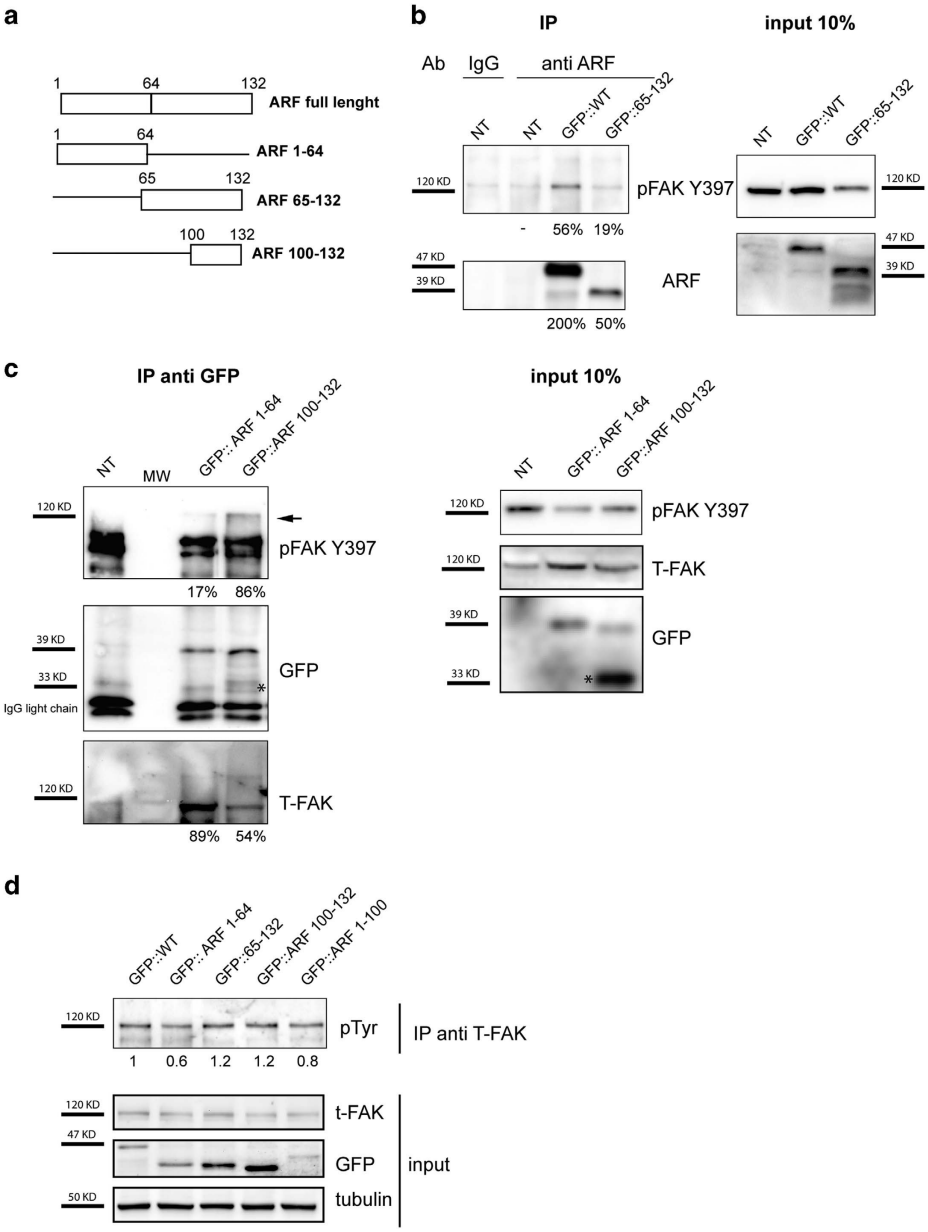

Figure 7. (**a**) Scheme of N-ter EGFP tagged ARF constructs used in this study. (**b**) HeLa cells were transiently transfected with wt and ARF 65–132 mutants, and after 24 h cells were re-plated and cytoplasmic extracts immunoprecipitated with anti-ARF antibody and analyzed by western blot with anti-pFAK Y397 and ARF antibodies. Panels of input are also shown on the right of immunoprecipitation experiment. Bands corresponding to the immunoprecipitated protein were quantified with ImageJ and reported as percentage of input, quantified in the same manner in order to obtain co-IP efficiency, indicated below the corresponding panel. (**c**) Cytoplasmic extracts of cells transfected with empty vector, ARF 1–64 and ARF 100–132 were immunoprecipitated with anti-GFP antibody analyzed by western blot with anti-pFAK Y397, t-FAK and GFP antibodies. Asterisk (*) indicates unspecific/degradation GFP products, arrow indicates immunoprecipitated FAK. Panel of input is also shown on the right of immunoprecipitation experiment. Efficiency of co-IP is quantified as described in **b**. (**d**) Cytoplasmic extracts were immunoprecipitated with anti-FAK antibody and analyzed by western blot with anti-pTyr antibody. Band intensity was compared with wt ARF-transfected sample arbitrarily set to 1. Panels of input probed with anti-FAK, GFP and tubulin antibodies are also shown.

C-dependent mechanism (Fontana, personal communication). Interestingly, it has been reported that p19ARF-deficient MEFs display a round phenotype, similar to the one reported in our study, accompanied by activation of the PI3K-Rac1 pathway and increased migration properties.[29,30] Despite significant divergence in amino-acid sequences, we show that this function is evolutionary conserved and the expression of p19 *per se* increases spreading efficiency (Figure 5c). In addition, our preliminary experiments show that, in line with the aforementioned article, ARF-depleted cells acquire increased migration properties.

Cell adhesion to the substrate is primarily mediated by integrins that, connecting extracellular matrix with cytoskeleton, induce cell survival pathways including phosphorylation and activation of FAK,[31,32] whose activation strongly correlates with tumor aggressiveness, cell migration and proliferation.[33–35] Here we provide evidence that p14ARF physically interacts with the FAK in its

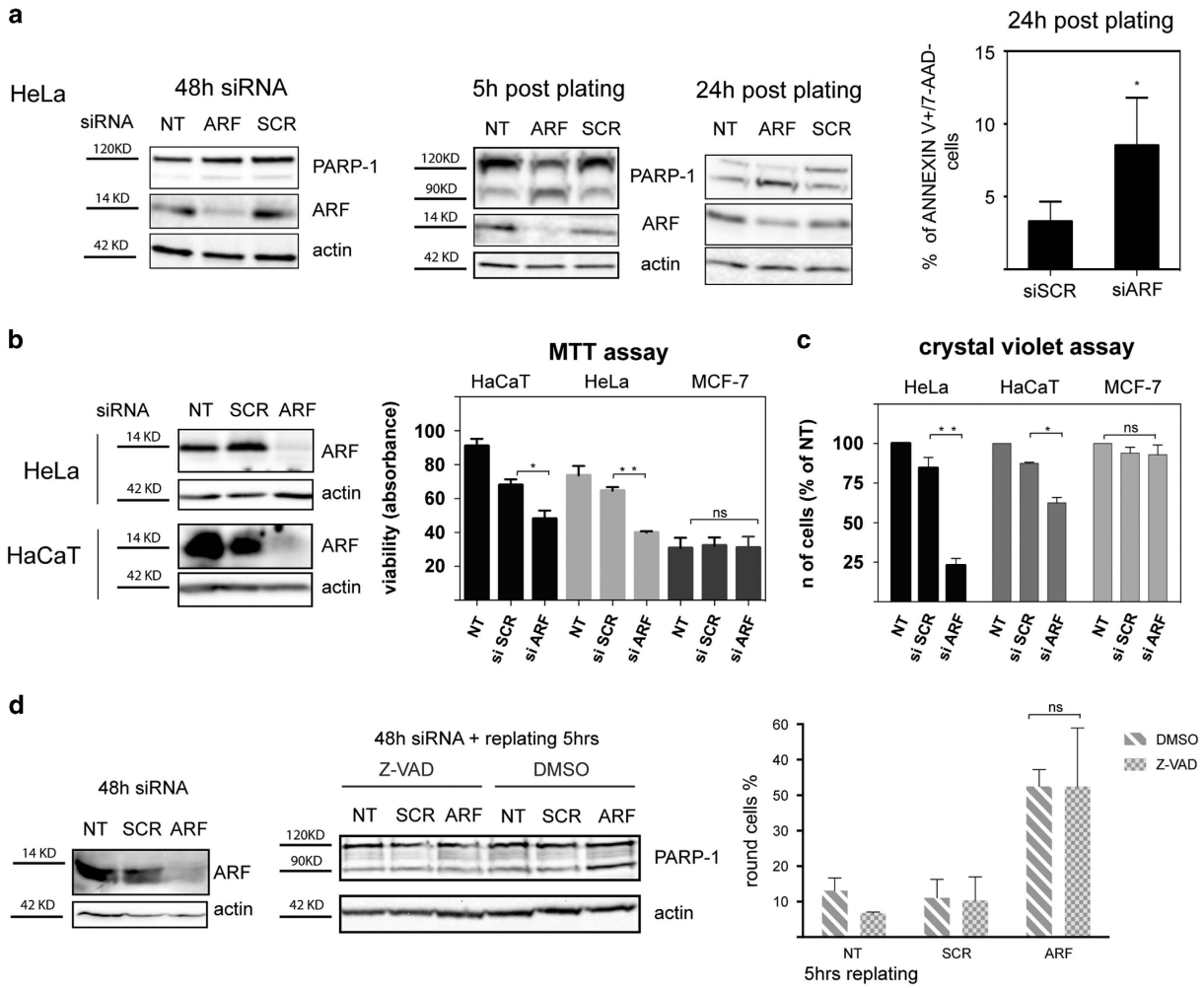

Figure 8. ARF depletion induces apoptosis. (**a**) HeLa cells were treated with the indicated siRNAs and analyzed by western blot 48 h later and 5 h and 24 h after plating. Silencing efficiency and viability was analyzed by western blot with anti-ARF and anti-PARP-1 antibody. Actin is a loading control. The percentage of early apoptotic cells was quantified by FACS through PE Annexin V staining. Percentage of PE Annexin V+/7-aminoactinomycin D-negative cells in siSCR and siARF-treated cells was reported in the graph. Cumulative data are expressed as a mean value ± s.d. of three independent experiments. Asterisk indicates statistically significant differences by paired two-tailed Student's *t*-test with $P < 0.05$. (**b**) HeLa, HaCaT and as negative control, MCF-7 cells (bearing INK4a/ARF locus deletion) cells were transiently transfected with the indicated siRNAs for 72 h. Silencing efficiency was analyzed by western blot with anti-ARF antibody. Actin is a loading control, whereas cell viability was analyzed by a MTT (3-(4,5-dimethylthiazol-2-yl)-2,5-diphenyltetrazolium bromide) based assay. The absorbance of each well (NT, siSCR and siARF) is reported. Graphs represent mean values ± s.d. of three independent experiments. Asterisks (*) indicate statistically significant differences with *P*-value obtained through the RM one-way ANOVA with the Greenhouse-Geisser correction $*P = 0.0158$, $**P = 0.0025$. No statistical (NS) difference between samples are indicated. (**c**) HeLa, HaCaT and MCF-7 were transiently transfected with the indicated siRNAs for 5 days, and cell viability analyzed by crystal violet staining of the plates (CVS assay). The absorbance of each well (NT, siSCR and siARF) was calculated as percentage of the control wells (NT) set to 100%. Statistically significant differences calculated as described $**P = 0.0002$, $*P = 0.0102$. (**d**) HeLa cells were treated with control or specific ARF siRNA for 48 h and then re-plated in presence of the general caspase inhibitor Z-VAD or DMSO as control for 5 h and analyzed by western blot to check silencing efficiency (left panel) and apoptosis (middle panels) as described before and phase-contrast microscopy for analysis of cell morphology. Quantification of percentage of cells with round phenotype was performed as described before. Cumulative data are expressed as a mean value ± s.d. of three independent experiments. For each experiment, 100 cells were analyzed for each transfection point. Unpaired two-tailed *t*-test shows NS difference between siARF DMSO and siARF Z-VAD-treated samples.

activated form. Given the observed reduction of total and phosphorylated FAK during the cell spreading process in ARF-depleted cells, we postulate that, through physical interaction, ARF can exert a protective role on FAK upon detachment and adhesion. Our experiments show that although the domains necessary for FAK interaction are present both in the N-ter and C-ter portion of the protein, the domain required for pFAK stabilization is restricted to the exon 2 encoded region. It has to be underlined that ARF region 100–132, required for both pFAK activation and survival, has an established role in autophagy as reported in Budina-Kolomets *et al.*[36] thus suggesting that ARF ability to regulate autophagy could be involved in this mechanism and it is independent from the reported ARF functions in mitochondrial homeostasis.[25] However, from experiments performed with mitotracker staining, we cannot exclude that ARF localization to cell periphery during the early phases of cell spreading (data not shown) could be in part mediated or primed by mitochondria accumulation to sites of actin remodeling.

It has been reported that sumoylated FAK[20] shows increased stability compared with the un-modified counterpart (Kadare *et al.*[20] and our unpublished data), whereas ARF has been shown to mediate sumoylation of its interacting partners.[21,37] Our data

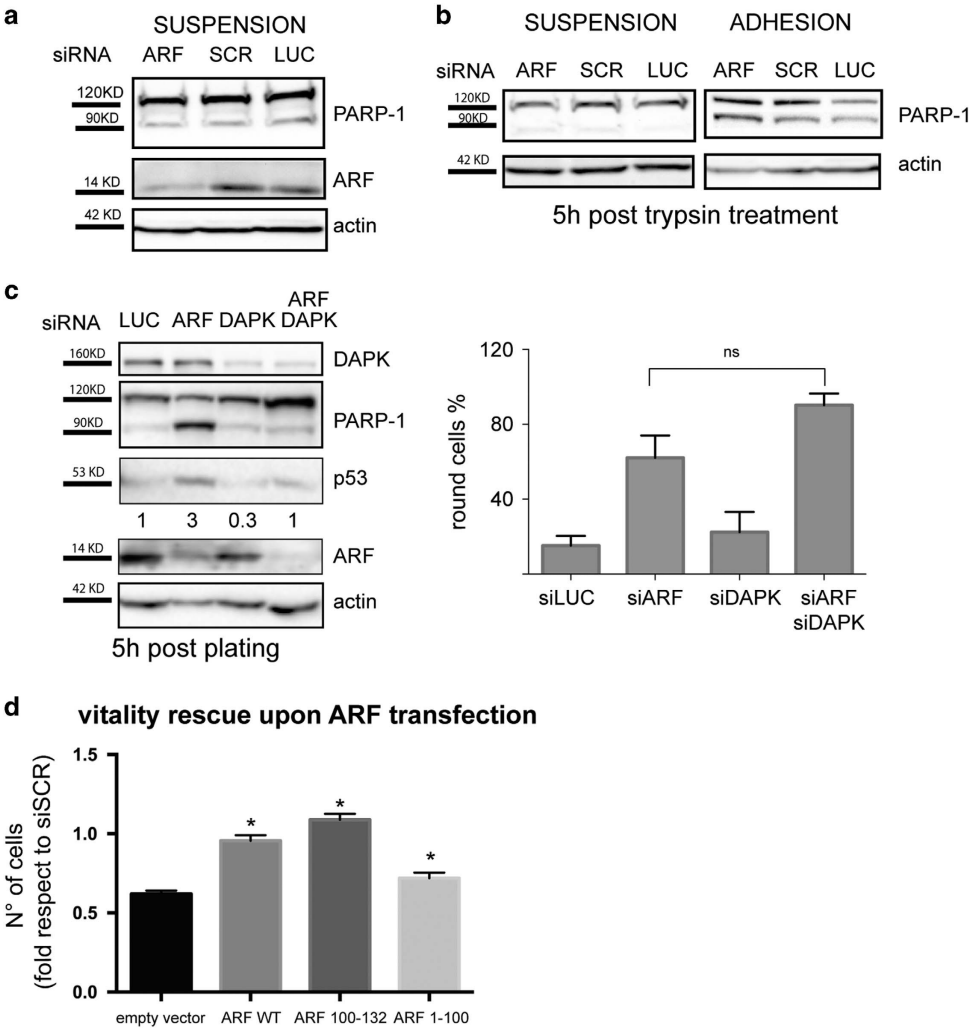

Figure 9. ARF depletion induces anoikis through a DAPK-dependent mechanism. (**a**) Western blot analysis of HeLa cells allowed to grow in suspension as spheres for 24 h and treated with control and specific ARF siRNA for 48 h. (**b**) Spheres were disaggregated by gentle trypsin treatment and re-placed in the same culture condition (**b**, left panels) or in adhesion (**b**, right panels) for 5 h. (**c**) HeLa cells grown in adherent conditions were treated with control or ARF and DAPK-specific siRNA alone or simultaneously for 72 h. Cells were re-plated as already described and analyzed by western blot analysis and phase-contrast microscopy. Silencing efficiency and vitality was analyzed by western blot with anti-ARF and anti-PARP-1 antibody. Actin is a loading control. WB are representative of at least three independent experiments. Normalized p53 band intensities are shown below respective wb panel, and are expressed as fold enrichment with respect to siSCR sample arbitrarily set to 1 (see Materials and methods section for details). Round phenotype was quantified and reported in graph as described. Cumulative data are expressed as a mean value ± s.d. of three independent experiments. For each experiment, 100–150 cells were analyzed for each transfection point. Analysis of variance show no statistical differences between the indicated values (NS) by paired two-tailed Wilcoxon test $P = 0.2$. (**d**) HeLa cells were transiently transfected with ARF of mutant vector as indicated for 24 h and were treated with control or ARF-3 siRNA (siUTR) for 72 h. Cell viability was analyzed by CVS (cristal violet staining) assay. The absorbance of each well treated with siARF-3 was calculated as fold of the control wells (siSCR) set to 1. Graphs represent mean values ± s.d. of two independent experiments. Analysis of variance shows statistical significant difference between empty vector and wt/mutant ARF-transfected points with P-value < 0.001 by Kruskal–Wallis test.

show that ARF expression induces the appearance of slow migrating FAK species, thus supporting the hypothesis that by interacting with FAK it could mediate its sumoylation and stabilization.

Proper organization of cytoskeletal structures allows the transduction of survival pathways inside the cells whose deregulation can result in anoikis.[38–42] Resistance to anoikis is a hallmark of malignant tumor cells, resulting in anchorage independence. DAPK is an actin-associated pro-apoptotic protein having an important role in tumor suppression[43,44] and anoikis.[26,45] Our data show that cell death induced by ARF depletion is DAPK dependent, as we observe anoikis rescue in doubly depleted ARF/DAPK cells. It has been previously reported that DAPK can phosphorylate ARF *in vitro* and thus promote p53-dependent apoptosis.[39] Recently, we have shown that phosphorylated ARF species are more stable in the cytoplasm.[46] As we noticed a decrease of ARF protein levels upon DAPK silencing (see Figure 8c), we speculate that DAPK could increase ARF stability through phosphorylation, suggesting the existence of a feedback loop between ARF and DAPK, in which ARF blocks DAPK-mediated apoptosis during cytoskeleton remodeling, whereas DAPK exerts a positive effect on ARF stability. Moreover, our data show an increase of p53 protein levels and of its transcriptional targets Puma and Apaf-1 (preliminary data not shown) upon ARF depletion, suggesting that DAPK apoptosis induction could be in part mediated through p53. Interestingly, it has been observed that ARF expression in spermatogonia prevents p53-dependent

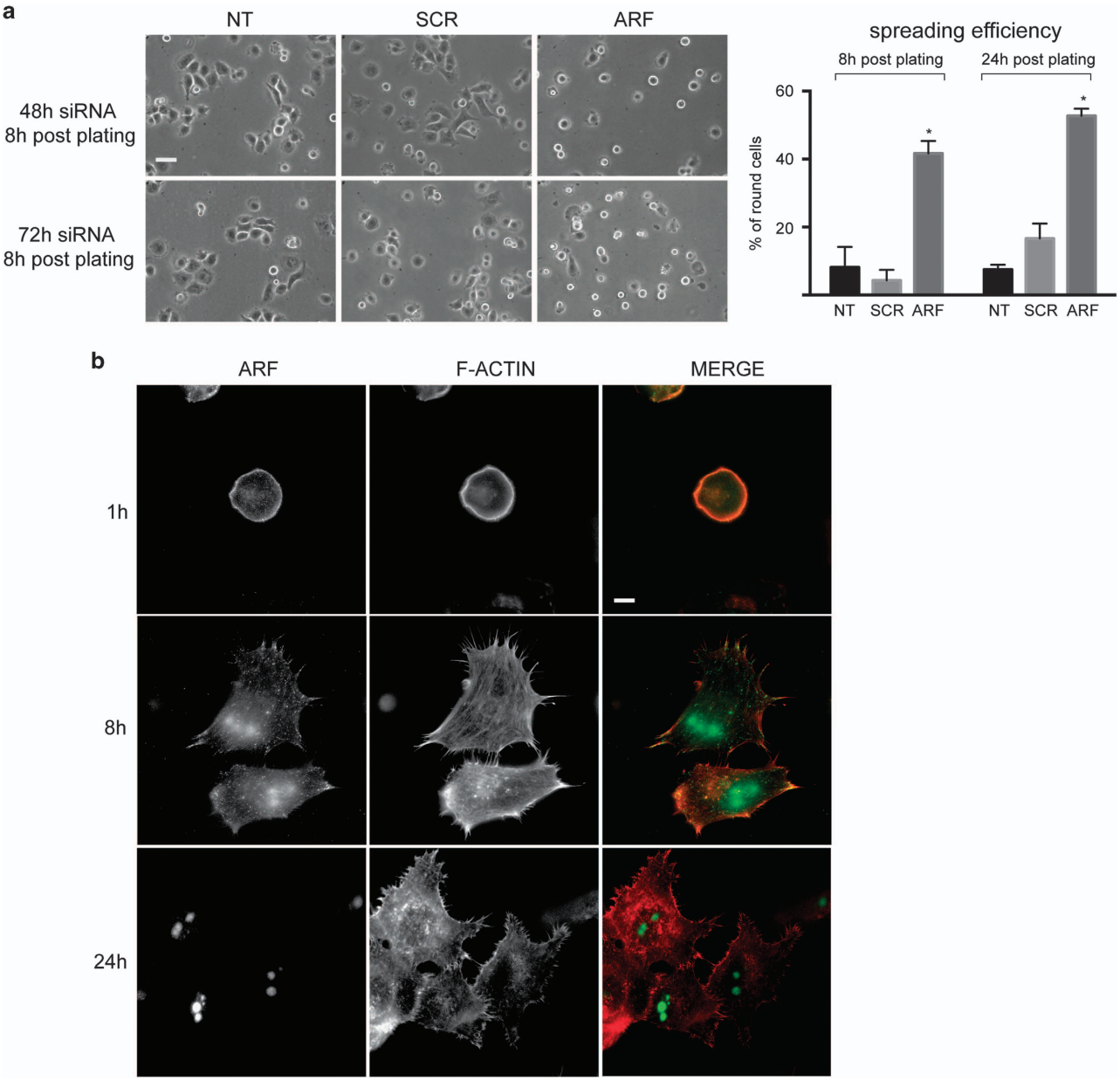

Figure 10. ARF is required for spreading and localizes to the plasma membrane of H1299 cells. (**a**) Contrast images of H1299 cells transiently transfected with the indicated siRNAs for 48 h and 72 h treated as described in Figure 4 and analyzed by phase-contrast microscope 8 h after plating, (scale bar, 30 μm). Quantification of round phenotype was performed as described and is shown in the graph on the right. Cumulative data are expressed as a mean value ± s.e.m. of at least three independent experiments. For each experiment, 100–150 cells were analyzed for each transfection point. Asterisks indicate statistically significant differences between ARF and SCR treated cells with *P*-value obtained by unpaired two-tailed *t*-test < 0.05. (**b**) H1299 cells were detached, re-suspended in growth medium, allowed to adhere onto coverslips and were fixed at different time points after plating (1, 8 and 24 h). Permeabilized cells were subjected to IF with anti-ARF antibody and stained with tetramethylrhodamine phalloidin to visualize actin cytoskeleton. Representative images showing ARF subcellular localization are shown for each time point. Images were taken by Nikon fluorescence microscopy (scale bar, 5 μm).

apoptosis.[47] Further experiments are needed to validate this hypothesis.

It has been reported that overexpression of DAPK induces morphological changes typical of apoptotic cells, such as cell rounding and shrinkage.[48] Our data only partially fit with these observations, as we do not observe a rescue of round phenotype in DAPK-depleted cells. In line with these results, we observe that H1299 cells, not expressing DAPK, show a round morphology upon ARF depletion and result in anoikis resistance.

DAPK-mediated apoptosis is accompanied by a specific decrease of FAK tyrosine phosphorylation.[45] As in H1299 we do not observe a decreased FAK activation upon ARF silencing, we hypothesized that the FAK downregulation observed in HeLa and HaCaT cells is at least in part due to activation of DAPK upon ARF depletion. In line with this hypothesis, re-introduction of both wt and death inactive DAPK mutant, induces a strong decrease of FAK levels upon cytoskeleton remodeling. More importantly, restoration of DAPK expression in H1299 cells induces apoptosis and this effect is further amplified by concomitant ARF silencing.

On this basis, we propose that, far from being simply inactive to restrain cell growth, ARF confers pro-survival properties by helping

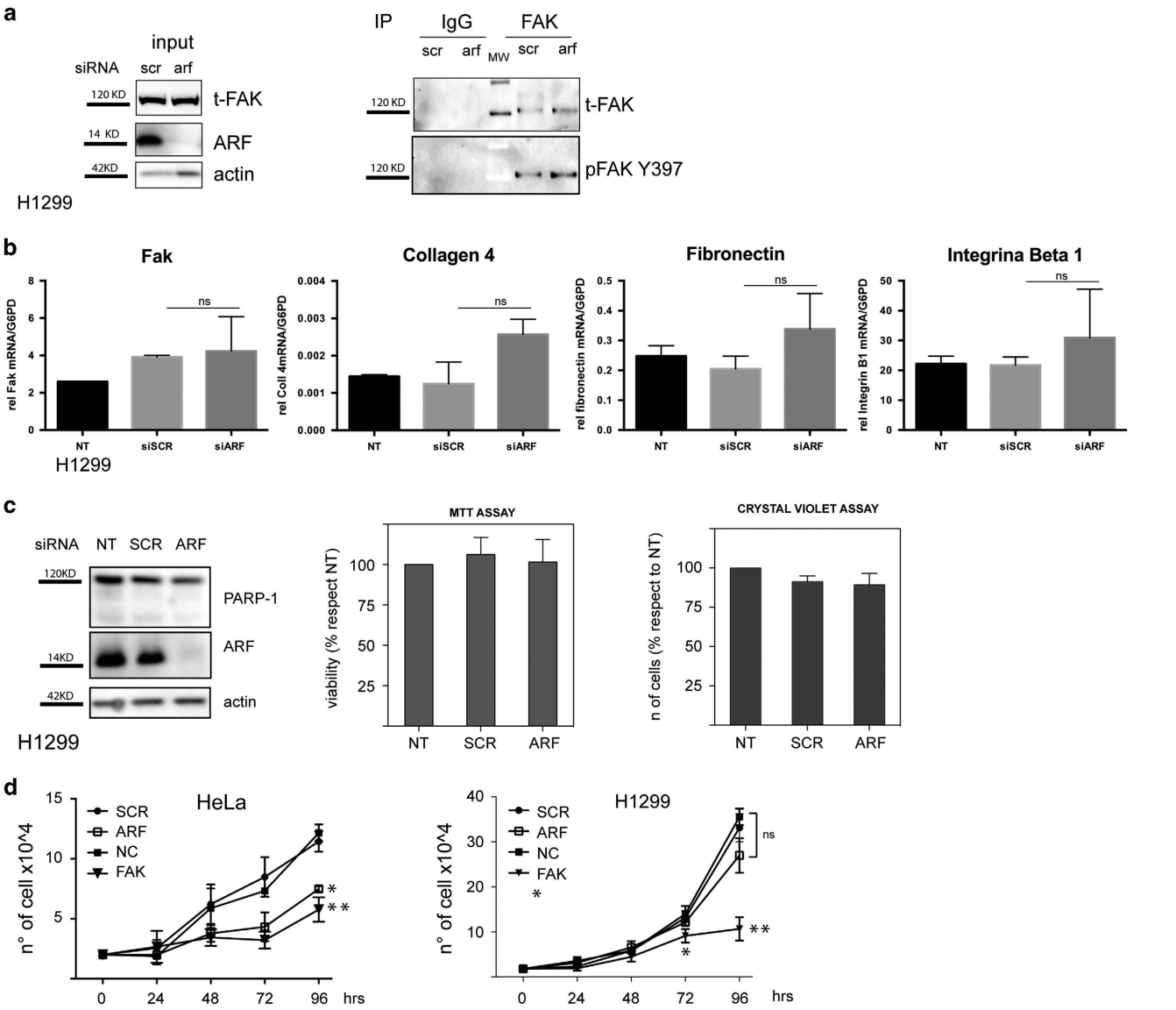

Figure 11. FAK levels and cell viability are unaffected by ARF depletion. (**a**) H1299 cells treated with control SCR and ARF-specific siRNA were detached and induced to adhere. Total cell extracts (8 h after re-plating) were immunoprecipitated with anti-FAK antibody or with IgG as negative control and analyzed by western blot with pFAK Y397 antibody and subsequently with anti-t-FAK antibody. Panels of inputs, representative of three independent experiments, probed with anti-FAK, ARF and actin antibodies are also shown. (**b**) Quantitative reverse transcriptase (qRT)–PCR analyses of FAK, collagen IV, fibronectin and integrin β1 mRNA levels normalized on G6PD expression in cells treated with the indicated siRNA are shown. Cumulative data are expressed as a mean value ± s.d. of three independent experiments. Statistical analysis has been performed as described in Figure 4. Not statistically significant differences are indicated (NS). (**c**) H1299 cells were transiently transfected with the indicated siRNAs and silencing efficiency analyzed by western blot with anti-ARF and actin as loading control. Viability was checked with PARP-1 antibody, MTT (3-(4,5-dimethylthiazol-2-yl)-2,5-diphenyltetrazolium bromide) and CVS (cristal violet staining) assay as described previously. Data are expressed in **c** and **d** are mean value ± s.d. of three independent experiments. (**d**) Growth curve of HeLa and H1299 cells treated with the indicated siRNA at different time points. Asterisks indicate statistically significant differences by unpaired two-tailed *t*-test, between FAK and NC sirna treated cells $^{**}P = 0.0048$, or between ARF and SCR sirna treated cells $^{*}P = 0.0085$ for HeLa cells. In H1299 cells, $^{*}P = 0.0217$ between FAK and NC at 72 h and $^{**}P = 0.0002$ at 96 h. Not statistically significant differences are indicated (NS).

cells to spread and protecting them from anoikis as illustrated in Figure 14. This is accomplished through inhibition of DAPK-induced apoptosis, and stabilization of FAK.

Conflicting data exist on ARF pro-oncogenic activity in some experimental settings. In particular, it has been reported that ARF contributes to prostate cancer progression by stabilization through SUMO modification of Slug protein.[37] Moreover, the ability of ARF to induce autophagy, a pro-survival mechanism related to the phenomenon of tumor dormancy,[49] also points to the hypothesis that in particular cellular contexts ARF could have a pro-proliferative or even oncogenic role. In this regard, it is interesting to note that the effect of ARF loss on cell morphology of prostate cells[37] is the opposite of that observed in MEF cells and in our experimental conditions.

Our findings point to a novel role of ARF on protection from cell anoikis. This could have a strong impact on tumor growth and dissemination. By providing insight into these previously unknown functions of this protein, this study may have important implications in development of novel strategies for cancer therapy.

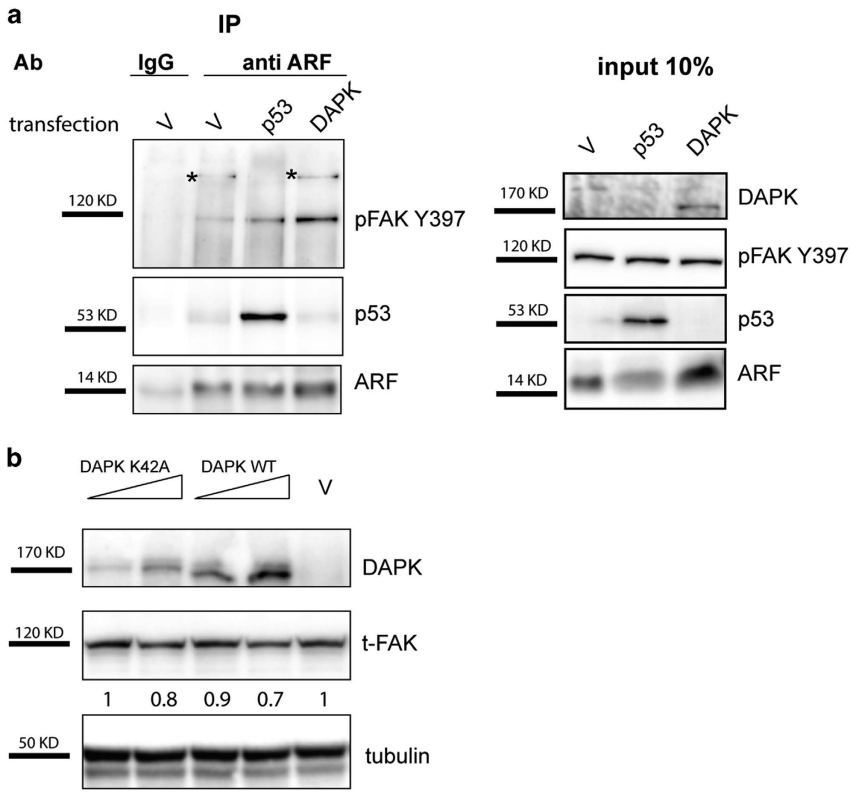

Figure 12. ARF interacts with FAK in H1299 cells. (**a**) H1299 cells were transiently transfected with empty vector (v) or either p53 or DAPK-expressing plasmids. After 24 h, cells were re-plated and cytoplasmic extracts immunoprecipitated with anti-ARF antibody and analyzed by western blot with anti-pFAK Y397, ARF and p53 antibodies. Panels of input are also shown on the right of immunoprecipitation experiment. (**b**) H1299 cells were transfected with an empty vector (v) or increasing amount of wt DAPK or DAPK K42A expression plasmids. Twenty-four hours after transfection, cells were lysed and cellular extracts were immunoblotted and analyzed with anti-FAK, anti-DAPK and anti-tubulin as loading control. WB shown are representative of at least three independent experiments. Normalized FAK band intensities are shown below each corresponding band, and are expressed as fold enrichment with respect to empty vector-transfected sample arbitrarily set to 1.

MATERIALS AND METHODS

HeLa cells were obtained from Dr Valeria R Villella, San Raffaele Scientific Institute, Milan, Italy. All other cell lines (H1299, HaCaT and MCF-7) were purchased from Cell Line Service (CLS, Eppelheim, Germany). Cells were grown as described,[15] transfected with Lipofectamine 2000, RNAiMAX reagent or electroporation (Neon transfection System, Life Technologies Carlsbad, CA, USA). Cells were routinely tested for mycoplasma contamination and kept in culture for no more than 6 weeks.

ARF siRNAs (harboring the stealth modification) anneal in the exon 1β of p14ARF transcript. ARF and p16INK4a siRNA sequences has been reported in Vivo *et al*.[8] and Kobayashi *et al*.[50] DAPK, FAK and luciferase siRNAs are available by Qiagen (Hilden, Germany). All siRNA were transiently transfected at a final concentration of 10 μM, except siRNA-3 that was used at 30 μM. Fibronectin purified from bovine plasma (Millipore, Billerica, MA, USA; 10 μg/ml). Z-VAD fmk (BioVision, Milpitas, CA, USA) was used at final concentration of 10 μM.

Quantitative reverse transcriptase–PCR analysis

Equal number of cells was lysed with RNA Mini Kit Ambion (Carlsbad, CA, USA). In all, 1 μg of total RNA of each sample was reverse-transcribed and quantitative PCR amplifications were performed as described in Vivo *et al*.[8] Primers were used: p16INK4a forward 5′-CCAACGCACCGAATAGTTACG-3′, reverse 5′-GCGCTGCCCATCATCATG-3′. FAK, DAPK, collagen IV, fibronectin and integrin β1 primers were purchased from Qiagen (Quantitect Primer Assay); G6PD forward 5′-ACAGAGTGAGCCCTTCTTCAA-3′ and reverse 5′-GGAGGCTGCATCATCGTACT-3′. Data presented represent the mean of three biological replicates.

Western blot was performed as described.[15] Band intensities were quantified by ImageJ Software (free software, NIH), normalized to actin and reported in graph as percentage of control. Each profile represents the mean of three independent experiments.

The list of antibodies are as follows: anti-PARP-1, (Cell Signaling Denvers, MA, USA, #9542); anti-ARF C-18, anti-actin I-19, anti-p53 DO-1, anti-caspase-3 H-277, anti-FAK C-20, anti-pFAK (Tyr397)-R for IF, (Santa Cruz Biotechnology, Heidelberg, Germany), anti-pFAK (Tyr397) (BD Milan, Italy; clone 14 for wb), anti-ARF Ab2 14PO2 (Neomarkers from Bio-Optica, Milan, Italy); anti-p19ARF (Novus Biologicals from Novus Italy, Milan, Italy; Ab80) anti-DAPK-55 mouse monoclonal antibody (Sigma Aldrich, Milan, Italy); anti-pPaxillin Tyr118 (Life Technologies) and anti-pTyr 05-321 (Upstate from Millipore, Darmstadt, Germany).

Cell viability assays. Cell viability was determined by the crystal violet staining method[51] or through a (3-(4,5-dimethylthiazol-2-yl)-2,5-diphenyl-tetrazolium bromide)) MTT based assay.[52] Dye uptake was measured at 580 nm using a spectrophotometer. Cell viability was calculated as dye intensity and compared with untreated samples.

Microscopy and IF. Live phase-contrast images were acquired using a (Nikon Eclipse microscope, Tokyo, Japan). Cell spreading was quantified as described in Tamura *et al*.[53] Fibronectin stimulation and IF were performed as described in Schlaepfer and Hunter[54] and Vivo *et al*.[46] Cells were incubated with Tetramethylrhodamine or fluorescein isothiocyanate-conjugated phalloidin for 30 min, followed by DAPI (Sigma-Aldrich) for 3 min and washed with PBS/0.05% Tween. Coverslip were mounted with Ibidi mounting medium (Ibidi GmbH, Martinsried, Germany).

Immunoprecipitation assays were performed either with cytoplasmic extracts or total cellular extracts (from 5×10^6 cells per sample). Subcellular fractionation was done as previously described.[15] For total cellular extracts, cells were harvested, lysed with RIPA buffer and incubated with anti-ARF antibody (C-18 Santa Cruz Biotechnology) or anti-FAK antibody.

Apoptosis was analyzed by PE Annexin V Apoptosis Detection Kit I (BD Biosciences; cat no. 559763) following the manufacturer's instructions.

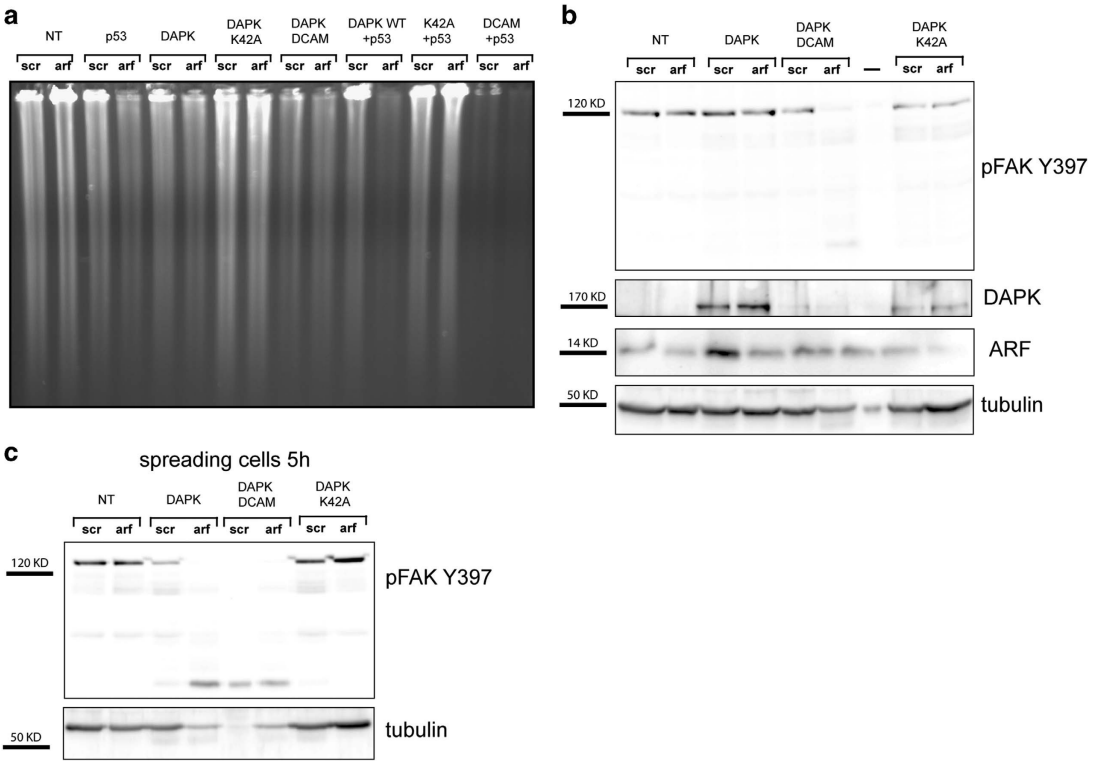

Figure 13. DAPK re-introduction in H1299 cells induces apoptosis and decrease of pFAK levels upon ARF silencing. (**a**) Genomic DNA content analysis for detection of apoptosis. H1299 cells were transiently transfected with the indicated vectors for 24 h and treated with siSCR control or ARF siRNA for 48 h. Genomic DNA was extracted and analyzed by agarose gel electrophoresis to analyze DNA integrity. (**b**) Western blot analysis showing pFAK Y397 levels upon transfection and silencing in the same experimental conditions. Tubulin was used as loading control. (**c**) Same experiment shown in **b** but collected 5 h upon spreading induction.

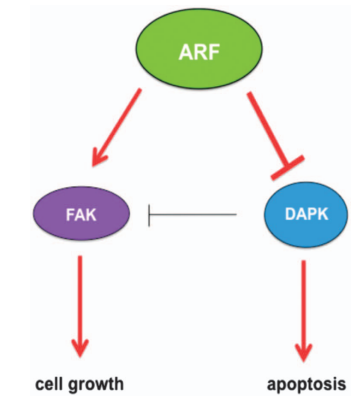

Figure 14. Proposed schematic model for ARF-mediated regulation of cell growth and inhibition of apoptosis. During cellular adhesion and spreading, ARF expression stabilizes activated FAK in the cytoplasm, probably mediating its sumoylation. FAK stabilization sustains cell growth. In parallel, ARF expression blocks DAPK-induced apoptosis, through both p53-dependent and -independent mechanism protecting cells from anoikis. In addition, ARF hampers DAPK downregulation of FAK activity. In cell-expressing p53, FAK stabilization can further results in FAK-mediated p53 degradation and thus inhibition of p53-dependent apoptosis.

DNA content analysis for detection of apoptotic cells was performed as described.[55]

Statistic. Data presented in this work was derived from experiments performed at least in triplicate (biological replicates), except when differently stated. The sample size of each experimental point is reported in the relative figure legend, as well as the specific statistical analysis performed. In all the experiments in which single cells were analyzed, 5–10 fields were randomly selected in the coverslip for each experimental point. Data have been analyzed to assay normal distribution with different tests, such as the D'Agostino and Pearson omnibus, the Shapiro–Wilk and the KS normality test. Analysis of data not showing a normal distribution were performed with the Wilcoxon, Mann–Whitney tests and Kruskal–Wallis test, otherwise *t*-test and analysis of variance were performed using GraphPad Prism 5.0 software (La Jolla, CA, USA).

CONFLICT OF INTEREST

The authors declare no conflict of interest.

ACKNOWLEDGEMENTS

We thank Dr Carlo Di Cristo and Dr Tiziana Parisi for critical revision of the manuscript. We thank Dr Valeria R Villella for providing HeLa cells, Dr Giovanna Benvenuto (Confocal Microscopy Service at the Stazione Zoologica Anton Dohrn, Naples) and Dr Per Guldberg for kindly providing GFP-tagged ARF mutants. This work was supported by grants awarded to GLM and AP from L.R.5 (2007), to VC and GLM from PO FESR 2007-2013 'DiMo' and 'Movie', respectively.

REFERENCES

1 Ozenne P, Eymin B, Brambilla E, Gazzeri S. The ARF tumor suppressor: structure, functions and status in cancer. *Int J Cancer* 2010; **127**: 2239–2247.
2 Kamijo T, Bodner S, van de Kamp E, Randle DH, Sherr CJ. Tumor spectrum in ARF-deficient mice. *Cancer Res* 1999; **59**: 2217–2222.
3 Ruas M, Peters G. The p16INK4a/CDKN2A tumor suppressor and its relatives. *Biochim Biophys Acta* 1998; **1378**: F115–F177.
4 Pollice A, Vivo M, La Mantia G. The promiscuity of ARF interactions with the proteasome. *FEBS Lett* 2008; **582**: 3257–3262.
5 Kotsinas A, Papanagnou P, Evangelou K, Trigas GC, Kostourou V, Townsend P *et al.* ARF: a versatile DNA damage response ally at the crossroads of development and tumorigenesis. *Front Genet* 2014; **5**: 236.

6 Gromley A, Churchman ML, Zindy F, Sherr CJ. Transient expression of the Arf tumor suppressor during male germ cell and eye development in Arf-Cre reporter mice. *Proc Natl Acad Sci USA* 2009; **106**: 6285–6290.
7 Li C, Finkelstein D, Sherr CJ. Arf tumor suppressor and miR-205 regulate cell adhesion and formation of extraembryonic endoderm from pluripotent stem cells. *Proc Natl Acad Sci USA* 2013; **110**: E1112–E1121.
8 Vivo M, Di Costanzo A, Fortugno P, Pollice A, Calabro V, La Mantia G. Down-regulation of DeltaNp63alpha in keratinocytes by p14ARF-mediated SUMO-conjugation and degradation. *Cell Cycle* 2009; **8**: 3537–3543.
9 Reef S, Zalckvar E, Shifman O, Bialik S, Sabanay H, Oren M *et al.* A short mitochondrial form of p19ARF induces autophagy and caspase-independent cell death. *Mol Cell* 2006; **22**: 463–475.
10 Humbey O, Pimkina J, Zilfou JT, Jarnik M, Dominguez-Brauer C, Burgess DJ *et al.* The ARF tumor suppressor can promote the progression of some tumors. *Cancer Res* 2008; **68**: 9608–9613.
11 Sanchez-Aguilera A, Sanchez-Beato M, Garcia JF, Prieto I, Pollan M, Piris MA. p14 (ARF) nuclear overexpression in aggressive B-cell lymphomas is a sensor of malfunction of the common tumor suppressor pathways. *Blood* 2002; **99**: 1411–1418.
12 Chen Z, Carracedo A, Lin HK, Koutcher JA, Behrendt N, Egia A *et al.* Differential p53-independent outcomes of p19(Arf) loss in oncogenesis. *Sci Signal* 2009; **2**: ra44.
13 Pimkina J, Humbey O, Zilfou JT, Jarnik M, Murphy ME. ARF induces autophagy by virtue of interaction with Bcl-xl. *J Biol Chem* 2009; **284**: 2803–2810.
14 Ferru A, Fromont G, Gibelin H, Guilhot J, Savagner F, Tourani JM *et al.* The status of CDKN2A alpha (p16INK4A) and beta (p14ARF) transcripts in thyroid tumour progression. *Br J Cancer* 2006; **95**: 1670–1677.
15 Vivo M, Ranieri M, Sansone F, Santoriello C, Calogero RA, Calabro V *et al.* Mimicking p14ARF phosphorylation influences its ability to restrain cell proliferation. *PloS ONE* 2013; **8**: e53631.
16 Zhao J, Guan JL. Signal transduction by focal adhesion kinase in cancer. *Cancer Metastasis Rev* 2009; **28**: 35–49.
17 Parsons JT, Horwitz AR, Schwartz MA. Cell adhesion: integrating cytoskeletal dynamics and cellular tension. *Nat Rev Mol Cell Biol* 2010; **11**: 633–643.
18 Westhoff MA, Serrels B, Fincham VJ, Frame MC, Carragher NO. SRC-mediated phosphorylation of focal adhesion kinase couples actin and adhesion dynamics to survival signaling. *Mol Cell Biol* 2004; **24**: 8113–8133.
19 Serrels B, Serrels A, Brunton VG, Holt M, McLean GW, Gray CH *et al.* Focal adhesion kinase controls actin assembly via a FERM-mediated interaction with the Arp2/3 complex. *Nat Cell Biol* 2007; **9**: 1046–1056.
20 Kadare G, Toutant M, Formstecher E, Corvol JC, Carnaud M, Boutterin MC *et al.* PIAS1-mediated sumoylation of focal adhesion kinase activates its autophosphorylation. *J Biol Chem* 2003; **278**: 47434–47440.
21 Tago K, Chiocca S, Sherr CJ. Sumoylation induced by the Arf tumor suppressor: a p53-independent function. *Proc Natl Acad Sci USA* 2005; **102**: 7689–7694.
22 Weber JD, Kuo ML, Bothner B, DiGiammarino EL, Kriwacki RW, Roussel MF *et al.* Cooperative signals governing ARF-mdm2 interaction and nucleolar localization of the complex. *Mol Cell Biol* 2000; **20**: 2517–2528.
23 Weber JD, Taylor LJ, Roussel MF, Sherr CJ, Bar-Sagi D. Nucleolar Arf sequesters Mdm2 and activates p53. *Nat Cell Biol* 1999; **1**: 20–26.
24 Llanos S, Clark PA, Rowe J, Peters G. Stabilization of p53 by p14ARF without relocation of MDM2 to the nucleolus. *Nat Cell Biol* 2001; **3**: 445–452.
25 Christensen C, Bartkova J, Mistrík M, Hall A, Lange MK, Ralfkiær U *et al.* A short acidic motif in ARF guards against mitochondrial dysfunction and melanoma susceptibility. *Nat Commun* 2014; **5**: 5348.
26 Chen RH, Wang WJ, Kuo JC. The tumor suppressor DAP-kinase links cell adhesion and cytoskeleton reorganization to cell death regulation. *J Biomed Sci* 2006; **13**: 193–199.
27 Kuo JC, Lin JR, Staddon JM, Hosoya H, Chen RH. Uncoordinated regulation of stress fibers and focal adhesions by DAP kinase. *J Cell Sci* 2003; **116**(Pt 23): 4777–4790.
28 Johnson CL, Lu D, Huang J, Basu A. Regulation of p53 stabilization by DNA damage and protein kinase C. *Mol Cancer Ther* 2002; **1**: 861–867.
29 Guo F, Gao Y, Wang L, Zheng Y. p19Arf-p53 tumor suppressor pathway regulates cell motility by suppression of phosphoinositide 3-kinase and Rac1 GTPase activities. *J Biol Chem* 2003; **278**: 14414–14419.
30 Guo F, Zheng Y. Involvement of Rho family GTPases in p19Arf- and p53-mediated proliferation of primary mouse embryonic fibroblasts. *Mol Cell Biol* 2004; **24**: 1426–1438.
31 Giancotti FG, Ruoslahti E. Integrin signaling. *Science* 1999; **285**: 1028–1032.
32 Frisch SM, Vuori K, Ruoslahti E, Chan-Hui PY. Control of adhesion-dependent cell survival by focal adhesion kinase. *J Cell Biol* 1996; **134**: 793–799.
33 Sulzmaier FJ, Jean C, Schlaepfer DD. FAK in cancer: mechanistic findings and clinical applications. *Nat Rev Cancer* 2014; **14**: 598–610.
34 Tancioni I, Uryu S, Sulzmaier FJ, Shah NR, Lawson C, Miller NL *et al.* FAK Inhibition disrupts a beta5 integrin signaling axis controlling anchorage-independent ovarian carcinoma growth. *Mol Cancer Ther* 2014; **13**: 2050–2061.
35 Fan H, Zhao X, Sun S, Luo M, Guan JL. Function of focal adhesion kinase scaffolding to mediate endophilin A2 phosphorylation promotes epithelial-mesenchymal transition and mammary cancer stem cell activities in vivo. *J Biol Chem* 2013; **288**: 3322–3333.
36 Budina-Kolomets A, Hontz RD, Pimkina J, Murphy ME. A conserved domain in exon 2 coding for the human and murine ARF tumor suppressor protein is required for autophagy induction. *Autophagy* 2013; **9**: 1553–1565.
37 Xie Y, Liu S, Lu W, Yang Q, Williams KD, Binhazim AA *et al.* Slug regulates E-cadherin repression via p19Arf in prostate tumorigenesis. *Mol Oncol* 2014; **8**: 1355–1364.
38 Puthalakath H, Huang DC, O'Reilly LA, King SM, Strasser A. The proapoptotic activity of the Bcl-2 family member Bim is regulated by interaction with the dynein motor complex. *Mol Cell* 1999; **3**: 287–296.
39 Buchheit CL, Weigel KJ, Schafer ZT. Cancer cell survival during detachment from the ECM: multiple barriers to tumour progression. *Nat Rev Cancer* 2014; **14**: 632–641.
40 Puthalakath H, Villunger A, O'Reilly LA, Beaumont JG, Coultas L, Cheney RE *et al.* Bmf: a proapoptotic BH3-only protein regulated by interaction with the myosin V actin motor complex, activated by anoikis. *Science* 2001; **293**: 1829–1832.
41 Frisch SM, Ruoslahti E. Integrins and anoikis. *Curr Opin Cell Biol* 1997; **9**: 701–706.
42 Frisch SM, Screaton RA. Anoikis mechanisms. *Curr Opin Cell Biol* 2001; **13**: 555–562.
43 Cohen O, Feinstein E, Kimchi A. DAP-kinase is a Ca2+/calmodulin-dependent, cytoskeletal-associated protein kinase, with cell death-inducing functions that depend on its catalytic activity. *EMBO J* 1997; **16**: 998–1008.
44 Inbal B, Cohen O, Polak-Charcon S, Kopolovic J, Vadai E, Eisenbach L *et al.* DAP kinase links the control of apoptosis to metastasis. *Nature* 1997; **390**: 180–184.
45 Wang WJ, Kuo JC, Yao CC, Chen RH. DAP-kinase induces apoptosis by suppressing integrin activity and disrupting matrix survival signals. *J Cell Biol* 2002; **159**: 169–179.
46 Vivo M, Matarese M, Sepe M, Di Martino R, Festa L, Calabro V *et al.* MDM2-mediated degradation of p14ARF: a novel mechanism to control ARF levels in cancer cells. *PloS ONE* 2015; **10**: e0117252.
47 Churchman ML, Roig I, Jasin M, Keeney S, Sherr CJ. Expression of arf tumor suppressor in spermatogonia facilitates meiotic progression in male germ cells. *PLoS Genet* 2011; **7**: e1002157.
48 Ivanovska J, Mahadevan V, Schneider-Stock R. DAPK and cytoskeleton-associated functions. *Apoptosis* 2014; **19**: 329–338.
49 Sosa MS, Bragado P, Aguirre-Ghiso JA. Mechanisms of disseminated cancer cell dormancy: an awakening field. *Nat Rev Cancer* 2014; **14**: 611–622.
50 Kobayashi T, Wang J, Al-Ahmadie H, Abate-Shen C. ARF regulates the stability of p16 protein via REGgamma-dependent proteasome degradation. *Mol Cancer Res* 2013; **11**: 828–833.
51 Vivo M, Calogero RA, Sansone F, Calabro V, Parisi T, Borrelli L *et al.* The human tumor suppressor arf interacts with spinophilin/neurabin II, a type 1 protein-phosphatase-binding protein. *J Biol Chem* 2001; **276**: 14161–14169.
52 Chiba K, Kawakami K, Tohyama K. Simultaneous evaluation of cell viability by neutral red, MTT and crystal violet staining assays of the same cells. *Toxicol In Vitro* 1998; **12**: 251–258.
53 Tamura M, Gu J, Matsumoto K, Aota S, Parsons R, Yamada KM. Inhibition of cell migration, spreading, and focal adhesions by tumor suppressor PTEN. *Science* 1998; **280**: 1614–1617.
54 Schlaepfer DD, Hunter T. Evidence for in vivo phosphorylation of the Grb2 SH2-domain binding site on focal adhesion kinase by Src-family protein-tyrosine kinases. *Mol Cell Biol* 1996; **16**: 5623–5633.
55 Koopman G, Reutelingsperger CP, Kuijten GA, Keehnen RM, Pals ST, van Oers MH. Annexin V for flow cytometric detection of phosphatidylserine expression on B cells undergoing apoptosis. *Blood* 1994; **84**:1415–1420.

Supplementary Information accompanies this paper on the Oncogene website (http://www.nature.com/onc)

Supplementary information

Fig S1

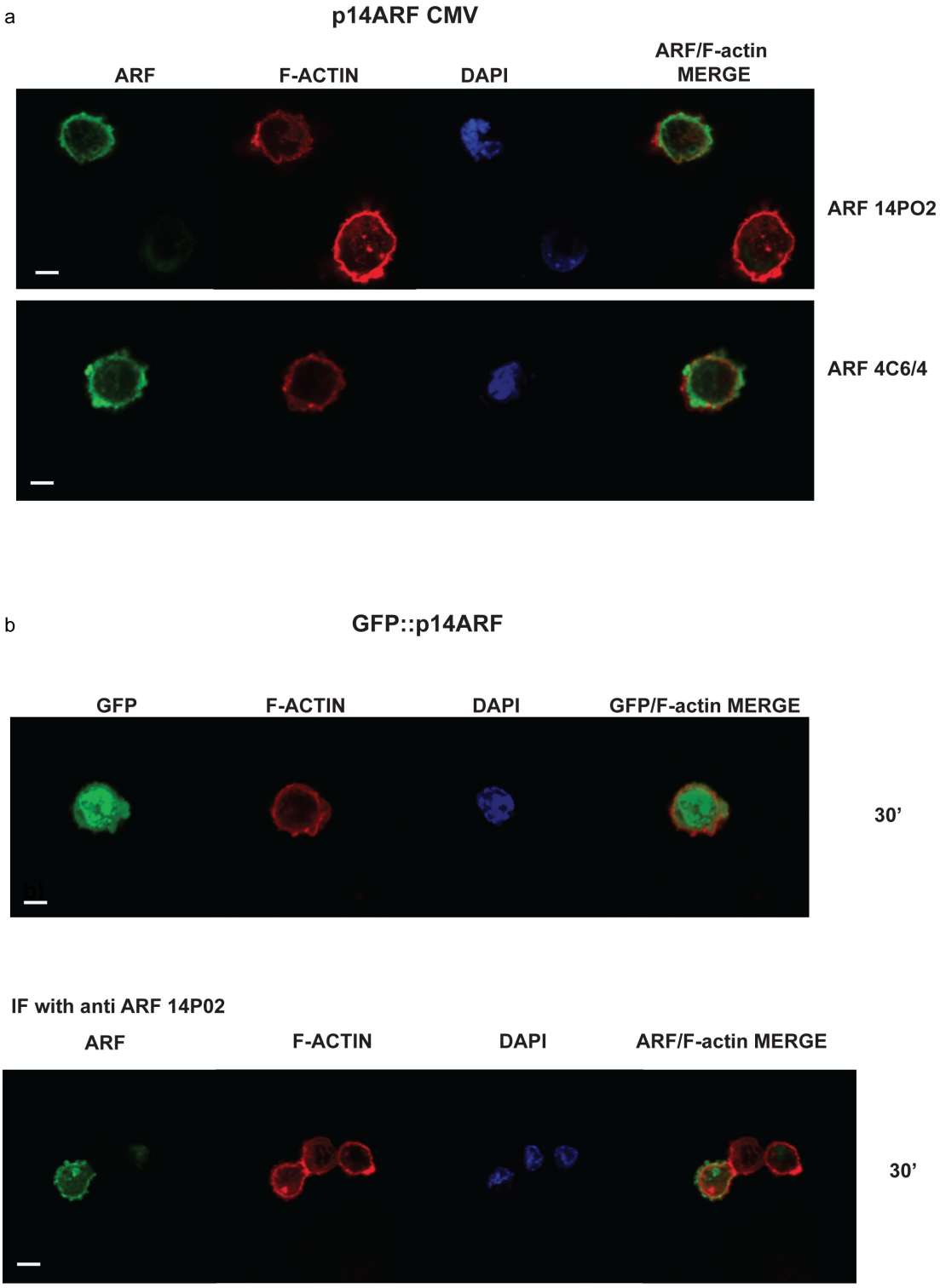

Fig. S1: p14ARF co-localization with F-actin using different type of anti-ARF antibodies and GFP tagged protein. a) MEF MDM2 -/- p53 -/- cells were transfected with p14ARF CMV

vector for 24h, then were detached by gentle trypsin treatment, resuspended in growth medium and allowed to adhere onto fibronectin coated coverslip. Immunofluorescence was performed as previously described using anti-ARF 14P02 (upper panel) or anti-ARF 4C6/A (lower panel) antibodies and both TRITC phalloidin and DAPI staining to visualize actin cytoskeleton and nuclei. b) Direct fluorescence analysis (upper panel) or IF with anti-ARF 14P02 antibody (lower panel) was performed in MEF transfected with GFP tagged protein. Representative images of ARF subcellular localization are shown. Images were taken with a Zeiss confocal laser-scanning microscope Axio Observer (scale bar, 7μm) using suitable lasers as described in Fig 1.

Fig S2

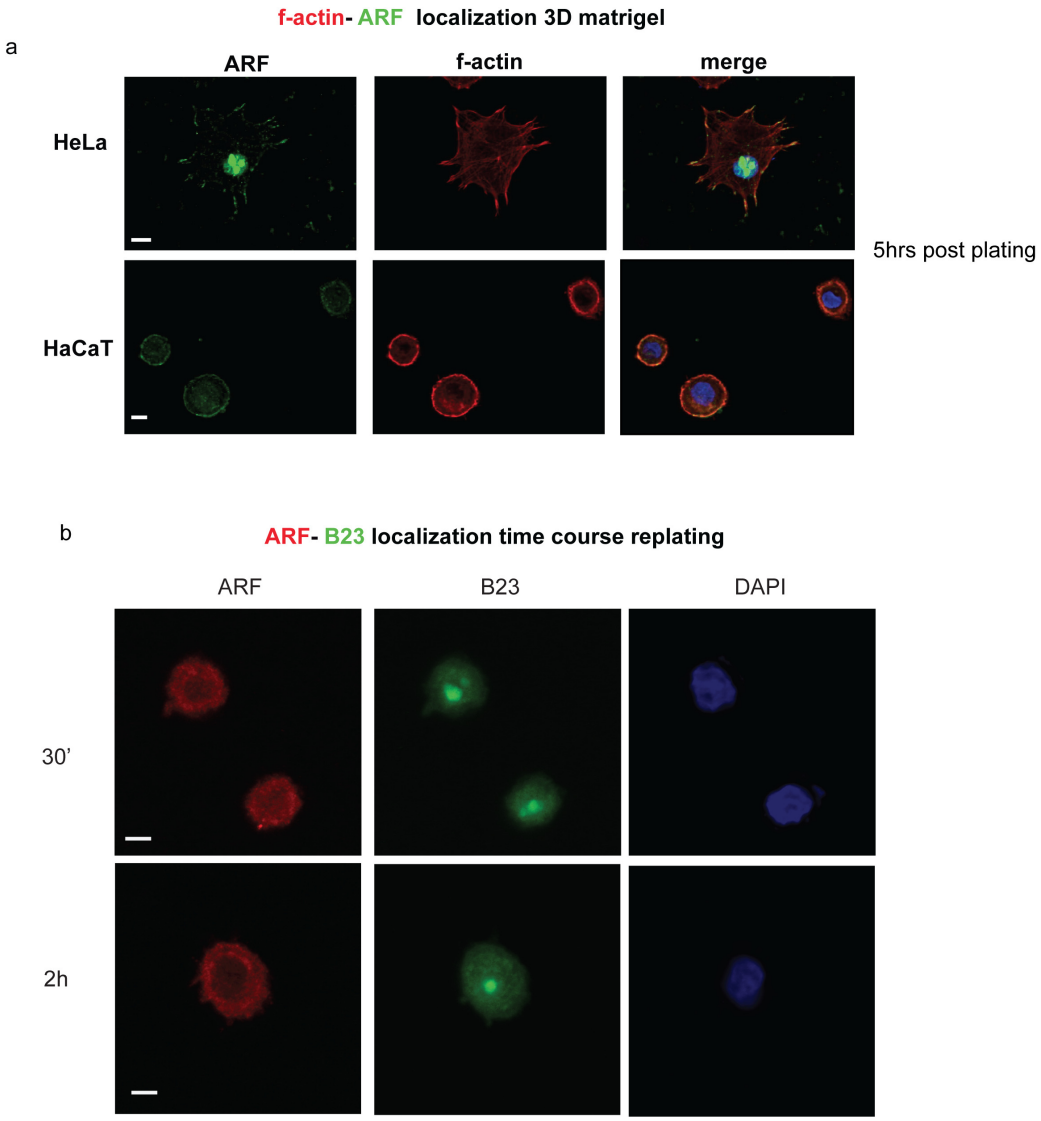

Fig. S2: a) p14ARF co-localizes with F-actin in 3D culture. Confocal images of ARF co-localization with TRITC phalloidin and merge with Dapi, in HeLa and HaCaT cells 5 hrs after plating in growth medium with Matrigel 2,5% (scale bar, 10μm). b) Representative images of ARF and B23 localization in HeLa cells after 30' and 2h post plating (scale bar, 10μm).

Fig S3

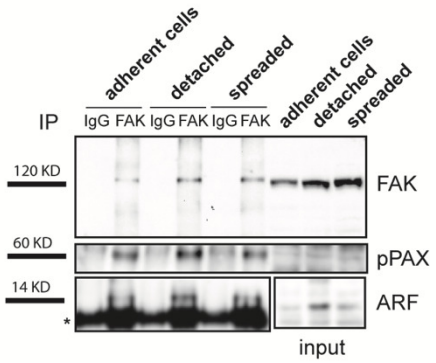

Fig. S3: Reverse immuno-precipitation with anti-FAK antibody in HeLa cells during adhesion. Cytoplasmic HeLa extracts collected in adherent cells, upon cell detachment and during spreading were subjected to immuno-precipitation with anti-FAK antibody or IgG as negative control and analysed by western blot with anti-FAK, anti-pPAX Tyr118 and anti-ARF antibodies. Inputs are also shown. * indicates IgG bands.

Fig S4

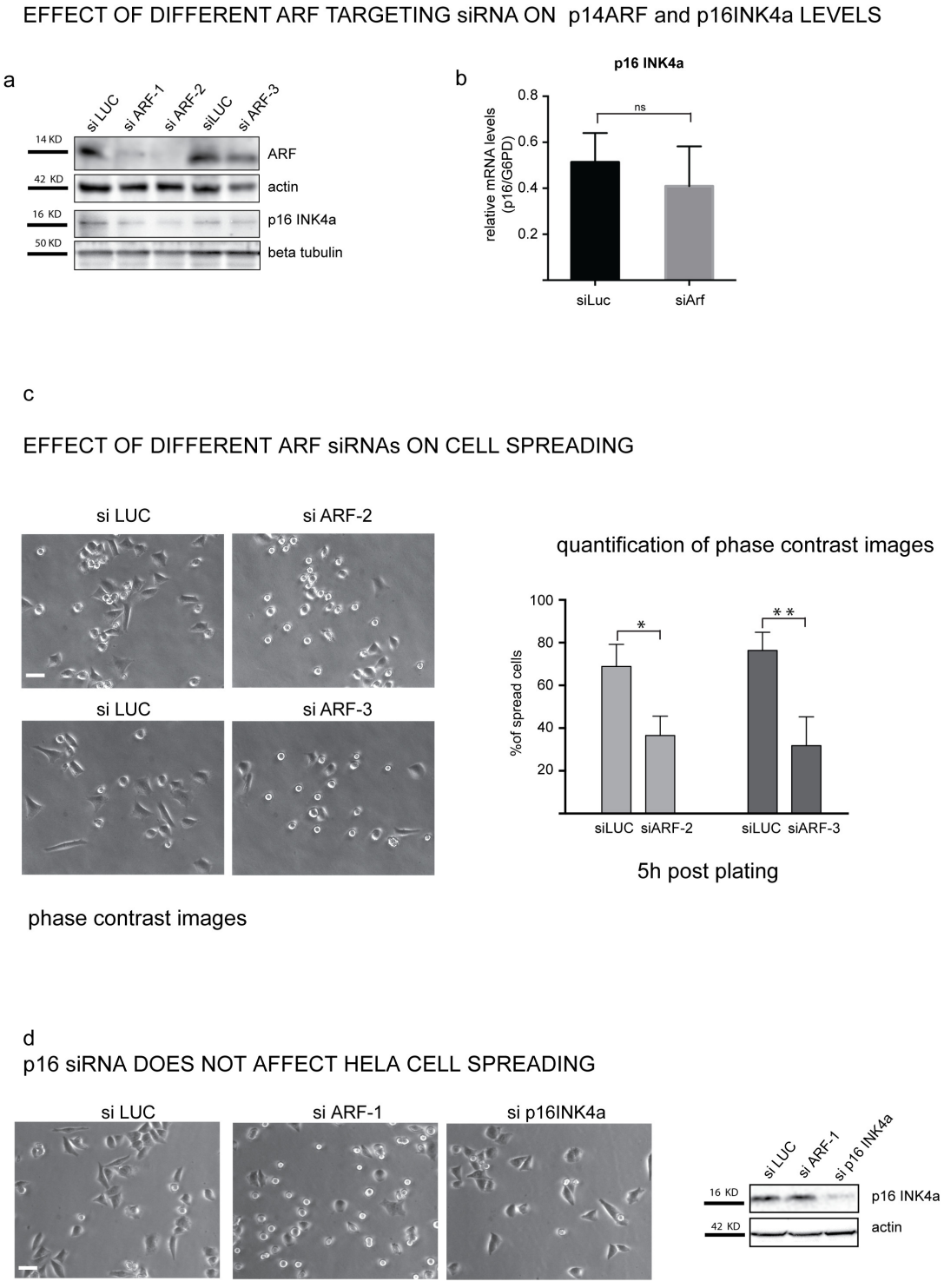

Fig. S4: a) HeLa cells were treated with the indicated stealth siRNAs for 48hrs and analysed by western blot 5 hrs after plating. Silencing efficiency was analysed by western blot with anti ARF and anti p16 INK4a antibodies. Actin and tubulin are loading control. b) INK4a levels

were analysed by quantitative real time PCR in control siLuc treated cells and in ARF depleted cells with a mix of the aforementioned specific ARF siRNA. Cumulative data are expressed as a mean value ± SD of 3 independent experiments. Statistical analysis performed by unpaired, two-tailed Mann-Whitney test show no statistical (ns) difference between siSCR and siARF samples. c) Contrast images of HeLa cells transiently transfected with the indicated siRNAs for 48hrs and analysed as described in Fig 3. Asterisks indicate statistically significant differences (P value <0.05) by unpaired two-tailed Student t test (*) = 0.0046; (**) = 0.0055. Number of cells analyzed for each experiment: SCR siRNA (50), siARF-2 (50), siARF-3 (50) (scale bar, 30 μm) d) Hela cells were treated with the indicated siRNA as described and silencing efficiency and spreading ability was analysed as described (scale bar, 30 μm).

Fig S5

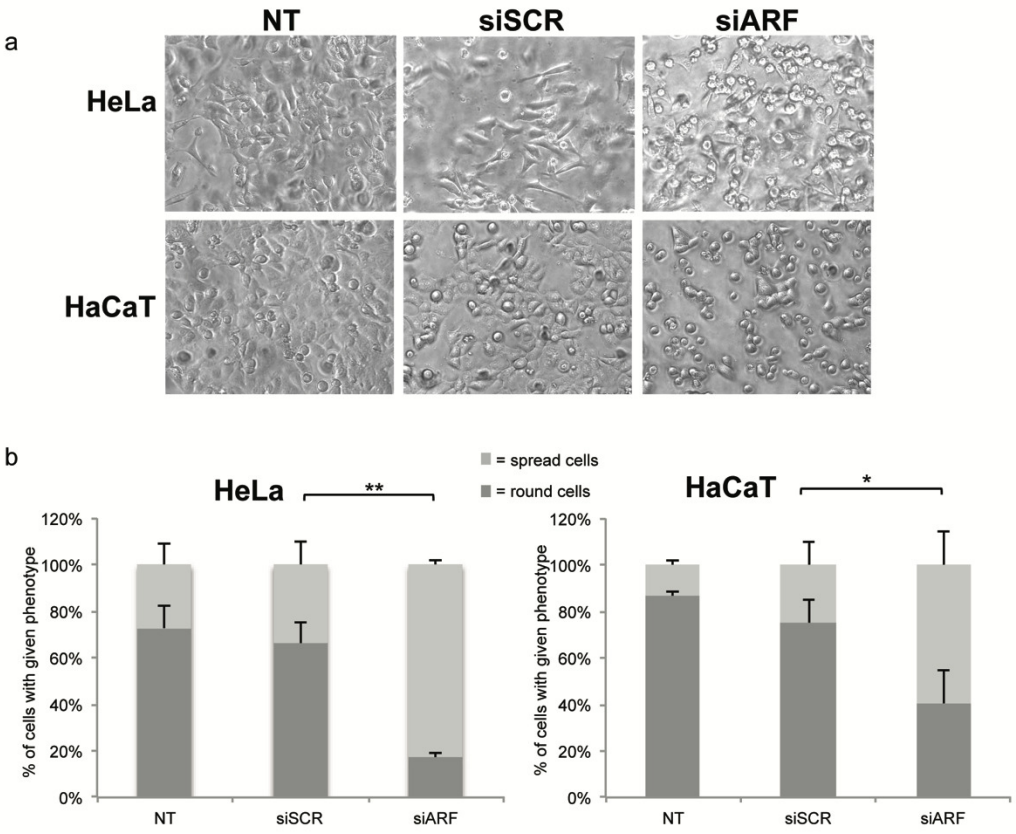

Fig. S5: p14ARF depletion affects cell morphology in 3D culture. a) Contrast images of HeLa and HaCaT cells transiently transfected with the indicated siRNAs for 48hrs, then detached by trypsinization and replated in growth medium containing Matrigel 2,5 %. Images were collected and analysed by phase-contrast microscope. b) To quantify the percentage of each phenotype, for each transfection point, we counted adherent and rounded cells in five different fields and pooled data from three to five experiments. Number of cells analysed for each experiment: siSCR (250), siARF (250), siLUC (250). The experiments are expressed as a mean value ± SEM of 3 independent experiments collected as biological replicates. The statistical analysis was performed by Student t-test *$P < 0.05$; ** $P < 0.01$.

Fig S6

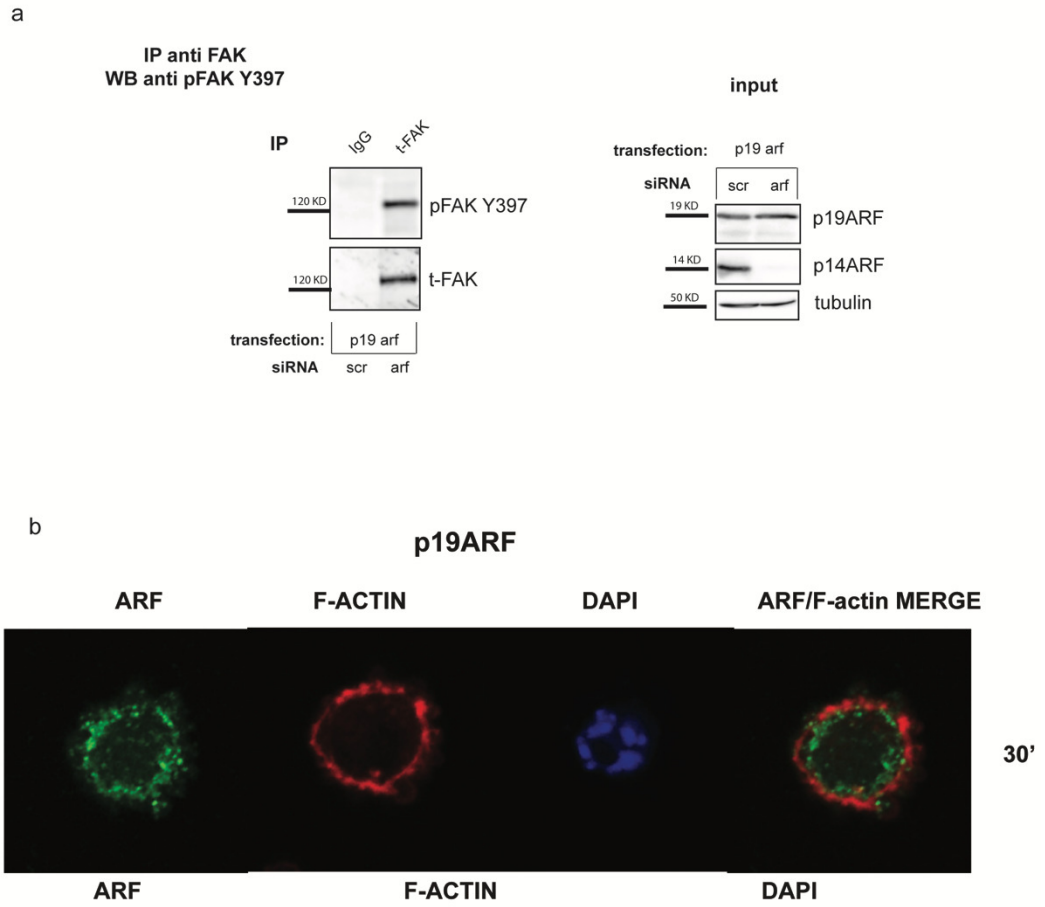

Fig. S6: a) p19ARF co-localizes with F-actin. MEF MDM2 -/- p53 -/- cells were transfected with p19ARF CMV vector for 24h, then were detached by gentle trypsin treatment, resuspended in growth medium and allowed to adhere onto fibronectin coated coverslip. Immunofluorescence was performed as previously described. Representative images of p19ARF subcellular localization are shown. Images were taken with a Zeiss confocal laser-scanning microscope Axio Observer (scale bar, 5μm). b) Re-introduction of p19ARF in ARF depleted cells restore pFAK expression. Rescue experiment was performed as described before. Analysis of pFAK Y397 and t-FAK protein levels upon rescue experiment by IP with anti t-FAK antibody performed as previously described. Panel of input probed with anti p19ARF and p14ARF antibodies is also shown on the right of immuno-precipitation experiment. Tubulin is used as loading control.

Fig S7

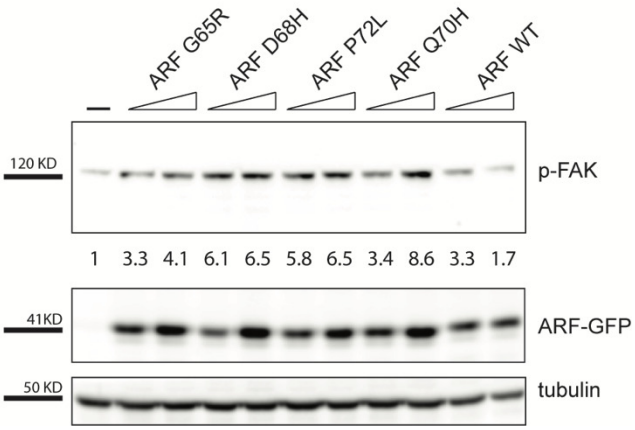

Fig. S7: CDKN2A missense mutations associated with melanoma did not affect pFAK protein levels. HeLa cells were transiently transfected with the indicated vectors for 24hrs and analysed by western blot with anti-pFAK Y397, anti-GFP antibodies. Tubulin is a loading control. Normalized pFAK Y397 band intensities, shown below each corresponding band, are expressed as fold enrichment respect to control cells arbitrarily set to 1.

Fig S8

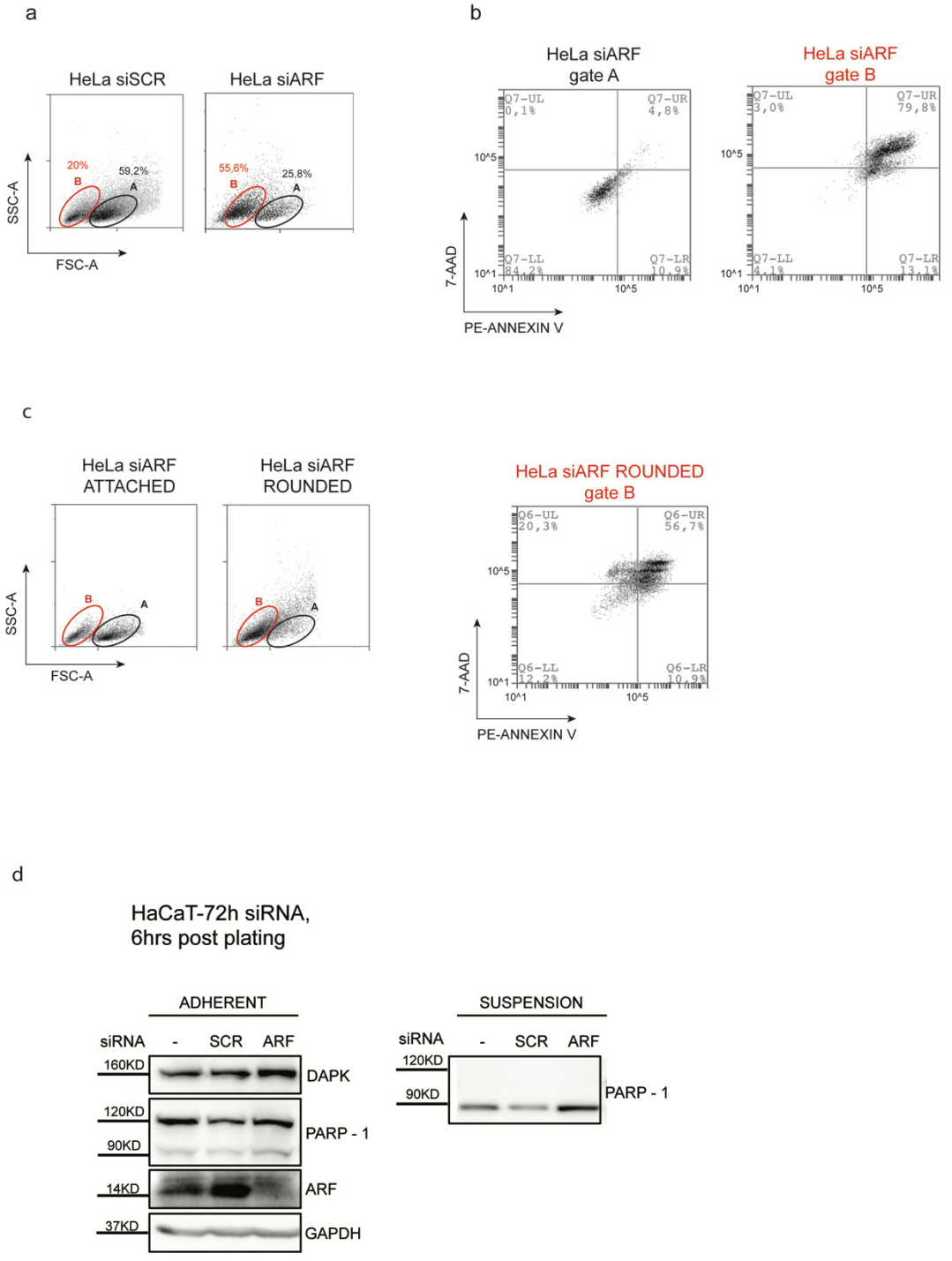

Fig. S8: Flow cytometric analysis of apoptosis in HeLa cells. HeLa cells were treated with the indicated siRNA and after 48h were replated as previously described. 24h after plating, adherent and rounded cells were collected (detached cells were collected with the supernatant, pelleted by centrifugation), washed and resuspended in 1x Annexin-V Binding buffer (BD

Biosciences) at 1x106 cells/ml. A total of 0.4x106 cells were stained with PE-conjugated Annexin-V (BD Biosciences) following manufacturer's instructions. An equal volume of 1x Annexin-V Binding buffer was added and samples were analysed within the next hour by flow cytometry with FACS Accuri C6 Flow Cytometer (BD Biosciences). Morphological analysis of ARF silenced cells by FACS showed the existence of two subpopulations of cells based on their size, with the population characterized by small size being the one in late apoptosis a) FSC (forward scatter) / SSC (side scatter) patterns and annexin-V/ 7-AAD staining (b) of cells gated for low FSC/high SSC profile (gate B-red circle) or high FSC/low SSC profile (gate A-black circle) are shown. Representative experiment out of three is shown (c) In ARF depleted cells, adherent and rounded cells were collected and analysed separately. FSC (forward scatter) / SSC (side scatter) patterns of each cell type and annexin-V/ 7-AAD staining of rounded cells gated for low FSC/high SSC profile (gate B) are shown.

ARF depletion induces apoptosis in HaCaT cells (d) Cells were treated with the indicated siRNAs and 72hrs later adherent and suspension cells were separately collected and analysed by western blot with anti PARP-1. Silencing efficiency was analysed by western blot with anti ARF antibody. GAPDH is a loading control.

Fig S9

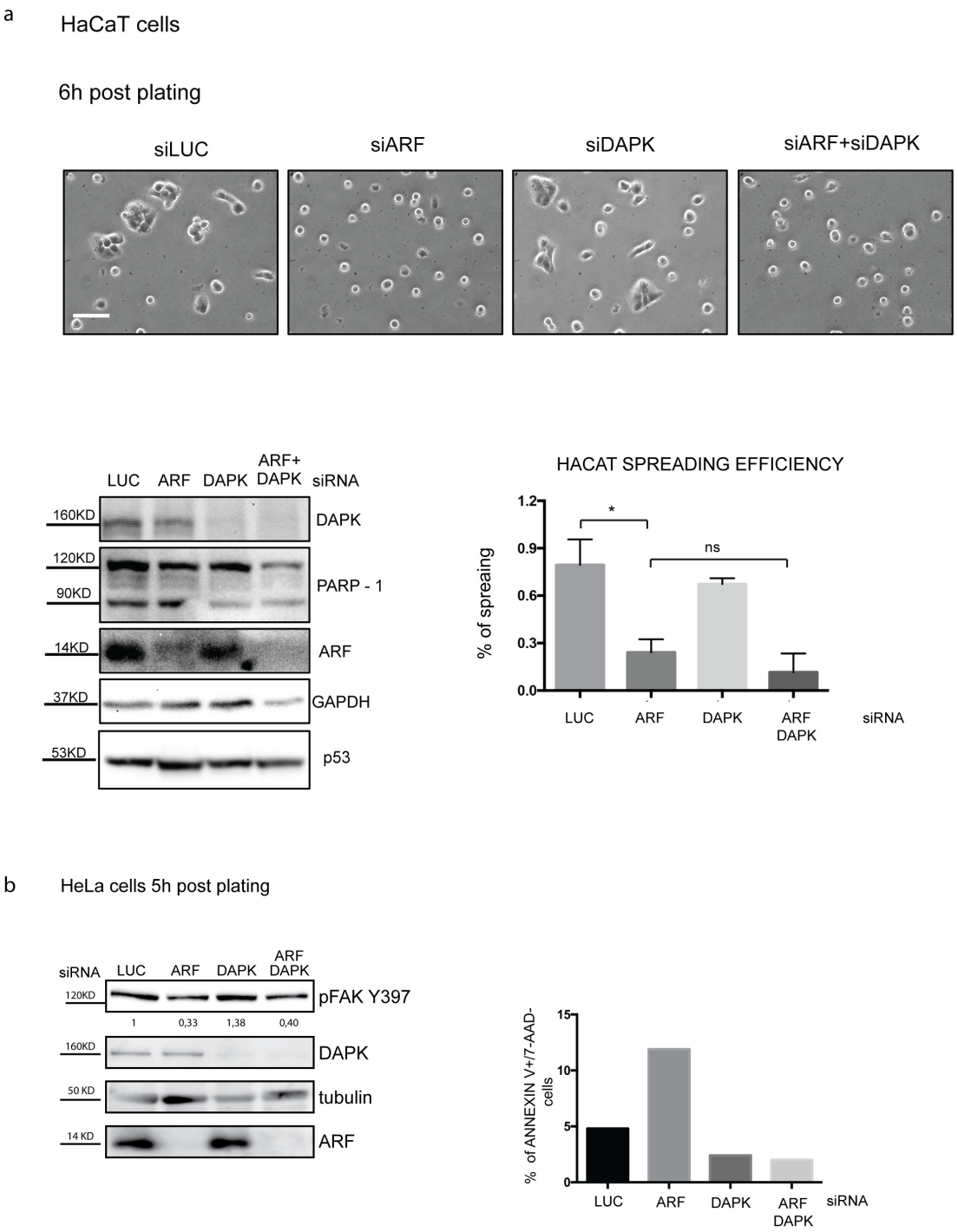

Fig. S9: ARF depletion induces apoptosis in HaCaT cells through a DAPK dependent mechanism. a) Cells grown in adherent conditions were treated with control or ARF and DAP kinase specific siRNA alone or simultaneously for 72hrs. Cells were replated as already described and analysed by western blot analysis and phase contrast microscopy. Representative images of replated cells (scale bar, 20μm). Graph represents cumulative data

expressed as a mean value ± SD of 2 independent experiments (biological replicates). Asterisk indicates statistically significant differences by unpaired two tailed Student T-test with *P<0.05; ns indicates no statistical (ns) difference. Silencing efficiency and vitality was analysed by western blot with anti ARF, anti DAPK, anti p53 and anti-PARP-1 antibody. GAPDH is a loading control. b) pFAK levels decrease are not induced by apoptosis (pFAK reduction in ARF KD cells is induced prior of apoptosis). HeLa cells grown in adherent conditions were treated with control or ARF and DAP kinase specific siRNA alone or simultaneously for 72hrs. Cells were replated as already described and analysed by western blot analysis. pFAK levels and silencing efficiency were analysed by western blot with anti pFAK Y397, ARF and DAPK antibodies. Tubulin is a loading control. Normalized pFAK Y397 band intensities, shown below each corresponding band, are expressed as fold enrichment respect to siLUC arbitrarily set to 1. Early apoptosis was evaluated 5h after plating by Annexin-V/7-AAD staining as previously described. Graph represents the percentage of apoptotic cells (PE-Annexin V positive and 7-AAD negative) observed in the indicated samples.

Fig S10

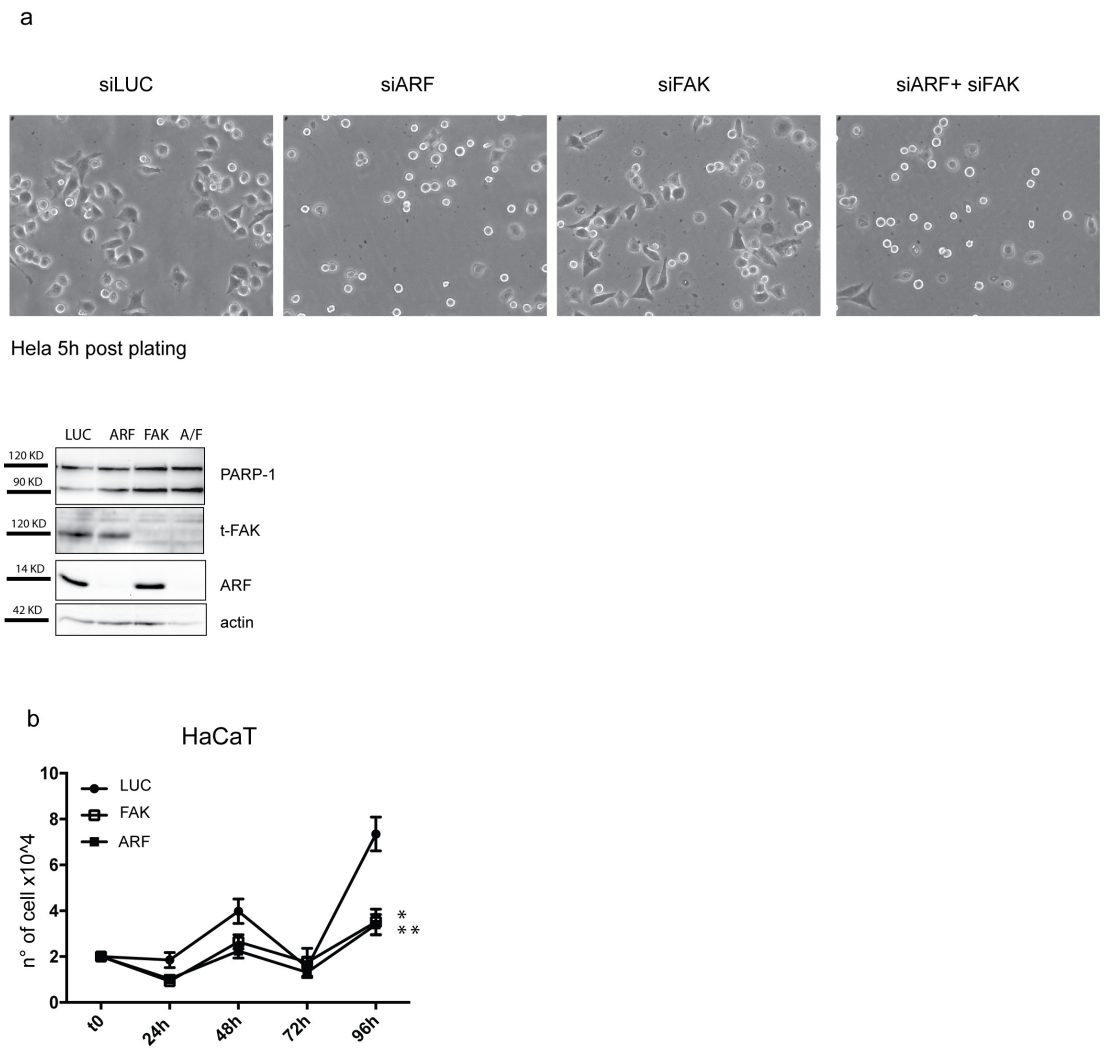

Fig. S10: FAK depletion does not affect cell morphology a) Contrast images of HeLa cells transiently transfected with the indicated siRNAs for 48hrs, detached by trypsinization and replated as previously described. Images were collected and analyzed by phase-contrast microscope 5 hrs post plating (scale bar, 30μm). Silencing efficiency and viability was analysed by western blot with anti-ARF, anti-t FAK and anti-PARP-1 antibody. Actin is a loading control. b) Growth curve of HaCaT cells treated with the indicated siRNA at different time points. Asterisks indicate statistically significant differences by unpaired two tailed T-test, between FAK and NC sirna treated cells *P= 0.0286, or between ARF and NC sirna treated cells **P=0.0108

CHAPTER 4

PKC DEPENDENT p14ARF PHOSPHORYLATION ON THREONINE 8 DRIVES CELL PROLIFERATION

Rosa Fontana, Felicia Sangermano, Viola Calabrò, Alessandra Pollice, Girolama La Mantia and Maria Vivo*

Dipartimento di Biologia, Università degli Studi di Napoli "Federico II"

Submitted in October 2017 on Scientific Reports

* corresponding author

maria.vivo@unina.it

ABSTRACT

ARF role as tumor suppressor has been challenged in the last years by several findings of different groups ultimately showing that its functions can be strictly context dependent. We previously showed that ARF loss in HeLa cells induces spreading defects, evident as rounding morphology of depleted cells, accompanied by a decrease of protein levels of phosphorylated Focal Adhesion Kinase (FAK) and anoikis. These data, together with previous finding that a PKC dependent signalling pathway can lead to ARF stabilization, led us to the hypothesis that ARF functions in cell proliferation might be regulated by phosphorylation. In line with this, we show here that upon cytoskeleton assembly ARF is induced through PKC activation. In line with this, constitutive-phosphorylated ARF mutant on the conserved threonine 8 (T8D) is able to mediate both cell spreading and FAK activation through inhibition of DAPK functions. Finally, ARF-T8D expression confers growth advantage to cells thus leading to the intriguing hypothesis that ARF phosphorylation could be a mechanism through which pro-proliferative or anti proliferative signals could be transduced inside the cells in both physiological and pathological conditions.

KEYWORDS: phosphorylation, stability, DAPK, FAK, anoikis

Introduction

The p14ARF protein, encoded by the INK4a/ARF locus, was initially described as a tumor suppressor that, in response to different oncogenic stimuli, by protecting p53 from proteasomal degradation, initiated a cell pathway leading to cell cycle block and/or apoptosis [1,2]. Further studies indicated that, apart from p53, ARF functionally interacts with a high number of factors, thus mediating cellular response also through p53-independent activities [3]. ARF has unexpectedly been found over expressed or stabilized in several types of cancers [4-6], to be involved in autophagy [7-9] and, recently, to have a role in protecting human melanocytes from free radicals arising upon mitochondrial dysfunction [10]. In addition to this, it also appears to play a role during development[11-13]. These observations led to the conclusion that, somehow, ARF role within the cell can be highly pleomorphic or context-dependent, ranging from halting cell growth in some cases to favour proliferation in others. We recently demonstrated that ARF plays an unexpected role in the cytoplasm in the organization of the cytoskeleton. During cell adhesion, ARF accumulates at sites of polymerized actin such as filopodia, where it co-localizes with and induces activation of the Focal Adhesion Kinase (FAK). Interesting this mechanism appears to be conserved in mouse. By aiding cytoskeleton assembly during spreading, ARF protects cells from anoikis blocking DAPK (Death Associated Protein Kinase) dependent apoptosis [14].

Our previous published data demonstrated that ARF is regulated through the activation of PKC pathway [15]. The involvement of phosphorylation in controlling ARF activities has been suggested by different experimental approaches [16-18 19]. Sequence prediction analysis shows that three PKC phosphorylation sites are present within ARF protein sequence, the threonine 8 and serine 52 in the functional active exon 1 beta encoded domain of the protein, while Serine 127 in the C-ter region of the protein. In vitro kinase assay shows that the protein can be specifically phosphorylated by PKC in vitro and that it is subjected to phosphorylation in vivo [15]. Mimicking the un-phosphorylatable status of the protein on Threonine 8 (T8A mutant), lying in the most conserved region of the protein, is highly unstable and displays the same ability of WT protein to restrain cell proliferation. Conversely, the T8D ARF mutant, that corresponds to the constitutive phosphorylation status of the protein, accumulates in the cytoplasm and is less efficient than the wt in halting cell growth. These data led to

the hypothesis that ARF function might be regulated by phosphorylation on this conserved residue. PKC plays important role in a number of cell functions [20]. Among these, it has been shown that it is involved in the regulation of cell morphology [21] through the phosphorylation of a high number of proteins involved in cell migration and in the generation of focal adhesion [22,23].

On the basis of this evidence, we sought to investigate if ARF role in cell spreading and its functional relation with FAK could be regulated by PKC activity. Here we show that during cytoskeleton remodelling induced by cell spreading, ARF protein levels increase in the cytoplasm through a PKC dependent mechanism. Mimicking the phosphorylation status of the protein is sufficient to drive its localization in the cytoplasm and rescue spreading defect of ARF silencing in HeLa cells as well as FAK phosphorylation, resulting in an increased proliferative ability. This is at least in part accomplished through the inhibition of DAPK negative effect on FAK during cell spreading. Taken together these data indicate that PKC activation can prime ARF involvement in cell spreading leading to increased FAK activation and cell proliferation.

Results

Threonine to Aspartic mutation in Threonine 8 is sufficient to affect ARF localization. The threonine 8 is highly conserved within ARF protein sequence. To analyse the relation between this site and the other PKC consensus sites, we constructed double (T8-S52) and triple (T8-S52-S127) mutants in which each single potential PKC site was replaced either with an alanine ("A" serie), that cannot be phosphorylated, or with an aspartic acid ("D"), that mimicks the phosphorylation status of the protein (as described in Vivo et al., 2013). ARF protein displays various degree of accumulation in nucleoli and/or scattered throughout the nucleoplasm [24,25]. We then tested if the inserted mutations could affect ARF subcellular localization by evaluating ARF subcellular localization in WT and mutant ARF proteins transfected U2OS cells by immunofluorescence. The experiment showed that both double and triple mutations mimicking the un-phosphorylatable status of the protein, although with small difference in the ratio of nucleoli/nucleoplasm staining (see Fig S1), show a localization pattern similar to WT and T8A mutant performed as control (Fig 1a). Transfection of the double and triple mutants of the "D" series showed for almost 50% (Fig 1a) of cells a nucleo-cytoplasmic localization of the protein, as reported for the T8D mutant [15]**.** These results suggest that Thr8 mutation alone is sufficient to determine ARF localization, while the other residues are not involved in this function. This allowed us to statistically analyse the role of T to A mutations vs T to D mutations. Comparing the percentages of nucleo-cytoplasmic localization of mutants of the A series with those of the D series, we obtained the plot shown in Fig 1b. We could observe how the localization of un-phosphorylatable ARF proteins (as well as of the WT) is significantly different from that of the "D" mutants. Collectively these results suggest that mimicking phosphorylation on threonine 8 alone is the signal sufficient to induce ARF accumulation in the cytoplasm.

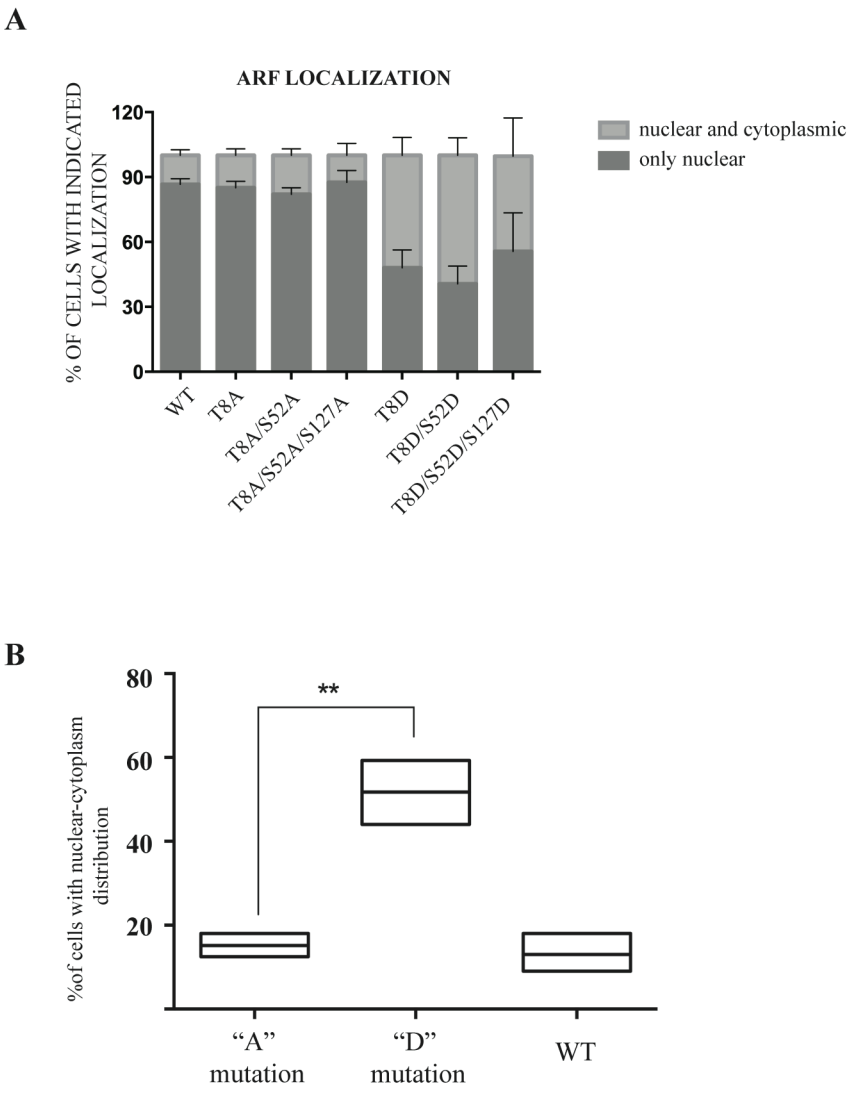

Figure 1. **Threonine 8 mutation affects ARF localization**

a) percentage of transfected cells showing nuclear and nuclear-cytoplasmic localization pattern + SD, n=3. b) nucleo-cytoplasmic localization of mutants of the A series vs D series. Analysis of variance by two-tailed paired t-test, ** P=0.0060.

ARF is induced during cytoskeleton reorganization through PKC activation. We recently put in light novel ARF functions in the organization of cytoskeleton. As T to D mutation on threonine 8 determines ARF localization in the cytoplasm together with its increased half-life [15] we now wondered if ARF phosphorylation could be the signal priming this ARF function. We first analysed if PKC activation could be detected during cytoskeleton remodelling. To this aim, we monitored levels of pPKC by western blot in HeLa cells during cell spreading. To follow spreading process over time, cytoplasmic protein extracts were collected from untreated (nt) and detached cells, as well as from replated cells five hours after seeding, when spreading process was almost completed. Cytoplasmic protein extracts were subjected to WB with an anti pPKC pan antibody that recognizes all the PKC isoforms phosphorylated at a carboxy-terminal residue homologous to serine 660 of PKC β II (activated pPKC). The experiment showed pPKC activation upon cell detachment (Fig 2a) mirrored by a parallel increase of ARF protein (Fig 2b, compare lane B with lane A and D). Treatment of cells with leptomycin B, that block nuclear export, does not block but rather increase ARF levels ruling out the hypothesis of re-localization of nuclear protein to the cytoplasm upon detachment (compare lane C with lane B Fig. 2b). As control, p53 levels increase in the nucleus of leptomycin treated cells.

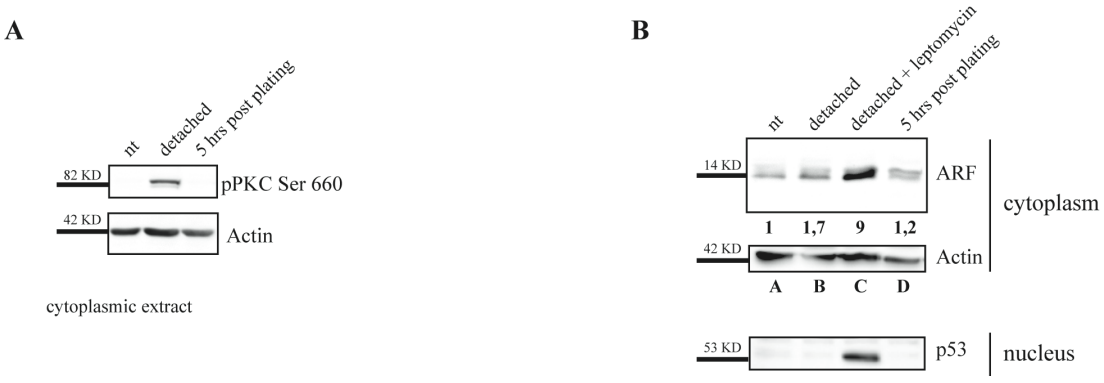

Figure 2. **Active PKC and ARF protein levels increase upon detachment** a) and b) Fractionated cellular extracts analysed by IB with anti pPKC Ser660, ARF, p53 and actin (loading control) antibodies. Representative western blots are shown. Quantification of ARF band intensities has been performed with Image J (See M&M for details) and are expressed as fold enrichment respect to NT sample, arbitrarily set to 1, using actin as normalizer.

To better analyse if the observed PKC activation is required to induce ARF increase, we knocked down PKC expression by RNA interference and analysed ARF cytoplasmic levels by western blot in HeLa cells. As control, cells were also treated with ARF specific siRNA. Untreated, control (siLuc and siSCR) and PKCalpha and ARF depleted cells were lysed 72hrs after transfection and subjected to subcellular fractionation. Cells were then subjected to trypsinization and divided in two aliquots. One was subjected to direct lysis (Fig 3a, detached cells), while the other replated and cells collected 24 hours after. In agreement with our hypothesis, ARF levels in PKC alpha depleted cells decrease with a similar efficiency to ARF depleted cells upon detachment, remaining low until 24h post plating. Western blot with anti-PKC antibody shows efficient silencing (Fig 3a)**,** although small fraction of PKC molecules is resistant to silencing in line with the notion that HeLa cells also expresses epsilon and delta PKC isoforms both recognized by this antibody (data not shown). Pharmacological inhibition of PKC with Bisindolylmaleimide I (Bim), an inhibitor of the catalytic subunit of PKC, confirms the requirement of catalytic active PKC in this process (Fig 3b)**.** Collectively these experiments show that during cytoskeleton remodelling PKC is activated resulting in increased cytoplasmic ARF protein levels.

A

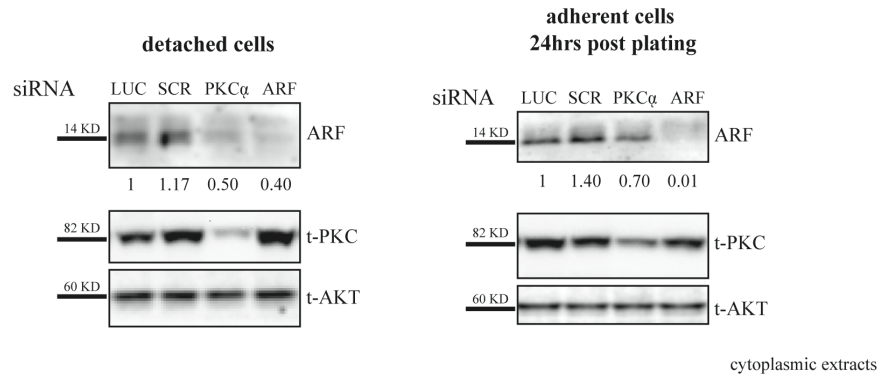

B

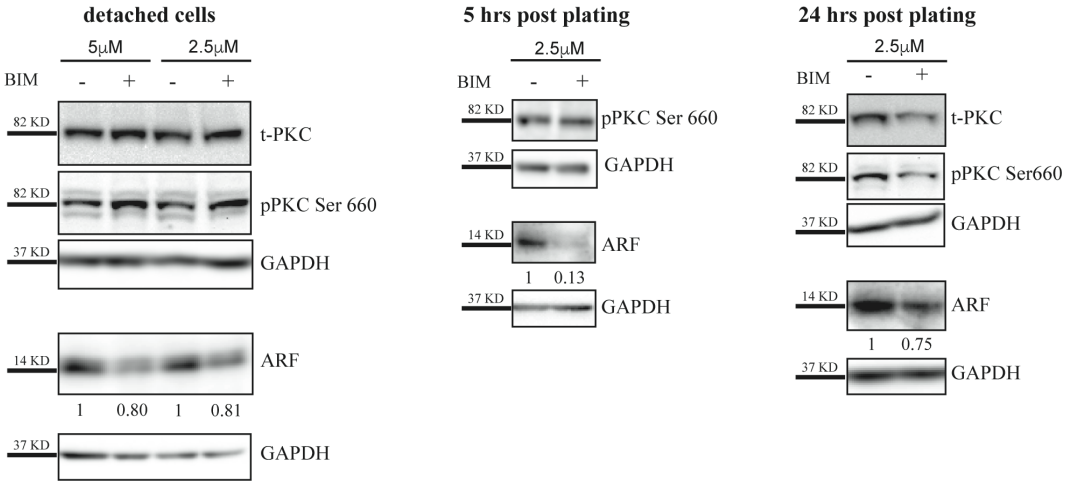

Figure 3. PKC activation is required for ARF induction

a) Cytoplasmic protein extracts of cells collected before or 24hours after replating analysed with anti ARF, t-PKC, and AKT (loading control) antibodies. ARF band intensities normalized versus AKT are shown as fold enrichment respect to siLUC. b) ARF and pPKC levels in HeLa cells treated with Bisindolylmaleimide I (Bim). Quantification of ARF band intensities has been performed as described.

ARF mutant mimicking T8 phosphorylation is involved in cell spreading. We previously showed that ARF silencing induces an evident morphological defect in different cell lines, including HeLa cells. In particular, due to inability of depleted cells to properly organize the cytoskeleton structures, cells display a striking round morphology [14].

In line with this, PKC depleted as well as Bim treated cells, showed spreading defects similarly to ARF depleted cells (Fig S2). We thus explored the hypothesis that ARF phosphorylation could have a role in this mechanism. We tested if mutant ARF proteins reintroduction is able to fulfil the function of the endogenous protein in rescue experiment. HeLa cells were transfected with either T8A or T8D expressing vectors and empty vector as control. Twenty-four hours later, cells were treated with scrambled or ARF-specific siRNA targeting endogenous ARF transcript. To monitor and compare spreading efficiency, cells were detached by trypsinization, replated and images of spreading cells collected 5hours post plating. The ability to spread was quantified and plotted as shown in Fig 4a. Less than 40% of ARF-depleted cells were able to properly spread both in empty vector and T8A expressing cells. In line with our hypothesis, T8D transfection is able to rescue spread morphology defect caused by ARF depletion in full. As shown previously rounding phenotype caused by ARF depletion is also accompanied by a decrease of FAK activation [14]. During cellular adhesion and upon integrin binding to the extra cellular matrix (ECM), FAK is activated through auto-phosphorylation of tyrosine 397 (Y397). This activation is followed by increased Src binding to FAK resulting in its massive phosphorylation onto several tyrosine residues within FAK sequence [26,27]. We thus preliminary checked if and which ARF mutant is also able to rescue FAK activation by western blot of crude extracts and of immunopurified FAK with anti pFAK antibodies. Results showed that in T8A expressing cells devoid of ARF expression, lower levels of both total and phosphorylated FAK are achieved, while no difference between siSCR and siARF could be detected in T8D expressing cells, mirroring the difference in spreading ability of the two mutants (Fig S3a). These experiments collectively suggest that T8A ARF mutant is impaired in both cytoskeleton re-organization and FAK stabilization. Interestingly, consequently to pFAK Y397 inactivation also downstream FAK phosphorylation events are impaired when endogenous ARF is replaced by T8A

mutant (Fig S3b). As ARF silencing affects both spreading and cell viability, we next checked if overexpression per se of either WT or mutant ARF proteins could induce an increase of FAK phosphorylation upon spreading induction. FAK immunoprecipitation followed by phospho-FAK immunodetection (both pFAKY397 and pTyr) showed that, although all proteins are able to positively induce FAK activation, T8D has the higher efficiency (Fig 4b).

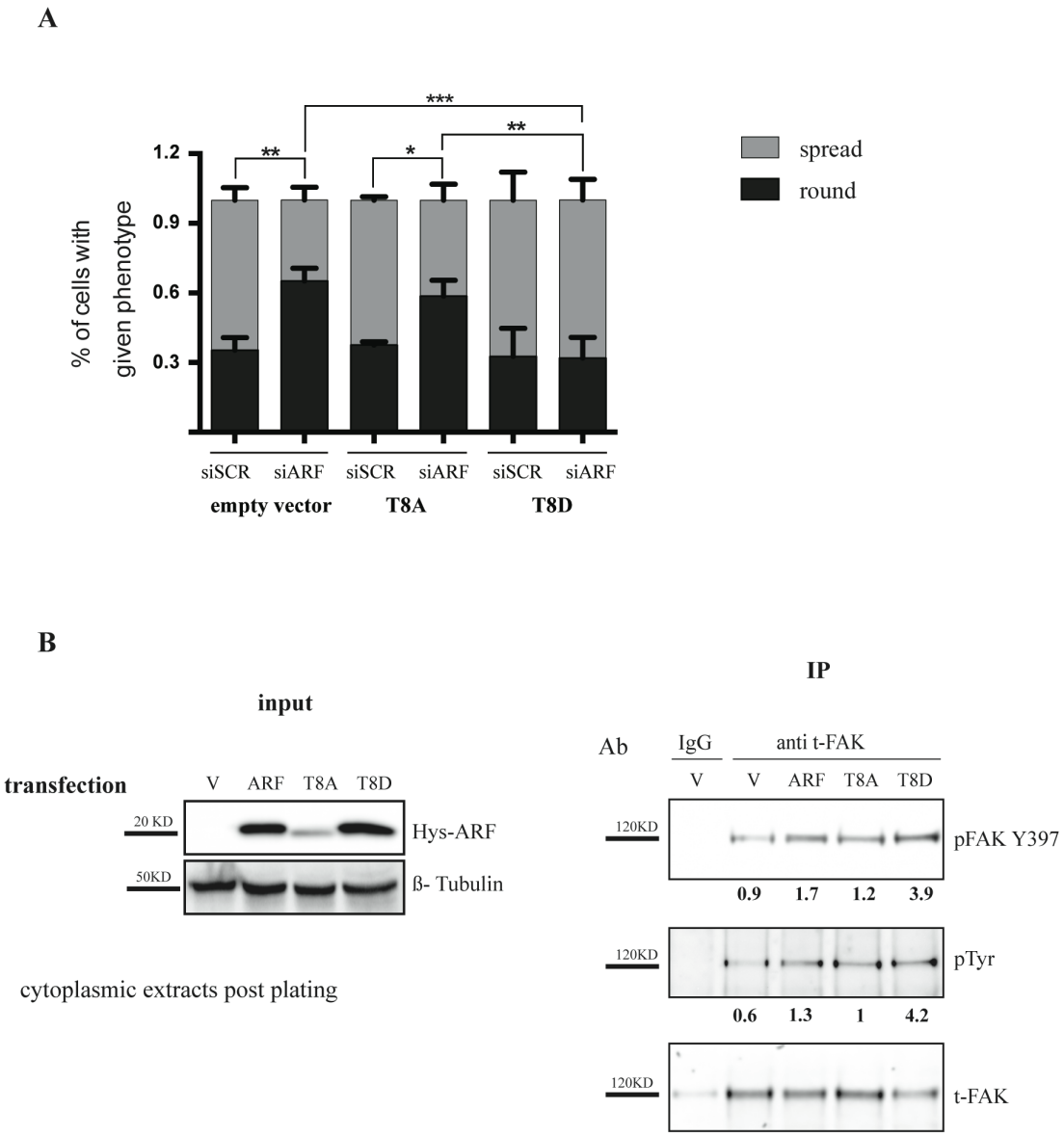

Figure 4. ARF T8D mutant rescues spreading defect of ARF depleted cells

a) Spreading efficiency of HeLa cells transiently transfected as indicated. Error bars represent SD with n=3. $P<0.05$ by two way Anova with Tukey correction. b) Cytoplasmic extracts of indicated transfected cells induced to spread were immuno-precipitated with anti t-FAK antibody and analysed by western blot with anti pFAK Y397, pTyrosine, t-FAK. Panels of input are also shown.

Mimicking ARF phosphorylation drives cell proliferation. Our previous studies showed that FAK activation correlates with ARF ability to confer pro-proliferative properties to cells. We thus analysed if T8D mutant, in virtue of its ability to strongly activate FAK phosphorylation, could also confer a growth advantage when expressed in cells. To this aim, HeLa cells, that endogenously express p14ARF protein and are characterized by inactivation of the p53 pathway, were transfected with plasmids encoding WT, T8A and T8D ARF mutants and empty vector (CMV) and cell growth was evaluated by comparing residual cell number 72hrs after transfection. Comparable number of viable cells were found in both empty vector and ARF transfected samples, thus meaning that ARF expression in these cells has no effect on cell growth, as expected [28-30]. Similar behaviour was observed in T8A expressing cells, while we constantly found an increased number of cells in T8D transfected samples (Fig. 5a). This suggested us that the T8D behaves as a constitutive active mutant. In addition, given that WT as well as the T8A protein has no effect on cell proliferation this could mean that in HeLa cells something can block this ARF function. Interestingly, in H1299 cells we did not observe differences in cell growth profiles of WT and mutant proteins transfected cells (Fig S3) and in this cell line we previously demonstrated that ARF-FAK pro-proliferative axis is interrupted due undetectable DAPK levels in this cell context. DAPK is a Serine/threonine kinase playing important roles in tumor suppression and apoptosis. We previously showed that ARF expression prevents DAPK mediated anoikis. It has been shown that FAK activation can be counteracted by DAP kinase expression [31,32] by disrupting signal transduction between integrin and FAK upon ECM interaction. We thus tested the hypothesis that ARF and/or T8D could be able to protect FAK by DAPK negative effect while T8A being less efficient. We thus checked the presence of DAPK in FAK immunoprecipitated samples, in presence of WT or T8A expression. Cells were transfected either with WT or T8A mutant expressing plasmids and 24h after transfection induced to spread. Immunoprecipitation was performed on cytoplasmic extracts followed by western blot with anti DAPK and anti-total FAK antibody. The experiment showed that a protein complex between FAK and DAPK is more abundant in T8A transfected cells than in WT transfected sample (Fig 5b, compare co-ip efficiency below DAPK panel).

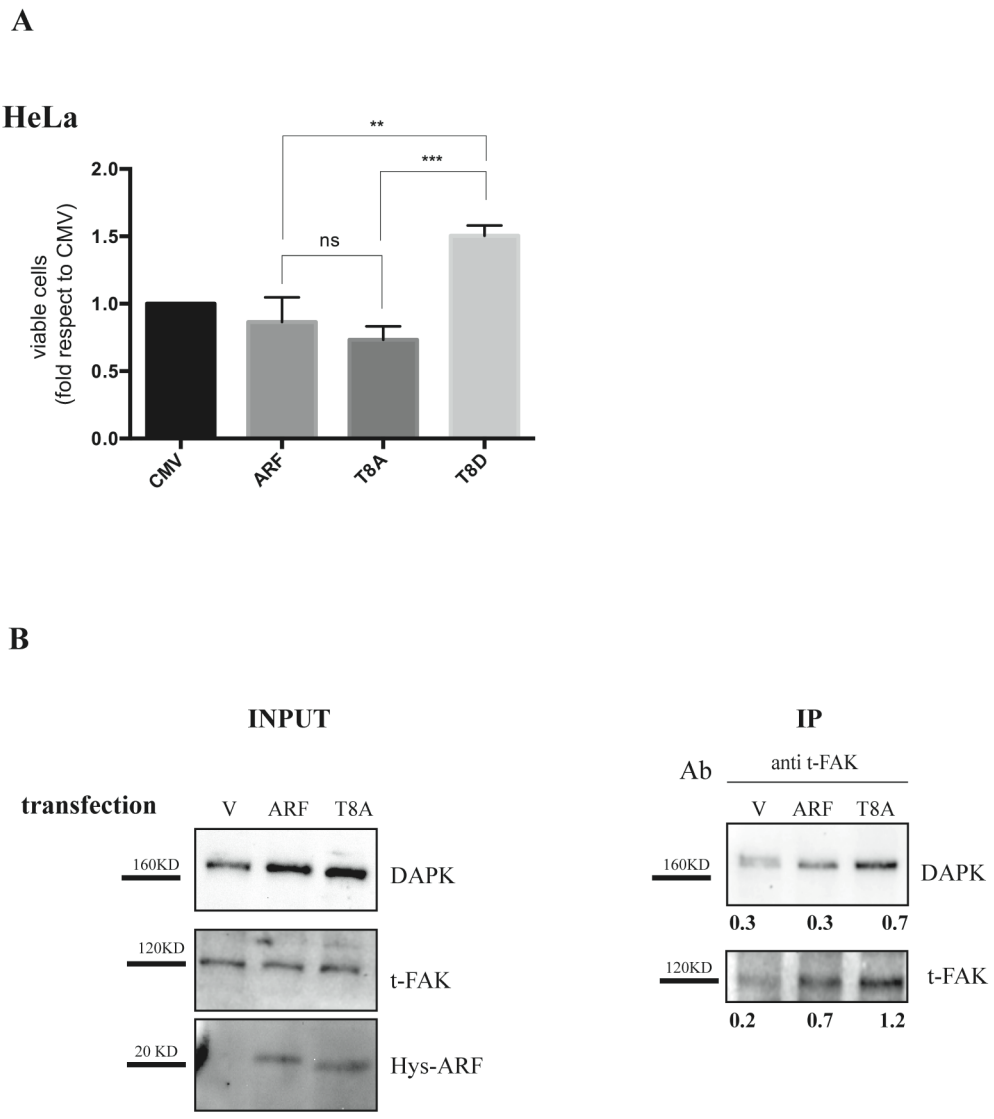

Figure 5. ARF T8D mutant promotes cell viability

a) The plots represent the relative cell number obtained with the indicated plasmids respect to empty vector set as 1. Error bars indicate S.D., n=3. $P<0.05$ by one-way ANOVA, using Tukey's multiple comparisons b) Cytoplasmic extracts of transfected cells were treated as described and were immuno-precipitated as indicated. FAK band intensities in IP panels are shown below each corresponding band. Panels of input are shown.

Discussion

Although to date the overwhelming majority of studies on ARF have focused on its tumor suppressor roles, a few of solid studies started to address the possibility that ARF might promote the survival of at least a subset of tumors. Here we presented evidences showing how p14ARF, upon PKC activation, is able to positively influence cell growth.

The PKC family consists of at least ten serine/threonine kinases playing a central role in cell proliferation, differentiation, survival and death [33,34]. We showed a novel and time-dependent ARF localization at focal adhesions thus highlighting ARF role in cytoskeleton organization upon cell spreading. We now further characterized this aspect, showing that this function is controlled by PKC activity and can account for some of ARF pro-proliferative capabilities. While mimicking a dephosphorylated status of the protein does not alter the nuclear localization of the protein, phosphorylation of Thr 8 is sufficient to lead to a strong increase of ARF protein levels in the cytoplasm. More interestingly, while the non-phosphorylatable mutant appears to retain the tumor suppressor properties of the WT protein, the T8D mutant instead behaves as a constitutive active mutant conferring pro-survival properties to the cells. Interestingly, also p21, a well-known tumor suppressor, has been shown to display that in some cell context its role as growth inhibitor has been substituted by promoting cell growth [35,36]. This behaviour, also shared by p14, suggests how the cell environment/status acts epistatically in directing tumor supressors functions.

The evidence that ARF functions can be thus modulated by phosphorylation events taking place on the conserved Threonine 8 leaves to the concept that ARF role in cell survival may more realistically depend on the cellular and/or tissue type and context, thus accounting for the controversy surrounding the topic.

By means of pharmacological studies, protein kinase C has been implicated as a key molecule involved in cell spreading and migration, in part through interaction with beta1-integrins [37-39]. Given the context dependency of ARF role within the cell, we focused on ARF function in cell spreading in a cell context in which ARF functions as tumor suppressor are blocked, thanks also to the inactivation of p53 pathway. Our data show that, during cytoskeleton remodelling induced by detachment, both the activated form of PKC and ARF protein levels increase in the cytoplasm. We previously showed

that ARF ability to favour cell spreading is accompanied by the transduction of growth signals arising from the integrin/FAK functional interaction [14]. We now added data showing that T8A can only in part rescue FAK activation, although this is not enough to allow cell spreading. This can be explained by decreased stability of the T8A mutant respect to T8D protein [15,40]. Our data depict a scenario in which during cell spreading or uncontrolled PKC activation, ARF stabilization and thus FAK activation could allow the pro-proliferative signal transduction within the cells. The so far described data, by reinforcing the previous finding, also provide a molecular mechanism based on the physical interaction between the Focal adhesion kinase and the DAPK. We found that during cell spreading DAPK interaction with FAK is un-favoured in presence of WT and T8D, being detectable only when cells express T8A.

Our data led us to conceive a model in which, during cell spreading and PKC activation, p14ARF protein levels increase in the cytoplasm. In this time frame, we found that DAPK interacts with FAK, maybe preventing its unwanted/unproper activation. The increase of ARF protein levels gradually interferes with this mechanism by displacing DAPK from FAK, and/or through the formation of an active complex in which DAPK inhibition of FAK is impaired (Fig 6). In absence of ARF phosphorylation we indeed observe a stable DAPK/FAK complex in which FAK is not activated, maybe sequestered from integrin binding. The more efficient immunoprecipitation of FAK in T8A transfected sample led us to speculate that ARF post-translational modification could somehow interfere with antibody binding to FAK thus favouring the hypothesis of the existence of a complex ARF-FAK-DAPK. This would indicate that the increased stability of ARF upon PKC activation wouldn't be sufficient to block DAPK activity, rather suggesting that a change in biochemical properties/binding ability of the protein to occurs. Further studies are needed to clarify this point. By interfering with the function of death associated protein kinase, ARF is able to induce full activation of the Focal Adhesion Kinase (Fig 6). This is associated with increased proliferation rate and higher level of ERK activation (data not shown) that mirrors FAK phosphorylation.

It has been widely reported that PKC mediated phosphorylation regulates composition and turn-over of focal adhesions where assembly and disassembly of actin fibres take place upon different environmental inputs. In particular, cellular motility and

invasivity, two of worst signals of cancer progression, are sustained by this highly dynamic phenomenon [20,41,42]. The involvement of PKC in tumor progression has thus gained recognition as potential therapeutic targets for the treatment of various malignancies. A deeper understanding of the PKC dependent ARF functions, both in physiological or pathological contexts, may provide useful informations about the environmental cues that determine ARF functions as tumor suppressor or tumor promoter.

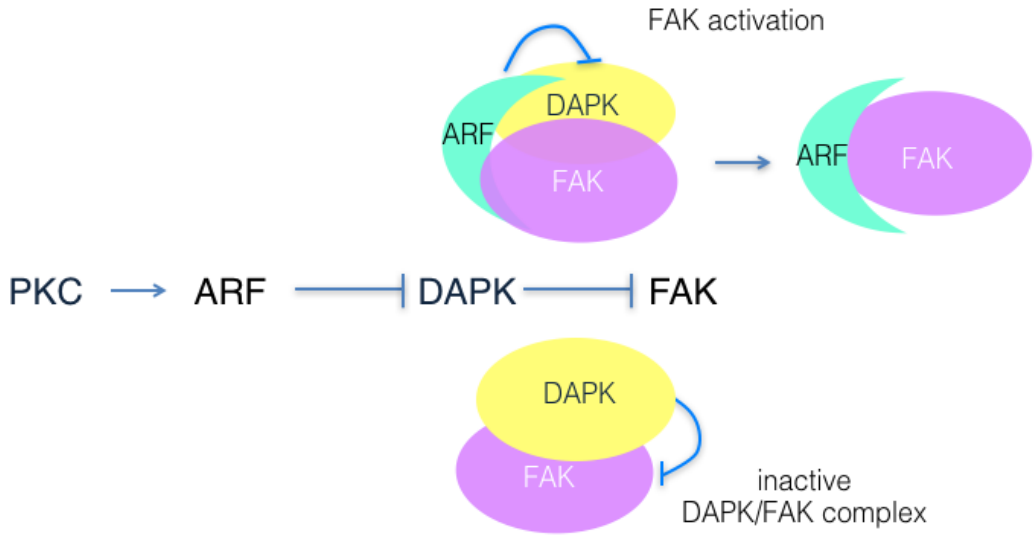

Figure 6. Upon PKC activation ARF stabilizes and activates the FAK. This is accomplished by disruption of the inactive FAK- DAPK complex.

Materials and Methods

Cell cultures, transfection and treatments HeLa cells were purchased from SIGMA. U2OS and H1299 were purchased from the American Type Culture Collection (ATTC) and authenticated by STR DNA Profiling Analysis. Cells were grown as described (Vivo et al., 2013) and were routinely tested for mycoplasma contamination by PCR based method and kept in culture for no more than 6 weeks after resuscitation. ARF mutants used in this study were generated as described (Vivo et al., 2013). The cells were transfected with Lipofectamine 2000 reagent (Invitrogen) or with electroporation (Neon transfection System, Life Technologies Carlsbad, CA, USA).

RNA interference experiments ARF siRNA (harbouring the stealth modification), that anneals in exon 1ß of p14ARF transcript, and scrambled siRNA (negative control) sequences have been reported in Vivo et al., 2009. PKC alfa and luciferase siRNAs are available by Qiagen (Hilden, Germany). For rescue experiment an ARF siRNA, that anneals in the 5'UTR region of ARF endogenous transcript, was used. All siRNAs were transfected using RNAiMAX reagent (Invitrogen). Rescue was performed as described in Vivo et al., 2017.

Treatments in this study were performed as follows: treatment with Bisindolylmaleimide I (from Calbiochem): 24 after plating, HeLa cells were treated either with DMSO or Bisindolylmaleimide I at 5 μM and 2,5 μM final concentrations for 2 hours then were detached by trypsin to synchronize the adhesion/spreading process. An aliquot of cells was harvested and total extracts prepared for subsequent analysis as described. Another aliquot of cells was replaced in presence of Bisindolylmaleimide I at 2,5 μM as final concentration and, after 5hrs and 24 hrs post plating, the cells were harvested and total extracts prepared as described.

Cell proliferation assay $4x10^6$ HeLa cells were transiently transfected by electroporation as described [14]. For H1299, $4x10^6$ cells were transiently transfected by electroporation with the indicated plasmid at 500ng as final concentration. After 72hrs from transfection, the cells were counted using ScepterTM automatic cell counter (Millipore) following the manufacturer's protocol. The data obtained were analysed using Scepter™ Software Pro (from Millipore). A multifunction plot representing the cell diameter (X-axis) and the cell counts (Y-axis) was created for each experiment and analysed. Cells were gated on the basis of their diameter: O1 for the whole cell

population, O2 for the cell population with low diameter (dead cells and debris) and O3 for the one with high diameter. The number of cells in O3 gate was used for the histogram showing in the figure.

Immunoprecipitation assays were performed either with cytoplasmic extracts or total cellular extracts (from 5×10^6 cells per sample). Subcellular fractionation was done as previously described (Vivo et al., 2013). For total cellular extracts, cells were harvested, lysed with Co-IP buffer (50mM Tris HCl pH 7.5, 150mM NaCl, 0,5% Np40, 5mM EDTA, 10% Glycerol, 100 mM NaF and 1mM NaVO3) and incubated with anti-FAK C-20 antibody as described in [14].

WB and antibodies Western blot (WB) analysis was performed as previously described (Vivo et al., 2013). Proteins were visualized by enhanced chemiluminescence (western blotting substrate Thermo Scientific). Images were acquired by ChemiDoc Imaging System equipped with a CCD camera (Bio-rad) through the Quantity One software. Representative experiments are shown for each protein. Full-length western blots are represented in supplementary information (supplemental data S5, S6, S7). Band intensities were quantified by ImageJ Software (http://imageJ.nih.gov/ij/ free software, NIH), normalized respect to loading control and reported as fold enrichment respect to control sample. List of antibodies used in this study: anti-ARF C-18, anti-p53 DO-1, anti-FAK C-20, anti-actin I-19, anti-ß-Tubulin H-235, anti-GAPDH 6C5 (Santa Cruz Biotechnology, Heidelberg, Germany), anti-pFAK (Tyr397) (BD Milan, Italy; clone 14 for wb), anti-DAPK-55 mouse monoclonal antibody (Sigma Aldrich, Milan, Italy); anti-pTyr 05-321 (Upstate from Millipore, Darmstadt, Germany), anti- PKC alpha, beta and gamma M110 (Millipore, Billerica, Massachusetts, Stati Uniti), anti- 6XHIS monoclonal antibody (Clontech), anti-AKT, anti-phospho PKC pan ßII Ser660 (Cell Signaling Technology, Leiden, The Netherlands).

IF and localization were performed as described in [15], using anti His antibody to detect WT and mutant ARF proteins.

Spreading efficiency HeLa cells were detached by trypsinization and replated at a density of $1x10^5$/ml. Live phase-contrast images were acquired using a Nikon Eclipse microscope (Tokyo, Japan) with 20x objective. 5 fields were randomly selected in the plates for each experimental point and images acquired with the Image Pro Plus

software (Media Cybernetics). To quantify the percentage of rounded cells, for each transfection point, we counted rounded (and adherent) cells in five different fields and pooled data from three to five experiments as described in [14].

Statistical analysis Data presented in this work derive from experiments performed at least in triplicate (biological replicates), except when differently stated. The sample size of each experimental point is reported in the relative figure legend, as well as the specific statistical analysis performed. In all the experiments in which single cells were analysed 5 to 10 fields were randomly selected in the coverslip for each experimental point. t-test and ANOVA were performed using GraphPad Prism 5.0 software.

ABBREVIATIONS

PKC Protein Kinase C; ARF Alternative Reading Frame; FAK Focal Adhesion Kinase; DAPK Death Associated Protein Kinase; ECM Extra Cellular Matrix; Bim Bisindolylmaleimide I.

AUTHOR CONTRIBUTIONS

M. V. and G.L.M. designed the research and wrote the paper with inputs from R.F., A.P., V. C.,

R.F., performed majority of the experiments with help from F.S. and M.V.

M.V. and G.L.M. supervised the project.

ACKNOWLEDGMENTS AND FUNDING

This work was supported by AIRC (Associazione Italiana Ricerca sul Cancro). The funder had no role in study design, data collection and analysis, decision to publish, or preparation of the manuscript.

CONFLICTS OF INTEREST

The authors declare that they have no conflict of interest.

REFERENCES

1 Kamijo, T., Bodner, S., van de Kamp, E., Randle, D. H. & Sherr, C. J. Tumor spectrum in ARF-deficient mice. *Cancer research* **59**, 2217-2222 (1999).

2 Sherr, C. J. & Weber, J. D. The ARF/p53 pathway. *Current opinion in genetics & development* **10**, 94-99 (2000).

3 Pollice, A., Vivo, M. & La Mantia, G. The promiscuity of ARF interactions with the proteasome. *FEBS letters* **582**, 3257-3262, doi:10.1016/j.febslet.2008.09.026 (2008).

4 Chen, Z. *et al.* Differential p53-independent outcomes of p19(Arf) loss in oncogenesis. *Science signaling* **2**, ra44, doi:10.1126/scisignal.2000053 (2009).

5 Ferru, A. *et al.* The status of CDKN2A alpha (p16INK4A) and beta (p14ARF) transcripts in thyroid tumour progression. *British journal of cancer* **95**, 1670-1677, doi:10.1038/sj.bjc.6603479 (2006).

6 Humbey, O. *et al.* The ARF tumor suppressor can promote the progression of some tumors. *Cancer research* **68**, 9608-9613, doi:10.1158/0008-5472.CAN-08-2263 (2008).

7 Budina-Kolomets, A., Hontz, R. D., Pimkina, J. & Murphy, M. E. A conserved domain in exon 2 coding for the human and murine ARF tumor suppressor protein is required for autophagy induction. *Autophagy* **9**, 1553-1565, doi:10.4161/auto.25831 (2013).

8 Pimkina, J. & Murphy, M. E. ARF, autophagy and tumor suppression. *Autophagy* **5**, 397-399 (2009).

9 Reef, S. *et al.* A short mitochondrial form of p19ARF induces autophagy and caspase-independent cell death. *Molecular cell* **22**, 463-475, doi:10.1016/j.molcel.2006.04.014 (2006).

10 Christensen, C. *et al.* A short acidic motif in ARF guards against mitochondrial dysfunction and melanoma susceptibility. *Nature communications* **5**, 5348, doi:10.1038/ncomms6348 (2014).

11 Gromley, A., Churchman, M. L., Zindy, F. & Sherr, C. J. Transient expression of the Arf tumor suppressor during male germ cell and eye development in Arf-Cre reporter mice. *Proceedings of the National Academy of Sciences of the*

United States of America **106**, 6285-6290, doi:10.1073/pnas.0902310106 (2009).

12 Li, C., Finkelstein, D. & Sherr, C. J. Arf tumor suppressor and miR-205 regulate cell adhesion and formation of extraembryonic endoderm from pluripotent stem cells. *Proceedings of the National Academy of Sciences of the United States of America* **110**, E1112-1121, doi:10.1073/pnas.1302184110 (2013).

13 van Oosterwijk, J. G., Li, C., Yang, X., Opferman, J. T. & Sherr, C. J. Small mitochondrial Arf (smArf) protein corrects p53-independent developmental defects of Arf tumor suppressor-deficient mice. *Proceedings of the National Academy of Sciences of the United States of America* **114**, 7420-7425, doi:10.1073/pnas.1707292114 (2017).

14 Vivo, M. *et al.* p14ARF interacts with the focal adhesion kinase and protects cells from anoikis. *Oncogene*, doi:10.1038/onc.2017.104 (2017).

15 Vivo, M. *et al.* Mimicking p14ARF phosphorylation influences its ability to restrain cell proliferation. *PloS one* **8**, e53631, doi:10.1371/journal.pone.0053631 (2013).

16 Inoue, R. & Shiraishi, T. PKCalpha is involved in phorbol ester TPA-mediated stabilization of p14ARF. *Biochemical and biophysical research communications* **330**, 1314-1318, doi:10.1016/j.bbrc.2005.03.117 (2005).

17 Raveh, T., Droguett, G., Horwitz, M. S., DePinho, R. A. & Kimchi, A. DAP kinase activates a p19ARF/p53-mediated apoptotic checkpoint to suppress oncogenic transformation. *Nature cell biology* **3**, 1-7, doi:10.1038/35050500 (2001).

18 Vivo, M. *et al.* Downregulation of DeltaNp63alpha in keratinocytes by p14ARF-mediated SUMO-conjugation and degradation. *Cell cycle* **8**, 3537-3543 (2009).

19 di Tommaso, A. *et al.* Residues in the alternative reading frame tumor suppressor that influence its stability and p53-independent activities. *Experimental cell research* **315**, 1326-1335, doi:10.1016/j.yexcr.2009.01.010 (2009).

20 Rosse, C. *et al.* PKC and the control of localized signal dynamics. *Nature reviews. Molecular cell biology* **11**, 103-112, doi:10.1038/nrm2847 (2010).

21 Leduc, C. & Etienne-Manneville, S. Regulation of microtubule-associated motors drives intermediate filament network polarization. *The Journal of cell biology* **216**, 1689-1703, doi:10.1083/jcb.201607045 (2017).

22 Anilkumar, N., Parsons, M., Monk, R., Ng, T. & Adams, J. C. Interaction of fascin and protein kinase Calpha: a novel intersection in cell adhesion and motility. *The EMBO journal* **22**, 5390-5402, doi:10.1093/emboj/cdg521 (2003).

23 Ng, T. *et al.* PKCalpha regulates beta1 integrin-dependent cell motility through association and control of integrin traffic. *The EMBO journal* **18**, 3909-3923, doi:10.1093/emboj/18.14.3909 (1999).

24 Llanos, S., Clark, P. A., Rowe, J. & Peters, G. Stabilization of p53 by p14ARF without relocation of MDM2 to the nucleolus. *Nature cell biology* **3**, 445-452, doi:10.1038/35074506 (2001).

25 Rodway, H., Llanos, S., Rowe, J. & Peters, G. Stability of nucleolar versus non-nucleolar forms of human p14(ARF). *Oncogene* **23**, 6186-6192, doi:10.1038/sj.onc.1207854 (2004).

26 Frame, M. C., Patel, H., Serrels, B., Lietha, D. & Eck, M. J. The FERM domain: organizing the structure and function of FAK. *Nature reviews. Molecular cell biology* **11**, 802-814, doi:10.1038/nrm2996 (2010).

27 Serrels, B. *et al.* A complex between FAK, RACK1, and PDE4D5 controls spreading initiation and cancer cell polarity. *Current biology : CB* **20**, 1086-1092, doi:10.1016/j.cub.2010.04.042 (2010).

28 Calabro, V., Parisi, T., Di Cristofano, A. & La Mantia, G. Suppression of Ras-mediated NIH3T3 transformation by p19ARF does not involve alterations of cell growth properties. *Oncogene* **18**, 2157-2162, doi:10.1038/sj.onc.1202532 (1999).

29 Pollice, A. *et al.* TBP-1 protects the human oncosuppressor p14ARF from proteasomal degradation. *Oncogene* **26**, 5154-5162, doi:10.1038/sj.onc.1210313 (2007).

30 Vivo, M. *et al.* The human tumor suppressor arf interacts with spinophilin/neurabin II, a type 1 protein-phosphatase-binding protein. *The Journal of biological chemistry* **276**, 14161-14169, doi:10.1074/jbc.M006845200 (2001).

31 Kuo, J. C., Wang, W. J., Yao, C. C., Wu, P. R. & Chen, R. H. The tumor suppressor DAPK inhibits cell motility by blocking the integrin-mediated polarity pathway. *The Journal of cell biology* **172**, 619-631, doi:10.1083/jcb.200505138 (2006).

32 Wang, W. J., Kuo, J. C., Yao, C. C. & Chen, R. H. DAP-kinase induces apoptosis by suppressing integrin activity and disrupting matrix survival signals. *The Journal of cell biology* **159**, 169-179, doi:10.1083/jcb.200204050 (2002).

33 Bosco, R. *et al.* Fine tuning of protein kinase C (PKC) isoforms in cancer: shortening the distance from the laboratory to the bedside. *Mini reviews in medicinal chemistry* **11**, 185-199 (2011).

34 Breitkreutz, D., Braiman-Wiksman, L., Daum, N., Denning, M. F. & Tennenbaum, T. Protein kinase C family: on the crossroads of cell signaling in skin and tumor epithelium. *Journal of cancer research and clinical oncology* **133**, 793-808, doi:10.1007/s00432-007-0280-3 (2007).

35 Evangelou, K., Galanos, P. & Gorgoulis, V. G. The Janus face of p21. *Molecular & cellular oncology* **3**, e1215776, doi:10.1080/23723556.2016.1215776 (2016).

36 Galanos, P. *et al.* Chronic p53-independent p21 expression causes genomic instability by deregulating replication licensing. *Nature cell biology* **18**, 777-789, doi:10.1038/ncb3378 (2016).

37 Parsons, M. *et al.* Site-directed perturbation of protein kinase C- integrin interaction blocks carcinoma cell chemotaxis. *Molecular and cellular biology* **22**, 5897-5911 (2002).

38 Zhang, X. A., Bontrager, A. L. & Hemler, M. E. Transmembrane-4 superfamily proteins associate with activated protein kinase C (PKC) and link PKC to specific beta(1) integrins. *The Journal of biological chemistry* **276**, 25005-25013, doi:10.1074/jbc.M102156200 (2001).

39 Li, Q. *et al.* Tetraspanin CD151 plays a key role in skin squamous cell carcinoma. *Oncogene* **32**, 1772-1783, doi:10.1038/onc.2012.205 (2013).

40 Vivo, M. *et al.* MDM2-mediated degradation of p14ARF: a novel mechanism to control ARF levels in cancer cells. *PloS one* **10**, e0117252, doi:10.1371/journal.pone.0117252 (2015).

41 Ivaska, J. *et al.* PKCepsilon-mediated phosphorylation of vimentin controls integrin recycling and motility. *The EMBO journal* **24**, 3834-3845, doi:10.1038/sj.emboj.7600847 (2005).

42 Rosse, C. *et al.* Binding of dynein intermediate chain 2 to paxillin controls focal adhesion dynamics and migration. *Journal of cell science* **125**, 3733-3738, doi:10.1242/jcs.089557 (2012).

Supplementary information

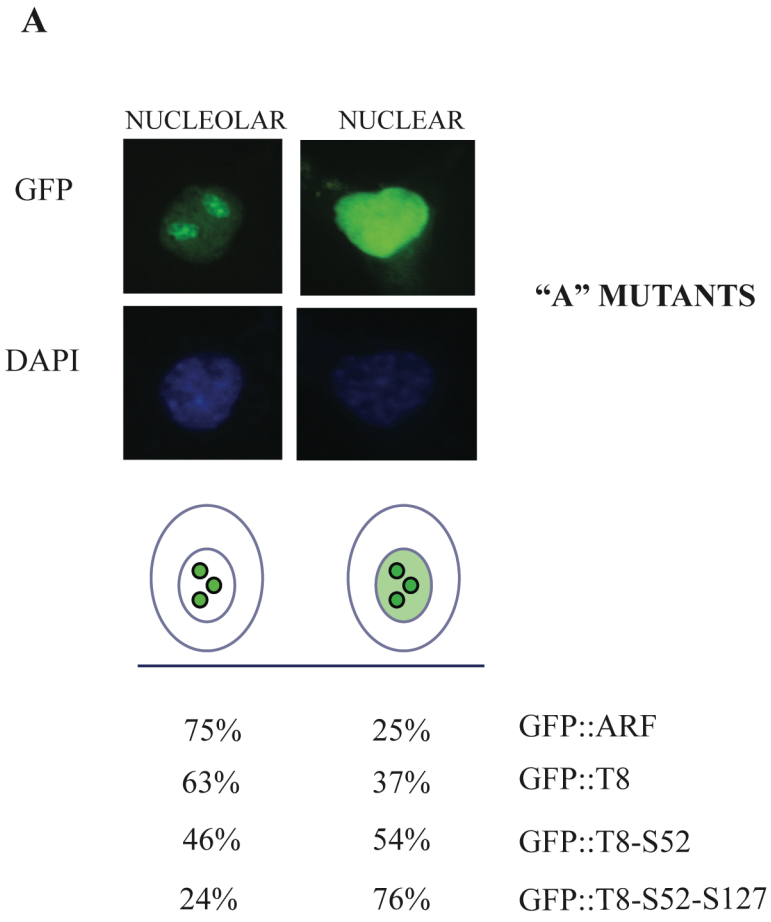

Figure S1. GFP tagged WT and mutant ARF proteins of the "A" series were expressed in NIH3T3 cells by transient transfection and subcellular localization analysed by fluorescence microscopy 24hrs later. Images were taken with a Nikon fluorescent microscope. a)

Visualization of the two different WT ARF localization patterns are shown on the top, while a schematic image of the nuclear and nucleolar staining is shown below IF panels. b) The histogram, representing the mean of three independent experiments, reports the percentage of transfected cells showing diffuse nuclear localization pattern. Standard deviations are also shown.

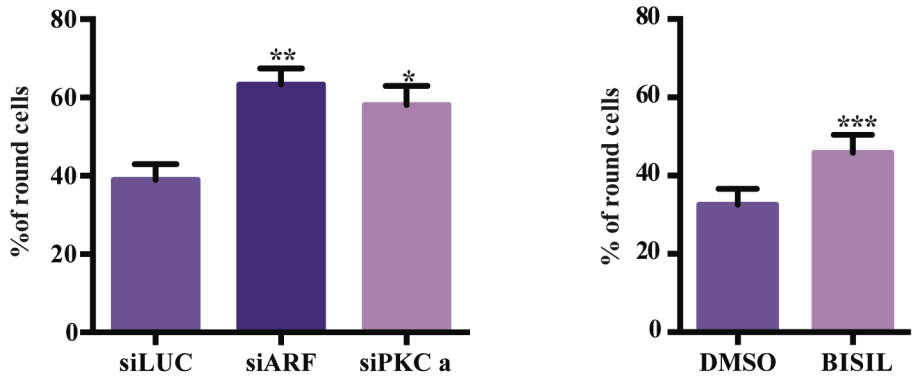

Figure S2. a) Spreading efficiency of HeLa cells transiently transfected with the indicated siRNAs for 48hrs, detached by trypsinization and replated at a density of $1x10^5$/ml. Cumulative data are expressed as a mean value ± SEM of 4 independent experiments. Number of cells analyzed for each experiment: siSCR (200), siARF (200), siPKC (200). Asterisks indicate statistically significant differences by RM One-way Anova with Tukey's correction between siARF and siPKC and the control siSCR, $P < 0.05$. b) spreading efficiency of Hela cells treated with BIM as described in Figure 4. Cumulative data are expressed as a mean value ± SEM of 5 independent experiments. Asterisks indicate statistically significant differences by two-tailed paired t-test. P=0.002

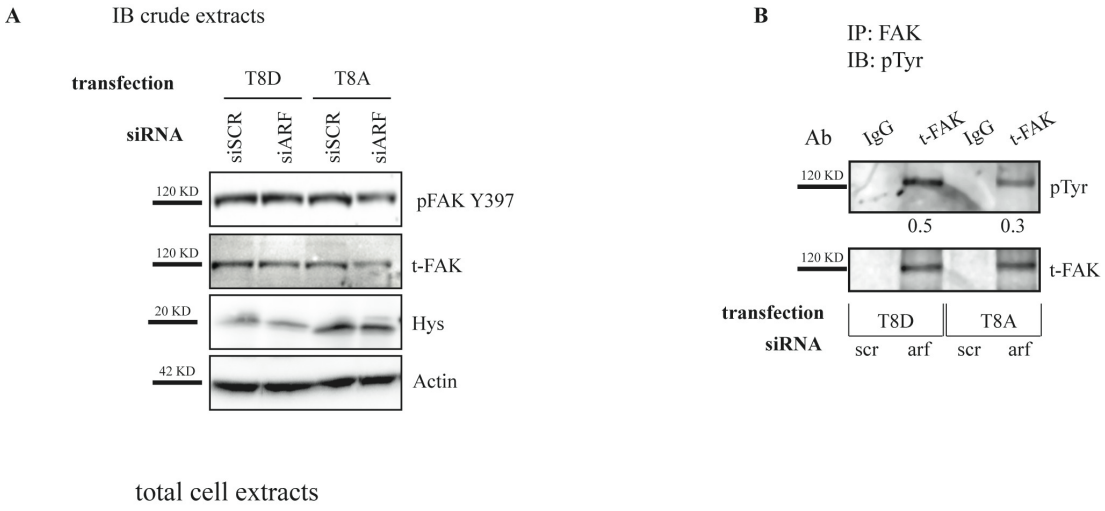

Figure S3. Immunoprecipitated cell extracts were analysed by IB as indicated. Panels of inputs are shown on the right. FAK band intensities in IP panels are shown below each corresponding band, and are expressed as ratio between pFAK and tFAK band intensity. Representative western blots are shown.

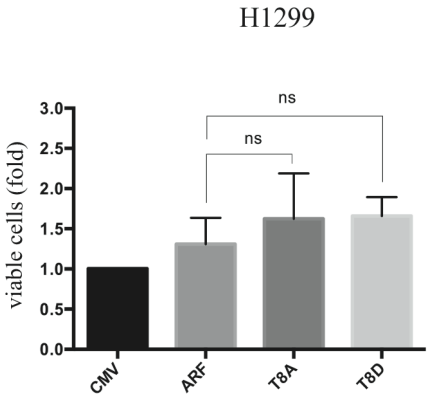

Figure S4. Equal number of H1299 cells were transfected with the indicated ARF and mutant expression vectors and empty vector as control (CMV). Seventy-two hours after transfection the cell number in each sample was analysed with the Scepter cell count as described in M & M section. The plot represents the relative cell number obtained with the indicated plasmids respect to the empty vector set arbitrarily as 1. Error bars indicate s.d. n=3 independent experiments. Asterisks indicate statistically significant differences. P values were determined with one-way ANOVA, using Tukey's multiple comparisons test ($P<0.05$)

CHAPTER 5

CONCLUSIONS

In primary cells, $p14^{ARF}$ is not detectably expressed, but in response to aberrantly sustained and increased levels of mitogenic signals, ARF transcription is induced and this protein promotes cell cycle arrest and/or apoptosis through both p53 dependent and independent pathways. Moreover, since its initial discovery, ARF was described with a prevalent nucleo/nucleolar localization, playing an important role in its stability and tumor suppressor functions.

Nevertheless, recently, different groups demonstrated that ARF is overexpressed in a significant fraction of human tumors (Eischen et al., 1999; Sànchez-Aguilera et al., 2002, Basso et al., 2005) and, in specific cases, a strong delocalization to the cytoplasm has been observed (Ferru et al., 2006). In line with this, Vivo and colleagues (2013) reported for the first time that, in some cell lines expressing high levels of $p14^{ARF}$, PKC activation induces its stabilization through phosphorylation and the protein predominantly accumulates in the cytoplasm, where it appears not able to efficiently control cell proliferation.

On the other hand, it has been suggested by several reports (Humbey et al., 2008; Chen et al., 2010; Xie et al., 2014; Xie et al., 2016) that in some tumors ARF can perform a pro-proliferative function depending on cellular and genetic context and on the state of tumor aggressiveness, through molecular mechanisms not yet clear.

Data presented in this thesis and in the provided papers add additional support to this new pro-proliferative role of ARF, giving further insight about the molecular mechanism.

We demonstrated for the first time that ARF promotes cell survival helping cells to spread. During cytoskeleton remodelling induced by cell spreading, we observed a strong PKC activation resulting in an ARF protein levels increase and stabilization in the cytoplasm. Along with this phenomenon, ARF is recruited to cell periphery at

points of focal adhesions, where co-localizes and interacts with the active Focal Adhesion Kinase (pFAK^{Y397}). Accordingly, we demonstrated that ARF silencing, causes spreading defects and actin cytoskeleton disorganization in both tumoral (Hela and H1299) and immortalized (HaCaT) cells. Interestingly, we also found that the reduced expression as well as catalytic activity inhibition of PKC causes spreading defects similarly to ARF depleted cells, highlighting the involvement of ARF phosphorylated form in this new function in adhesion/spreading process.

In line with this, our rescue experiments show that the ARF T8D mutant (mimicking the phosphorylation status of the protein) displaying a nucleo/cytoplasmic localization, promotes cell spreading in ARF depleted cells, unlike the T8A version, which is mainly localized in the nucleus and preserves the ARF tumor suppressor functions.

ARF-FAK-DAPK circuit

The observation that, during spreading, ARF silencing causes a reduction of FAK tyrosine phosphorylation and apoptotic cell death in HeLa and HaCaT cells led us to deeply investigate this relation. We reported that the cytoskeleton disorganization induced by ARF KD causes anoikis through a mechanism dependent on the Death-Associated Protein Kinase. The DAPK is a pro-apoptotic serine/threonine kinase, that is activated and induces apoptosis following cytoskeleton–matrix disengagement (Chen et al., 2006; Kuo et al., 2003). A link between ARF and DAPK has been previously shown. In particular, DAPK can promote ARF phosphorylation *in vitro* leading to p53 dependent apoptosis *in vivo* (Raveh et al., 2001). However, we demonstrated here that ARF silencing results in a DAPK increase upon cell detachment, thus suggesting that p14^{ARF} blocks DAPK functions avoiding DAPK-dependent cell death. In line with our data, it has been reported that DAPK-dependent apoptosis is accompanied by a specific decrease of FAK tyrosine phosphorylation (Wang et al., 2002). Furthermore, in H1299, where DAPK expression is undetectable, we do observe neither apoptosis nor pFAK decrease upon ARF depletion. Finally, restoration of DAPK expression in ARF KD H1299 cells induces a strong decrease of FAK levels and cell death, in line with what we observed in HeLa cells. It is worth to report that, during cell spreading, DAPK interaction with FAK is favoured when cells express T8A, suggesting that in absence of ARF phosphorylation a stable DAPK/FAK

complex in which FAK is not activated exists. This model is supported by our data showing that only the T8D protein expression but not the T8A version, is able to induce pFAK stabilization and cell proliferation.

On this basis, we propose that, far from being simply inactive to restrain cell growth, ARF confers pro-survival properties by helping some tumor cells to spread and protecting them from anoikis, through inhibition of DAPK-induced apoptosis and stabilization of FAK (Fig.4).

One of the main way through which ARF regulates the function of its binding partners is promoting their sumoylation (Sherr, 2006). In agreement with this, we demonstrated that ARF promotes FAK sumoylation, which has been associated with increased protein stability, catalytically activation and preferential nuclear localization (Kadare et al., 2003). In the nucleus, FAK impairs transcription of p53-dependent genes either through the direct binding with p53 or promoting its proteasome degradation by MDM2 (Golubovskaya et al., 2005; Lim et al., 2008).

Interestingly, our data show that in Hela cells, although p53 pathway is partially disabled by HPV-encoded E6 mediated degradation, an increase of p53 protein levels and of its transcriptional targets Puma and Apaf-1 (preliminary data not shown) occurs upon ARF depletion, suggesting that the observed apoptosis induction could be in part mediated through p53. In line with this, it has been observed that also during spermatogenesis, ARF expression transiently occurs and prevents p53-dependent apoptosis (Gromley et al., 2009).

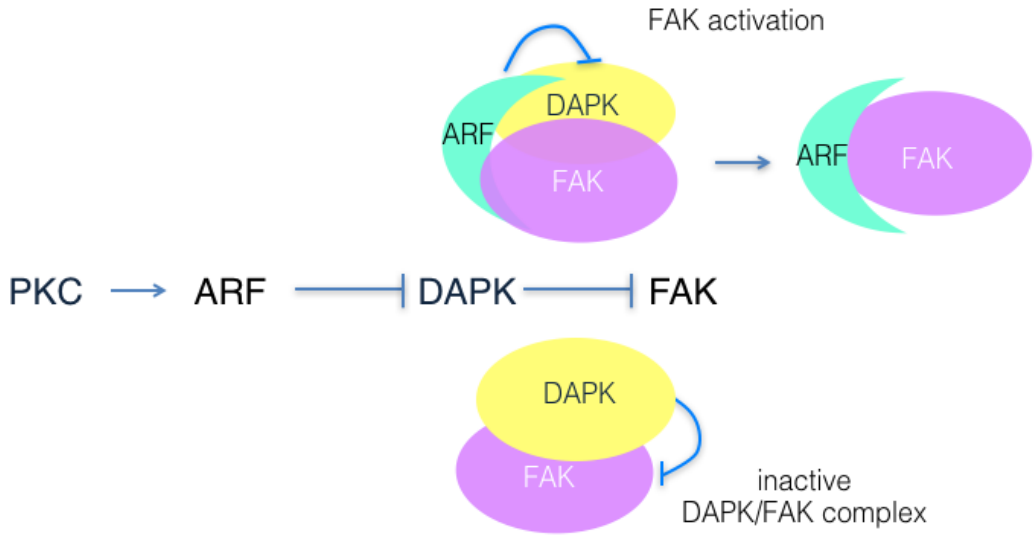

Figure 4: Schematic model of the ARF-DAPK-FAK pathway.

Different groups demonstrated that ARF induces autophagy, a molecular mechanism that seems to be a double-edged sword in cancer because can have both pro- and anti-metastatic roles depending on cellular context and state of tumor aggressiveness. While Abida and Gu (2008) reported that autophagy contributes to ARF tumor suppression functions, Humbey and colleagues (2008) demonstrated that autophagy induced by $p19^{ARF}$ is necessary to promote lymphoma survival both *in vitro* than *in vivo*, in response to nutrient deprivation. These data suggest that ARF induced autophagy may be cytoprotective only in specific type of tumors.

Interestingly, we demonstrated that the conserved domain 100-132 (in ARF exon 2 encoded region), that it has been described to be necessary to induce autophagy (Budina-Kolomets et al., 2013), is able to promote FAK activation and cell survival, during spreading (Vivo et al., 2017).

Autophagy can promote metastatic processes protecting matrix-detached epithelial cells from anoikis (Fung et al., 2008). In line with these data, Sandilands and colleagues (2011) demonstrated that in detached cells or in cells with low level of activated FAK, the block of autophagy induces anoikis.

Since it has also been reported that FAK can induce autophagy through ERK/JNK/c-JUN signalling cascade (Nollet and Miranti, 2013), we speculate that, in response to different stress, such as the cytoskeleton re-organization during spreading, ARF can induce autophagy promoting FAK activation to safeguard tumor cell survival.

On the other hands, it has been reported that AuTophaGy-related (ATG) proteins (a group of proteins required for progression through specific stages of the autophagy pathway) are localized at focal adhesions where they show co-localization with FAK (Sandilands et al., 2011). Moreover, the basal autophagy regulates cell spreading, in particular cell protrusion extension (Kadandale and Kiger, 2010), and is required for focal adhesion turnover and cell migration (Sharifi et al., 2016). Again, it is possible to suppose that ARF can promote cell spreading through its ability to induce autophagy.

In line with this hypothesis, our preliminary data seem to indicate that during spreading, the block of autophagic flux through chloroquine treatment induces HeLa cells to acquire rounded shape similarly to ARF depleted cells.

Further experiments will be necessary to validate our hypothesis and clarify the possible involvement of autophagy in this new ARF function in adhesion/spreading and/or in tumor progression.

Another unresolved question deriving from our data is whether this new ARF role in cell spreading could represent a way through which this protein performs its oncogenic activity. Indeed, the adhesion/spreading process is strictly connected to cell migration, which is essential to promote tumor invasiveness and metastasis.
Interestingly, it has been reported that $p19^{ARF}$-deficient MEFs display a round phenotype, similar to the one reported in our study, accompanied by activation of the PI3K-Rac1 pathway and increased migration properties (Guo et al., 2003 and 2004).
In line with the aforementioned article, our preliminary experiments show that ARF-depleted HeLa cells acquire increased migration properties.
On the other hand, adhesion/spreading interplay has a well-documented role not only in malignancy but also in physiological processes such as embryogenesis. Indeed, it has been reported that during the late stages of extraembryonic endoderm (ExEn) differentiation in cultured embryoid bodies (EBs), $p19^{ARF}$ expression is required for the proper migration and sorting of differentiating ExEn cells to their final location on the EB periphery (Li et al., 2013). Further analyses are necessary to clarify this point.

Finally, our data show that ARF involvement in cytoskeleton organization relies on an evolutionary conserved function/mechanism, suggesting a possible physiological role, as the mouse $p19^{ARF}$ protein is able to rescue spread morphology defect caused by $p14^{ARF}$ silencing. Moreover, the ARF exon 2 encoded region (aa. 65-132), which shows a stronger degree of identity between human and mouse respect to the exon 1ß, is required for FAK binding, its activation and cell spreading. These observations add an important element in the understanding of the function(s) of exon 2 sequences, in which the majority of mutations in human cancer have been identified so far.

CHAPTER 6

REFERENCES

Abida W.M., Gu W. p53-Dependent and p53-independent activation of autophagy by ARF. Cancer Res. 2008 Jan 15;68(2):352-7.

Ayrault O., Andrique L., Larsen C.J., Seite P. Human Arf tumor suppressor specifically interacts with chromatin containing the promoter of rRNA genes. Oncogene. 2004 Oct 21;23(49):8097-104.

Ayrault O., Andrique L., Fauvin D., Eymin B., Gazzeri S., Séité P. Human tumor suppressor p14ARF negatively regulates rRNA transcription and inhibits UBF1 transcription factor phosphorylation. Oncogene. 2006 Dec 7;25(58):7577-86.

Balaburski G.M., Hontz R.D., Murphy M.E. p53 and ARF: unexpected players in autophagy. Trends Cell Biol. 2010 Jun;20(6):363-9.

Basso K., Margolin A.A., Stolovitzky G., Klein U., Dalla-Favera R., Califano A. Reverse engineering of regulatory networks in human B cells. Nat Genet. 2005 Apr;37(4):382-90.

Brady S.N., Yu Y., Maggi L.B. Jr, Weber J.D. ARF impedes NPM/B23 shuttling in an Mdm2-sensitive tumor suppressor pathway. Mol Cell Biol. 2004 Nov;24(21):9327-38.

Budina-Kolomets A., Hontz R.D., Pimkina J., Murphy M.E. A conserved domain in exon 2 coding for the human and murine ARF tumor suppressor protein is required for autophagy induction. Autophagy. 2013 Oct;9(10):1553-65.

Calabrò V., Mansueto G., Santoro R., Gentilella A., Pollice A., Ghioni P., Guerrini L., La Mantia G. Inhibition of p63 transcriptional activity by p14ARF: functional and physical link between human ARF tumor suppressor and a member of the p53 family. Mol Cell Biol. 2004 Oct;24(19):8529-40.

Carmeliet P. VEGF as a key mediator of angiogenesis in cancer. Oncology. 2005;69 Suppl 3:4-10.

Carnero A., Hudson J.D., Price C.M., Beach D.H. p16INK4A and p19ARF act in overlapping pathways in cellular immortalization. Nat Cell Biol. 2000 Mar;2(3):148-55.

Chen D., Kon N., Li M., Zhang W., Qin J., Gu W. ARF-BP1/Mule is a critical mediator of the ARF tumor suppressor. Cell. 2005 Jul 1;121(7):1071-83.

Chen D., Shan J., Zhu W.G., Qin J., Gu W. Transcription-independent ARF regulation in oncogenic stress-mediated p53 responses. Nature. 2010 Mar 25;464(7288):624-7.

Chen R.H., Wang W.J., Kuo J.C. The tumor suppressor DAP-kinase links cell adhesion and cytoskeleton reorganization to cell death regulation. J Biomed Sci. 2006 Mar;13(2):193-9.

Chen X., Barton L.F., Chi Y., Clurman B.E., Roberts J.M. Ubiquitin-independent degradation of cell-cycle inhibitors by the REGgamma proteasome. Mol Cell. 2007 Jun 22;26(6):843-52.

Chen Z., Carracedo A., Lin H.K., Koutcher J.A., Behrendt N., Egia A., Alimonti A., Carver B.S., Gerald W.,2 Teruya-Feldstein J., Loda M., Pandolfi P.P. Differential p53- independent outcomes of p19(Arf) loss in oncogenesis. Sci Signal. 2009 Aug 18; 2(84): ra44.

Chin L., Pomerantz J., DePinho R.A. The INK4a/ARF tumor suppressor: one gene– two products–two pathways. Trends Biochem Sci. 1998 Aug;23(8):291-6.

Christensen C., Bartkova J., Mistrík M., Hall A., Lange M.K., Ralfkiær U., Bartek J., Guldberg P. A short acidic motif in ARF guards against mitochondrial dysfunction and melanoma susceptibility. Nat Commun. 2014 Nov 5; 5:5348.

Collins C.J., Sedivy J.M. Involvement of the INK4a/Arf gene locus in senescence. Aging Cell. 2003 Jun;2(3):145-50.

De Stanchina E., McCurrach M.E., Zindy F., Shieh S.Y., Ferbeyre G., Samuelson A.V., Prives C., Roussel M.F., Sherr C.J., and Scott W.L. E1A signaling to p53 involves the p19ARF tumor suppressor. Genes Dev. 1998 Aug 1; 12(15): 2434–2442.

Di Tommaso A., Hagen J., Tompkins V., Muniz V., Dudakovic A., Kitzis A., Ladeveze V., Quelle D.E. Residues in the alternative reading frame tumor suppressor that influence its stability and p53-independent activities. Exp Cell Res. 2009 Apr 15;315(7):1326-35.

Dominguez-Brauer C., Chen Y.J., Brauer P.M., Pimkina J., Raychaudhuri P. ARF stimulates XPC to trigger nucleotide excision repair by regulating the repressor complex of E2F4. EMBO Rep. 2009 Sep; 10(9): 1036–1042.

Dubiel W., Pratt G., Ferrell K., Rechsteiner M. Purification of an 11 S regulator of the multicatalytic protease. J Biol Chem. 1992; 267:22369–22377.

Duro D., Bernard O., Della Valle V., Berger R., and Larsen, C.J. A new type of p16INK4a/MTS1 gene transcript expressed in B-cell malignancies. Oncogene. 1995 Jul 6;11(1):21-9.

Eischen M.C., Weber J.D., Roussel M.F., Sherr C.J., Cleveland J.L. Disruption of the ARF–Mdm2–p53 tumor suppressor pathway in Myc-induced lymphomagenesis. Genes Dev. 1999 Oct 15; 13(20): 2658–2669.

Esteller M., Tortola S., Toyota M., Capella G., Peinado M.A., Baylin S.B., Herman J.G. Hypermethylation-associated inactivation of p14(ARF) is independent of p16(INK4a) methylation and p53 mutational status. Cancer Res. 2000 Jan 1;60(1):129-33.

Eymin B., Leduc C., Coll J.L., Brambilla E., Gazzeri S. p14ARF induces G2 arrest and apoptosis independently of p53 leading to regression of tumours established in nude mice. Oncogene. 2003 Mar 27;22(12):1822-35.

Eymin B., Claverie P., Salon C., Leduc C., Col E., Brambilla E., Khochbin S., Gazzeri S. p14ARF activates a Tip60-dependent and p53-independent ATM/ATR/CHK pathway in response to genotoxic stress. Mol Cell Biol. 2006 Jun;26(11):4339-50.

Fatyol K., Szalay A.A. The p14ARF tumor suppressor protein facilitates nucleolar sequestration of hypoxia-inducible factor-1alpha (HIF-1alpha) and inhibits HIF-1-mediated transcription. J Biol Chem. 2001 Jul 27;276(30):28421-9.

Ferrara N., Davis-Smyth T. The biology of vascular endothelial growth factor. Endocr Rev. 1997 Feb;18(1):4-25.

Ferru A., Fromont G., Gibelin H., Guilhot J., Savagner F., Tourani J.M., Kraimps J.L., Larsen C.J., Karayan-Tapon L. The status of CDKN2A alpha (p16INK4A) and beta (p14ARF) transcripts in thyroid tumour progression. Br J Cancer. 2006 Dec 18; 95(12): 1670–1677.

Freedman D.A., Levine A.J. Nuclear export is required for degradation of endogenous p53 by MDM2 and human papillomavirus E6. Mol Cell Biol. 1998 Dec;18(12):7288-93.

Fung C., Lock R., Gao S., Salas E., Debnath J. Induction of autophagy during extracellular matrix detachment promotes cell survival. Mol Biol Cell. 2008;19: 797–806.

García M.A., Collado M., Muñoz-Fontela C., Matheu A., Marcos-Villar L., Arroyo J., Esteban M., Serrano M., Rivas C. Antiviral action of the tumor suppressor ARF. EMBO J. 2006 Sep 20;25(18):4284-92.

Gil J., Peters G. Regulation of the INK4b-ARF-INK4a tumour suppressor locus: all for one or one for all. Nat Rev Mol Cell Biol. 2006 Sep;7(9):667-77.

Gilley J. and Fried M. One INK4 gene and no ARF at the Fugu equivalent of the human INK4A/ARF/INK4B tumour suppressor locus. Oncogene. 2001 Nov 1;20(50):7447-52.

Golubovskaya V.M., Finch R., Cance W.G. Direct interaction of the N-terminal domain of focal adhesion kinase with the N-terminal transactivation domain of p53. J. Biol. Chem. 2005;280(26):25008–25021.

Gromley A., Churchman M.L., Zindy F., Sherr C.J. Transient expression of the Arf tumor suppressor during male germ cell and eye development in Arf-Cre reporter mice. Proc Natl Acad Sci U S A. 2009 Apr 14;106(15):6285-90.

Guo F, Gao Y, Wang L, Zheng Y. p19Arf-p53 tumor suppressor pathway regulates cell motility by suppression of phosphoinositide 3-kinase and Rac1 GTPase activities. J Biol Chem. 2003 Apr 18;278(16):14414-9.

Guo F, Zheng Y. Involvement of Rho family GTPases in p19Arf- and p53-mediated proliferation of primary mouse embryonic fibroblasts. Mol Cell Biol. 2004 Feb;24(3):1426-38.

Hainaut P., Soussi T., Shomer B., Hollstein M., Greenblatt M., Hovig E., Harris C.C., Montesano R. Database of p53 gene somatic mutations in human tumors and cell lines: updated compilation and future prospects. Nucleic Acids Res. 1997 Jan 1;25(1):151-7.

Haindl M., Harasim T., Eick D., Muller S. The nucleolar SUMO-specific protease SENP3 reverses SUMO modification of nucleophosmin and is required for rRNA processing. EMBO Rep. 2008 Mar;9(3):273-9.

Hall M., Peters G. Genetic alterations of cyclins, cyclin-dependent kinases, and Cdk inhibitors in human cancer. Adv Cancer Res. 1996; 68:67-108.

Hemmati P.G., Gillissen B., von Haefen C., Wendt J., Stärck L., Güner D., Dörken B., Daniel P.T. Adenovirus-mediated overexpression of p14(ARF) induces p53 and Bax-independent apoptosis. Oncogene. 2002 May 9;21(20):3149-61.

Hershko A., Ciechanover A. The ubiquitin system. Annu Rev Biochem. 1998;67: 425-79.

Honda R., Tanaka H., Yasuda H. Oncoprotein MDM2 is a ubiquitin ligase E3 for tumor suppressor p53. FEBS Lett. 1997 Dec 22;420(1):25-7.

Honda R., Yasuda H. Association of p19(ARF) with Mdm2 inhibits ubiquitin ligase activity of Mdm2 for tumor suppressor p53. EMBO J. 1999 Jan 4;18(1):22-7.

Humbey O., Pimkina J., Zilfou J.T., Jarnik M., Dominguez-Brauer C., Burgess D.J. Eischen C.M., Murphy M.E. The ARF tumor suppressor can promote the progression of some tumors. Cancer Res. 2008 Dec 1;68(23):9608-13.

Inoue R., Shiraishi T. PKCalpha is involved in phorbol ester TPA-mediated stabilization of p14ARF. Biochem Biophys Res Commun. 2005 May 20;330(4):1314-8.

Itahana K., Bhat K.P., Jin A., Itahana Y., Hawke D., Kobayashi R., Zhang Y. Tumor suppressor ARF degrades B23, a nucleolar protein involved in ribosome biogenesis and cell proliferation. Mol Cell. 2003 Nov;12(5):1151-64.

Itahana K., Zhang Y. Mitochondrial p32 Is a Critical Mediator of ARF-Induced Apoptosis. Cancer Cell. 2008 Jun; 13(6): 542–553.

Junttila M.R., Evan G.I. p53--a Jack of all trades but master of none. Nat Rev Cancer. 2009 Nov;9(11):821-9.

Kadandale P., Kiger A.A. Role of selective autophagy in cellular remodeling "Self-eating" into shape. Autophagy. 2010 Nov 16; 6(8): 1194–1195.

Kadaré G., Toutant M., Formstecher E., Corvol J.C., Carnaud M., Boutterin M.C., Girault J.A. PIAS1-mediated sumoylation of focal adhesion kinase activates its autophosphorylation. J Biol Chem. 2003 Nov 28;278(48):47434-40.

Kamb A., Shattuck-Eidens D., Eeles R., Liu Q., Gruis N. A., Ding W., Hussey C., Tran T., Miki Y., Weaver-Feldhaus J., McClure M., Aitken J.F., Anderson D.E., Bergman W., Frants R., Goldgar D. E., Green A., MacLennan R., Martin N.G., Meyer L.J., Youl P., Zone J.J., Skolnick M.H., Cannon-Albright L. A. Analysis of the p16gene(cdkN2) as a candidate for the chromosome 9p melanoma susceptibility locus. Nat Genet. 1994 Sep;8(1):23-6.

Kamijo T., Weber J.D., Zambetti G., Zindy F., Roussel M.F., Sherr C.J. Functional and physical interactions of the ARF tumor suppressor with p53 and Mdm2. Proc Natl Acad Sci U S A. 1998 Jul 7;95(14):8292-7.

Kamijo T., Bodner S., van de Kamp E., Randle D.H., Sherr C.J. Tumor spectrum in ARF-deficient mice. Cancer Res 1999; 59: 2217–2222.

Kawagishi H., Nakamura H., Maruyama M., Mizutani S., Sugimoto K., Takagi M., Sugimoto M. ARF suppresses tumor angiogenesis through translational control of VEGFA mRNA. Cancer Res. 2010 Jun 1;70(11):4749-58.

Kim, S.H., Mitchell M., Fujii H., Llanos S. and Peters, G. Absence of p16INK4a and truncation of ARF tumor suppressors in chickens. Proc Natl Acad Sci U S A. 2003 Jan 7;100(1):211-6.

Kobayashi T., Wang J., Al-Ahmadie H., Abate-Shen C. ARF regulates the stability of p16 protein via REGγ-dependent proteasome degradation. Mol Cancer Res. 2013 Aug; 11(8): 828–833.

Konishi N., Nakamura M., Kishi M., Nishimine M., Ishida E., Shimada K. Heterogeneous methylation and deletion patterns of the INK4a/ARF locus within prostate carcinomas. Am J Pathol. 2002 Apr;160(4):1207-14.

Kotsinas A., Papanagnou P., Evangelou K., Trigas G.C., Kostourou V., Townsend P., Gorgoulis V.G. ARF: a versatile DNA damage response ally at the crossroads of development and tumorigenesis. Front Genet. 2014; 5: 236.

Kuo J.C., Lin J.R., Staddon J.M., Hosoya H., Chen R.H. Uncoordinated regulation of stress fibers and focal adhesions by DAP kinase. J Cell Sci. 2003 Dec 1;116(Pt 23):4777-90.

Kuo M.L., den Besten W., Bertwistle D., Roussel M.F., Sherr C.J. N-terminal polyubiquitination and degradation of the Arf tumor suppressor. Genes Dev. 2004 Aug 1;18(15):1862-74.

Laud K., Marian C., Avril M.F., Barrois M., Chompret A., Goldstein A.M., Tucker M.A., Clark P.A., Peters G., Chaudru V., Demenais F., Spatz A., Smith M.W., Lenoir G.M., Bressac-de Paillerets B.; French Hereditary Melanoma Study Group. Comprehensive analysis of CDKN2A (p16INK4A/p14ARF) and CDKN2B genes in 53 melanoma index cases considered to be at heightened risk of melanoma. J Med Genet. 2006 Jan;43(1):39-47.

Lee Y.K., Park J.Y., Kang H.J., Cho H.C. Overexpression of p16INK4A and p14ARF in haematological malignancies. Clin Lab Haematol. 2003 Aug;25(4):233-7.

Lessard F., Morin F., Ivanchuk S., Langlois F., Stefanovsky V., Rutka J., Moss T. The ARF tumor suppressor controls ribosome biogenesis by regulating the RNA polymerase I transcription factor TTF-I. Mol Cell. 2010 May 28;38(4):539-50.

Li C., Finkelstein D., Sherr C.J. Arf tumor suppressor and miR-205 regulate cell adhesion and formation of extraembryonic endoderm from pluripotent stem cells. Proc Natl Acad Sci U S A. 2013 Mar 19;110(12):E1112-21.

Li X., Lonard D.M., Jung S.Y., Malovannaya A., Feng Q., Qin J., Tsai S.Y., Tsai M.J., O'Malley B.W. The SRC-3/AIB1 coactivator is degraded in a ubiquitin-and ATP-independent manner by the REGgamma proteasome. Cell. 2006; 124:381–392.

Liggett W.H. Jr. and Sidransky, D. Role of the p16 tumor suppressor gene in cancer. J Clin Oncol. 1998 Mar;16(3):1197-206.

Lilienbaum A. Relationship between the proteasomal system and autophagy. Int J Biochem Mol Biol. 2013; 4(1): 1–26.

Lim S.T., Chen X.L., Lim Y., Hanson D.A., Vo T.T., Howerton K., Larocque N., Fisher S.J., Schlaepfer D.D., Ilic D. Nuclear FAK promotes cell proliferation and survival through FERM-enhanced p53 degradation. Mol. Cell. 2008;29(1):9–22.

Liu X., Liu Z., Jang S.W., Ma Z., Shinmura K., Kang S., Dong S., Chen J., Fukasawa K., Ye K. Sumoylation of nucleophosmin/B23 regulates its subcellular localization, mediating cell proliferation and survival. Proc Natl Acad Sci U S A. 2007 Jun 5; 104(23): 9679–9684.

Llanos S., Clark P.A., Rowe J., Peters G. Stabilization of p53 by p14ARF without relocation of MDM2 to the nucleolus. Nat Cell Biol. 2001 May;3(5):445-52.

Lohrum M.A.E., Ashcroft M., Kubbutat M.H.G., Vousden K.H. Contribution of two independent MDM2-binding domains in p14ARF to p53 stabilization. Curr Biol. 2000 May 4;10(9):539-42.

Ma C.P., Slaughter C.A., DeMartino G.N. Identification, purification, and characterization of a protein activator (PA28) of the 20 S proteasome (macropain). J Biol Chem. 1992 May 25;267(15):10515-23.

Maggi L.B. Jr., Winkeler C.L., Miceli A.P., Apicelli A.J., Brady S. N., Kuchenreuther M. J., Weber J. D. ARF tumor suppression in the nucleolus. Biochim Biophys Acta. 2014 Jun;1842(6):831-9.

Maiuri MC, et al. Functional and physical interaction between Bcl-X(L) and a BH3-like domain in Beclin-1. EMBO J 2007; 26:2527–2539.

Mao L., Merlo A., Bedi G., Shapiro G.I., Edwards C.D., Rollins B.J., Sidransky D. A novel p16INK4A transcript. Cancer Res. 1995 Jul 15;55(14):2995-7.

McKeller R.N., Fowler J.L., Cunningham J.J., Warner N., Smeyne R.J., Zindy F., Skapek S.X. The Arf tumor suppressor gene promotes hyaloid vascular regression during mouse eye development. Proc. Natl. Acad. Sci. U.S.A. 2002; 99:3848–3853.

Menéndez S., Khan Z., Coomber D.W., Lane D.P., Higgins M., Koufali M.M., Lain S. Oligomerization of the human ARF tumor suppressor and its response to oxidative stress. J Biol Chem. 2003 May 23;278(21):18720-9.

Mochly-Rosen D., Das K., Grimes K.V. Protein kinase C, an elusive therapeutic target? Nat Rev Drug Discov. 2012 Dec;11(12):937-57.

Momand J., Zambetti G.P., Olson D.C., George D., Levine A.J. The mdm-2 oncogene product forms a complex with the p53 protein and inhibits p53-mediated transactivation. Cell. 1992 Jun 26;69(7):1237-45.

Nakamura M., Watanabe T., Klangby U., Asker C., Wiman K., Yonekawa Y., Kleihues P., Ohgaki H. p14ARF deletion and methylation in genetic pathways to glioblastomas. Brain Pathol. 2001 Apr;11(2):159-68.

Nishizuka Y. Protein kinase C and lipid signaling for sustained cellular responses. FASEB J. 1995 Apr;9(7):484-96.

Nollet E.A., Miranti C.K. Integrin and Adhesion Regulation of Autophagy and Mitophagy- Chapter 21 in “Autophagy - A Double-Edged Sword - Cell Survival or Death?” Dr. Yannick Bailly (Ed.), 2013, InTech, DOI: 10.5772/55398.

Oliner J.D., Pietenpol J.A., Thiagalingam S., Gyuris J., Kinzler K.W., Vogelstein B. Oncoprotein MDM2 conceals the activation domain of tumour suppressor p53. Nature. 1993 Apr 29;362(6423):857-60.

Orlando G., Khoronenkova S.V., Dianova I.I., Parsons J.L., Dianov G.L. ARF induction in response to DNA strand breaks is regulated by PARP1. Nucleic Acids Res. 2014 Feb; 42(4): 2320–2329.

Ozenne P., Eymin B., Brambilla E., Gazzeri S. The ARF tumor suppressor: structure, functions and status in cancer. Int J Cancer 2010; 127: 2239–2247.

Pattingre S., Tassa A., Qu X., Garuti R., Liang X.H., Mizushima N., Packer M., Schneider M.D., Levine B. Bcl-2 antiapoptotic proteins inhibit Beclin 1-dependent autophagy. Cell. 2005 Sep 23;122(6):927-39.

Pollice A., Nasti V., Ronca R., Vivo M., Lo Iacono M., Calogero R., Calabrò V., La Mantia G. Functional and physical interaction of the human ARF tumor suppressor with Tat-binding protein-1. J Biol Chem. 2004 Feb 20;279(8):6345-53.

Pollice A., Sepe M., Villella V.R., Tolino F., Vivo M., Calabrò V., La Mantia G. TBP-1 protects the human oncosuppressor p14ARF from proteasomal degradation. Oncogene. 2007 Aug 2;26(35):5154-62.

Pollice A., Vivo M., La Mantia G. The promiscuity of ARF interactions with the proteasome. FEBS Lett. 2008 Oct 15;582(23-24):3257-62.

Pomerantz J., Schreiber-Agus N., Liegeois N.J., Silverman A., Alland L., Chin L., Potes J., Chen K., Orlow I., Lee H.W., Cordon-Cardo C., DePinho R.A. The Ink4a tumor suppressor gene product, p19Arf, interacts with MDM2 and neutralizes MDM2's inhibition of p53. Cell. 1998 Mar 20;92(6):713-23.

Quelle D.E., Zindy F., Ashmun R.A. and Sherr C.J. Alternative reading frames of the *INK4a* tumor suppressor gene encode two unrelated proteins capable of inducing cell cycle arrest. Cell. 1995 Dec 15;83(6):993-1000.

Quelle, D.E., Cheng M., Ashmun R.A., Sherr, C.J. Cancer-associated mutations at the INK4a locus cancel cell cycle arrest by p16INK4a but not by the alternative reading frame protein p19ARF. Proc Natl Acad Sci U S A. 1997 Jan 21; 94(2): 669–673.

Raveh T., Droguett G., Horwitz M.S., DePinho R.A., Kimchi A. DAP kinase activates a p19ARF/p53-mediated apoptotic checkpoint to suppress oncogenic transformation. Nature cell biology. 2001; 3(1):1-7.

Reef S., Zalckvar E., Shifman O., Bialik S., Sabanay H., Oren M., Kimchi A. A short mitochondrial form of p19ARF induces autophagy and caspase-independent cell death. Mol Cell. 2006 May 19;22(4):463-75.

Reef S., Shifman O., Oren M., Kimchi A. The autophagic inducer smARF interacts with and is stabilized by the mitochondrial p32 protein. Oncogene. 2007 Oct 11;26(46):6677-83.

Rizos H., Darmanian A.P., Holland E.A., Mann G.J., Kefford R.F. Mutations in the INK4a/ARF melanoma susceptibility locus functionally impair p14ARF. J Biol Chem. 2001 Nov 2;276(44):41424-34.

Rizos H., Woodruff S., Kefford R.F. p14ARF interacts with the SUMO-conjugating enzyme Ubc9 and promotes the sumoylation of its binding partners. Cell Cycle. 2005 Apr;4(4):597-603.

Rocha S., Campbell K.J., Perkins N.D. p53- and Mdm2-independent repression of NF-kappa B transactivation by the ARF tumor suppressor. Mol Cell. 2003 Jul;12(1):15-25.

Rocha S., Garrett M.D., Campbell K.J., Schumm K., Perkins ND. Regulation of NF-kappaB and p53 through activation of ATR and Chk1 by the ARF tumour suppressor. EMBO J. 2005 Mar 23;24(6):1157-69.

Rodway H., Llanos S., Rowe J., Peters G. Stability of nucleolar versus non-nucleolar forms of human p14(ARF). Oncogene. 2004 Aug 19;23(37):6186-92.

Roth J., Dobbelstein M., Freedman D.A., Shenk T., Levine A.J. Nucleo-cytoplasmic shuttling of the hdm2 oncoprotein regulates the levels of the p53 protein via a pathway used by the human immunodeficiency virus rev protein. EMBO J. 1998 Jan 15;17(2):554-64.

Ruas M., Peters G. The p16INK4a/CDKN2A tumor suppressor and its relatives. Biochim Biophys Acta. 1998 Oct 14;1378(2):F115-77.

Sanchez-Aguilera A., Sanchez-Beato M., Garcia J.F., Prieto I., Pollan M., Piris M.A. p14 (ARF) nuclear overexpression in aggressive B-cell lymphomas is a sensor of mal- function of the common tumor suppressor pathways. Blood 2002; 99: 1411–1418.

Sandilands E., Serrels B., McEwan D.G., Morton J.P., Macagno J.P., McLeod K., Stevens C., Brunton V.G., Langdon W.Y., Vidal M., Sansom O.J., Dikic I., Wilkinson S., Frame M.C. Autophagic targeting of Src promotes cancer cell survival following reduced FAK signalling. Nat Cell Biol. 2011 Dec 4;14(1):51-60.

Saporita A.J., Maggi L.B. Jr., Apicelli A.J., Weber J.D. Therapeutic targets in the ARF tumor suppressor pathway. Curr Med Chem. 2007;14(17):1815-27.

Schutte M., Hruban R.H., Geradts J., Maynard R., Hilgers W., Rabindran S.K., Moskaluk C.A., Hahn S.A., Schwarte-Waldhoff I., Schmiegel W., Baylin S.B., Kern S.E., Herman J.G. Abrogation of the Rb/p16 tumor-suppressive pathway in virtually all pancreatic carcinomas. Cancer Res. 1997 Aug 1;57(15):3126-30.

Serrano M. The INK4a/ARF locus in murine tumorigenesis. Carcinogenesis. 2000 May;21(5):865-9.

Sharifi M.N., Mowers E.E., Drake L.E., Collier C., Chen H., Zamora M., Mui S., Macleod K.F. Autophagy promotes focal adhesion disassembly and cell motility of metastatic tumor cells through the direct interaction of paxillin with LC3. Cell Rep. 2016 May 24; 15(8): 1660–1672.

Sharpless N.E. and DePinho R.A. The INK4A/ARF locus and its two gene products. Curr Opin Genet Dev. 1999 Feb;9(1):22-30.

Sharpless N.E., Sherr C.J. Forging a signature of in vivo senescence. Nat Rev Cancer. 2015 Jul;15(7):397-408.

Sherburn T.E., Gale J.M. and Ley R.D. Cloning and characterization of the CDKN2A and p19ARF genes from Monodelphis domestica. DNA Cell Biol. 1998 Nov;17(11):975-81.

Sherr C.J. Tumor surveillance via the ARF-p53 pathway. Genes Dev. 1998 Oct 1;12(19):2984-91.

Sherr C.J. The INK4a/ARF network in tumour suppression. Nat Rev Mol Cell Biol. 2001 Oct;2(10):731-7.

Sherr C.J. Divorcing ARF and p53: an unsettled case. Nat Rev Cancer. 2006 Sep;6(9):663-73.

Silva J., Domínguez G., Silva J.M., García J.M., Gallego I., Corbacho C., Provencio M., España P., Bonilla F. Analysis of genetic and epigenetic processes that influence p14ARF expression in breast cancer. Oncogene. 2001 Jul 27;20(33):4586-90.

Stone S., Jiang P., Dayananth P., Tavtigian S.V., Katcher H., Parry D., Peters G., Kamb A. Complex structure and regulation of the P16 (MTS1) locus. Cancer Res. 1995 Jul 15;55(14):2988-94.

Stott F.J., Bates S., James M.C., McConnell B.B., Starborg M., Brookes S., Palmero I., Ryan K., Hara E., Vousden K.H., Peters G. The alternative product from the human CDKN2A locus, p14(ARF), participates in a regulatory feedback loop with p53 and MDM2. EMBO J. 1998 Sep 1;17(17):5001-14.

Su X., Cho M.S., Gi Y.J., Ayanga B.A., Sherr C.J., Flores E.R. Rescue of key features of the p63-null epithelial phenotype by inactivation of Ink4a and Arf. EMBO J. 2009 Jul 8;28(13):1904-15.

Sugimoto M., Kuo M.L., Roussel M.F., Sherr C.J. Nucleolar Arf tumor suppressor inhibits ribosomal RNA processing. Mol Cell. 2003 Feb;11(2):415-24.

Sun Y., Jiang X., Chen S., Fernandes N., Price B.D. A role for the Tip60 histone acetyltransferase in the acetylation and activation of ATM. Proc Natl Acad Sci U S A. 2005 Sep 13;102(37):13182-7.

Swafford D.S., Middleton S.K., Palmisano W.A., Nikula K.J., Tesfaigzi J., Baylin S.B., Herman J.G. and Belinsky S.A. Frequent Aberrant Methylation of p16INK4a in Primary Rat Lung Tumors. Mol Cell Biol. 1997 Mar;17(3):1366-74.

Tago K., Chiocca S., Sherr C.J. Sumoylation induced by the Arf tumor suppressor: a p53-independent function. Proc Natl Acad Sci U S A. 2005 May 24;102(21):7689-94.

Tao W., Levine A.J. P19(ARF) stabilizes p53 by blocking nucleo-cytoplasmic shuttling of Mdm2. Proc Natl Acad Sci U S A. 1999 Jun 8;96(12):6937-41.

Tsujimoto H., Hagiwara A., Sugihara H., Hattori T., Yamagishi H. Promoter methylations of p16INK4a and p14ARF genes in early and advanced gastric cancer. Correlations of the modes of their occurrence with histologic type. Pathol Res Pract. 2002;198(12):785-94.

Van Oosterwijk J.G., Li C., Yang X., Opferman J.T., Sherr C.J. Small mitochondrial Arf (smArf) protein corrects p53-independent developmental defects of Arf tumor suppressor-deficient mice. Proc Natl Acad Sci U S A. 2017 Jul 11; 114(28): 7420–7425.

Vivo M., Di Costanzo A., Fortugno P., Pollice A., Calabrò V., La Mantia G. Downregulation of DeltaNp63alpha in keratinocytes by p14ARF-mediated SUMO-conjugation and degradation. Cell Cycle. 2009 Nov 1;8(21):3545-51.

Vivo M., Ranieri M., Sansone F., Santoriello C., Calogero R.A., Calabrò V., Pollice A., La Mantia G. Mimicking p14ARF phosphorylation influences its ability to restrain cell proliferation. PLoS One. 2013;8(1):e53631.

Vivo M., Matarese M., Sepe M., Di Martino R., Festa L., Calabrò V., La Mantia G., Pollice A. MDM2-mediated degradation of p14ARF: a novel mechanism to control ARF levels in cancer cells. PLoS One. 2015 Feb 27;10(2):e0117252.

Vivo M., Fontana R., Ranieri M., Capasso G., Angrisano T., Pollice A., Calabrò V., La Mantia G. p14ARF interacts with the focal adhesion kinase and protects cells from anoikis. Oncogene. 2017 Aug 24;36(34):4913-4928.

Vonlanthen S., Heighway J., Tschan M.P., Borner M.M., Altermatt H.J., Kappeler A., Tobler A., Fey M.F., Thatcher N., Yarbrough W.G., Betticher D.C. Expression of p16INK4a/p16alpha and p19ARF/p16beta is frequently altered in non-small cell lung cancer and correlates with p53 overexpression. Oncogene. 1998 Nov 26;17(21):2779-85.

Vousden K.H., Lu X. Live or let die: the cell's response to p53. Nat Rev Cancer. 2002 Aug;2(8):594-604.

Wang W.J., Kuo J.C., Yao C.C., Chen R.H. DAP-kinase induces apoptosis by suppressing integrin activity and disrupting matrix survival signals. J Cell Biol 2002; 159: 169–179.

Weber J.D., Kuo M.L., Bothner B., Di Giammarino E.L., Kriwacki R.W., Roussel M.F., Sherr C.J. Cooperative signals governing ARF–Mdm2 interaction and nucleolar localization of the complex. Mol Cell Biol. 2000 Apr; 20(7): 2517–2528.

Woods Y.L., Xirodimas D.P., Prescott A.R., Sparks A., Lane D.P., Saville M.K. p14 Arf promotes small ubiquitin-like modifier conjugation of Werners helicase. J Biol Chem. 2004 Nov 26;279(48):50157-66.

Xie Y., Liu S., Lu W., Yang Q., Williams K.D., Binhazim A.A., Carver B.S., Matusik R.J., Chen Z. Slug regulates E-cadherin repression via p19Arf in prostate tumorigenesis. Mol Oncol. 2014 Oct; 8(7): 1355–1364.

Xie Y., Lu W., Liu S., Yang Q., Goodwin J.S., Sathyanarayana S.A., Pratap S., Chen Z. MMP7 interacts with ARF in nucleus to potentiate tumor microenvironments for prostate cancer progression in vivo. Oncotarget. 2016 Jul 26;7(30):47609-47619.

Xirodimas D.P., Chisholm J., Desterro J.M., Lane D.P., Hay R.T. P14ARF promotes accumulation of SUMO-1 conjugated (H)Mdm2. FEBS Lett. 2002 Sep 25;528(1-3):207-11.

Yarbrough W.G., Bessho M., Zanation A., Bisi J.E., Xiong Y. Human tumor suppressor ARF impedes S-phase progression independent of p53. Cancer Res. 2002 Feb 15;62(4):1171-7.

Yu J., Zhang S.S., Saito K., Williams S., Arimura Y., Ma Y., Ke Y., Baron V., Mercola D., Feng G.S., Adamson E., Mustelin T. PTEN regulation by Akt-EGR1-ARF-PTEN axis. EMBO J. 2009 Jan 7;28(1):21-33.

Zhang Y., Xiong Y., Yarbrough W.G. ARF promotes MDM2 degradation and stabilizes p53: ARF-INK4a locus deletion impairs both the Rb and p53 tumor suppression pathways. Cell. 1998 Mar 20;92(6):725-34.

Zhang Y., Xiong Y. Mutations in human ARF exon 2 disrupt its nucleolar localization and impair its ability to block nuclear export of MDM2 and p53. Mol Cell. 1999 May;3(5):579-91.

Zindy F., Williams R.T., Baudino T.A., Rehg J.E., Skapek S.X., Cleveland J.L., Roussel M.F., Sherr C.J. Arf tumor suppressor promoter monitors latent oncogenic signals in vivo. Proc. Natl. Acad. Sci. U.S.A. 2003; 100:15930–15935.